Permeable Landscapes for Climate Change

The Nature Conservancy, Eastern Conservation Science

Mark G. Anderson, Melissa Clark, and Brad H. McRae

March 2015

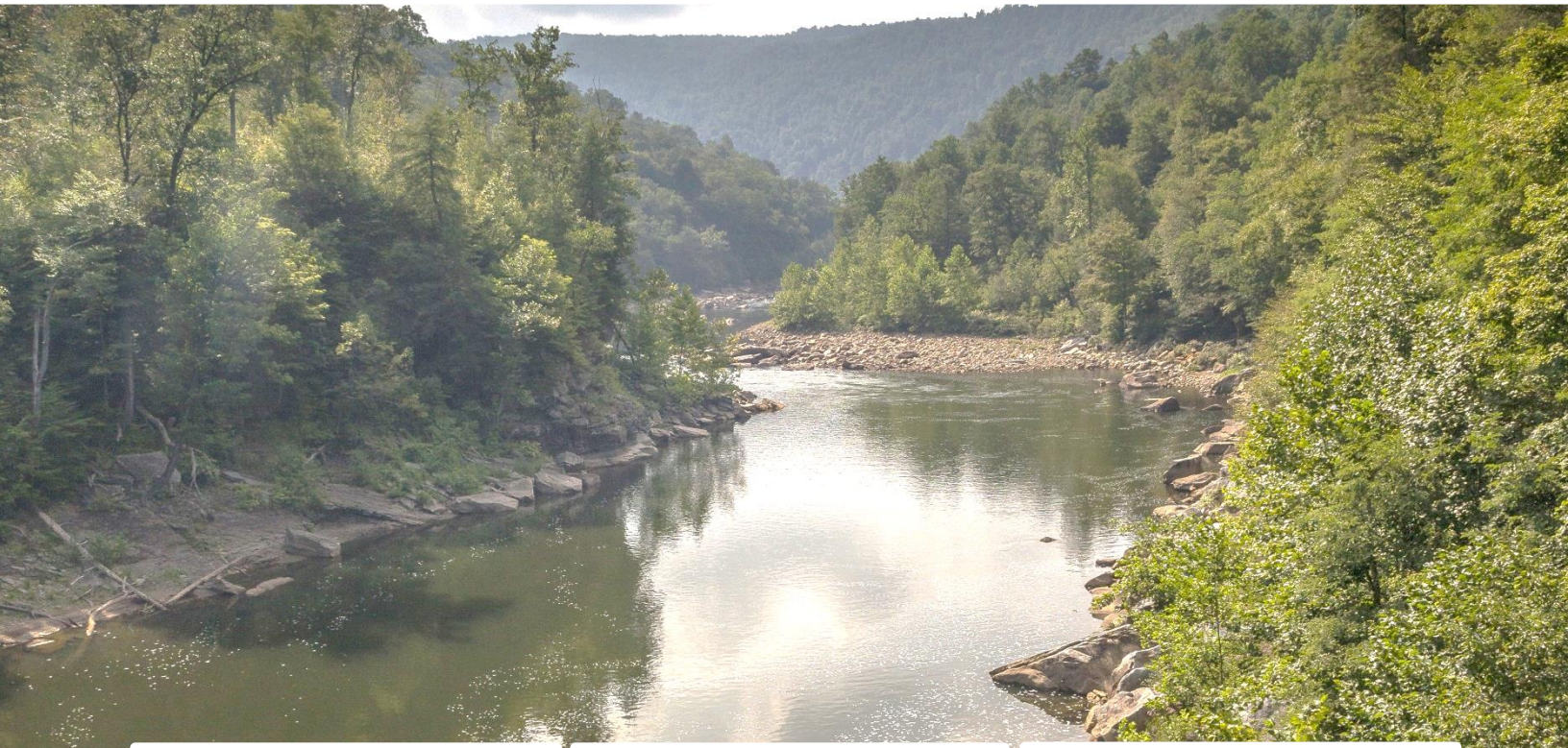

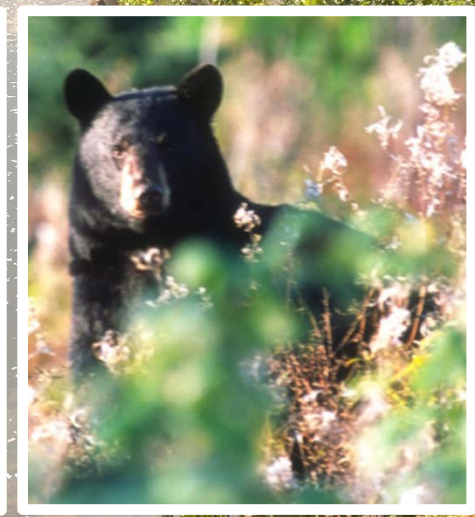

The Nature Conservancy

Protecting nature. Preserving life.

Mark G. Anderson, Melissa Clark, and Brad H. McRae

The Nature Conservancy
Eastern Conservation Science
Eastern Regional Office
99 Bedford St, 5th Floor
Boston, MA 02111

Please cite as:

Anderson, M.G. Clark, M. and McRae, B.H. 2015. Permeable Landscape for Climate Change. The Nature Conservancy, Eastern Conservation Science, Eastern Regional Office. Boston, MA.

Funding for this project was supported by a grant from the U.S. Department of the Interior, Fish and Wildlife Service

North Atlantic LCC
North Atlantic Landscape Conservation Cooperative

About the Cover:
Background: © Kent Mason Cheat River, Cheat River Canyon in West Virginia.
Bottom Left: © Kent Mason An Eastern Newt (Notophthalmus viridescens), sometimes called the "Red-spotted Newt" at Bear Rocks Preserve. The Nature Conservancy's Bear Rocks Preserve in West Virginia. High above Canaan Valley, in Dolly Sods, where a flat, windswept expanse of subalpine heath barrens opens up to the sky. Stunted red spruce, ancient bogs and forlorn boulders define this haunting landscape, where creatures typically found in more northern environs roam oblivious to their geologic isolation. The Nature Conservancy's 477-acre Bear Rocks Preserve is a cornerstone of this wonderfully diverse and complex ecosystem, which lies on a ridge crest that forms part of the Eastern Continental Divide.
Bottom Center: © David Dadurka Bee balm blooms in Cranesville Swamp Preserve, a unique sub-arctic swamp, or "frost pocket" of land located in the central Appalachian mountains of Maryland comprised of bog peatland, wet meadows, shrubland, and forest communities and home to diverse plant and animal life, including 43 species classified by Maryland conservationists as being endangered or rare
Bottom Right: © Vicki Nolan Black Bear in Maine

Acknowledgements

We wish to thank Andrew Milliken, Scott Schwenk, and Steve Fuller of the USFW North Atlantic Landscape Conservation Cooperative for their advice, support, and patience as we worked through the complexities of this project. Analie Barnett, Andy Finton, Barbara Vickery, Dan Coker, Dave Theobald, Josh Royte, Judy Dunscomb, Nels Johnson, Sally Palmer, and Thomas Minney provided helpful perspectives on how to think about landscape permeability. Special thanks to Arlene Olivero and Analie Barnett for help with the riparian climate corridors and Charles Ferree for the regional landform model.

Abstract

In response to climate change, species' ranges are shifting northward at rates of 10-20 km per decade and upslope at rates of 11 m per decade. How do conservationists ensure that the landscape remains permeable enough to allow such large-scale movement, particularly by populations that disperse slowly? In this spatial study we introduce two approaches that may facilitate permeability in the Northeastern USA. In the first approach, range-shift linkages, we identify areas where northward and upslope movements become concentrated due to roads and development patterns or where intact natural areas with large temperature gradients occur. We modeled the former using a wall-to-wall Circuitscape analysis that combined upslope and northward movements with anthropogenic resistance. We modeled the latter using a moving window approach to identify concentrations of natural cover that connect natural areas across temperature gradients. In the second approach, riparian climate corridors, we identified stretches of intact floodplains that span large temperature gradients. For these, we created units using a 30 m floodplain model, and ranked the units based on attributes such as their size, length of temperature gradients, and degree of local connectedness. The results highlight places that may be regionally important for facilitating adaptation.

.

Table of Contents

Introduction

Objective and Background

In response to a changing climate, populations of plants and animals are rapidly moving northward and upslope or finding refuge along relatively cool, moist riparian areas. Essentially, they are shifting their distributions to keep up with changing conditions. How do conservationists ensure that the landscape remains permeable enough to allow such large-scale movement, particularly by populations that disperse slowly? In this spatially-explicit study of the Northeast and Mid-Atlantic region, we explore this question using new methods designed to evaluate the patterns of permeability across the entire region. We focus on understanding and identifying two types of landscape linkages that that may be critical in facilitating movement and sustaining the diversity of the region:

Range Shift Linkages: Areas of land where northward and upslope movements become concentrated due to roads and development patterns, or intact natural areas with large temperature gradients. These are regional and local areas where the range shifts of many species will likely converge.

Riparian Climate Corridors: Intact floodplains containing large temperature gradients. These benefit species by offering a cool, moist environment that tracks gradual temperature change.

Our objective was to highlight regionally and locally significant places that may warrant conservation action because of the role they play in maintaining the permeability of the landscape. Towards that end we develop conceptual models and appropriate analytical methods to assess the region for places with characteristics important to range shifts or gradual riparian movements. In this report, we describe what these characteristics are, explain our assessment methods, and present our results. We do this separately for each linkage type and we make the data available for others to explore.

This report is a complement to an earlier study of climate-resilient sites (Anderson et al. 2012) which identified site more likely to retain species and ecological processes in the face of climate change based on their geophysical properties. Together, these studies provide information necessary to identify a new type of "core and linkage" conservation network, one specifically designed to accommodate the dynamics expected as species adapt to climate change. However, measuring and maintaining connectivity has much greater uncertainty to it than identifying and conserving a core area. Further, the effects of connectivity conservation are not well understood and may be overestimated (Hodgson 2009). Nevertheless, it is clear that species distributions and ecological processes are in flux, and constituents of every major terrestrial taxa group are shifting their ranges. Thus, core areas, even climate resilient ones, must be embedded in a permeable landscape if they are to function as envisioned. Our hope is that synergies between the two strategies add up to more effective conservation and if implemented will help sustain the diversity of the Northeast.

Permeability vs. Connectivity

Climate change is expected to accelerate the natural dynamics of the Northeast, shifting seasonal temperature and precipitation patterns and altering disturbance cycles of fire, wind, drought, and flood. The implication of this change on wildlife and plants is relatively unknown. Rapid periods of climate change in the Quaternary saw many shifts in species distributions but few extinctions, perhaps because the landscape was highly connected by natural cover (Botkin et al. 2007). Now, pervasive fragmentation disrupts ecological processes and impedes the ability of many species to move or adapt to changes. The concern is that broad-scale degradation will result from the impaired ability of nature to adjust to rapid change, creating a world dominated by depleted environments and weedy generalist species. Not surprisingly, the need to maintain connectivity has emerged as a point of agreement among scientists (Heller and Zavaleta 2009, Krosby et al. 2010). When done in conjunction with protecting and restoring sufficient areas of high quality habitat, maintaining a permeable landscape should facilitate the expected range shifts of species responding to a changing climate.

We use the term 'permeability' instead of 'connectivity' because the conservation literature commonly defines 'connectivity' as the capacity of individual species to move between areas of habitat via corridors and linkage zones (Fischer and Lindenmayer 2006). Accordingly, the analysis of landscape connectivity typically entails identifying linkages between specific places, usually patches of good habitat or natural landscape blocks, with respect to a particular species (Beier et al. 2011). Moreover, traditional models identify areas that facilitate species movements at one point in time between their current habitats and within their current distributions (Hannah 2011) and thus don't identify areas that would allow species to track climate-driven range shifts (Nunez 2013). In contrast, facilitating the large-scale ecological reorganization expected from climate change - many types of organisms, over many generation, with directional influence – requires a broader and more inclusive analysis, one appropriate to thinking about the transformation of whole regions.

Landscape permeability is a measure of landscape structure: the hardness of barriers, the connectedness of natural cover, and the arrangement of land uses. It is defined as the degree to which regional landscapes, encompassing a variety of natural, semi-natural and developed land cover types, will sustain ecological processes and are conducive to the movement of many types of organisms (Meiklejohn et al. 2010). Accordingly, we developed methods that would map permeability as a continuous surface, not as a set of discrete cores and linkages, and quantify the physical arrangement and relative resistance of natural and modified habitats. The software we used (Circuitscape) "sees" the landscapes as a surface with varying degrees of permeability, simultaneously putting up resistances to movement, and promoting movement.

Because permeability is a multidimensional characteristic, we developed two separate analytical models to assess different aspects of its local and regional nature. The **wall-to-wall approach**, looks at upslope and north-south flow patterns across the entire region and measures how flow patterns become slowed, redirected, or channeled into concentration areas, due to the spatial arrangements of cities, towns, farms, roads, and natural land. The **moving window** approach starts with a focal cell and looked at the anthropogenic resistance to flows outward in all directions following temperature gradients in the cell's local 10 km neighborhood.

Permeability for Range Shifts

In this chapter, we analyze the landscape of the Northeast US to identify areas that may facilitate the range shifts necessary for plants and wildlife to adjust to a changing climate. In the first section, we spatially model the upslope and northward movements necessary for species to adapt to a warming climate and then we model how these become blocked or channeled based on anthropogenic impediments. We use a wall-to-wall analysis to identify regional scale pinch points and blockage areas. In the second section, we identify intact areas with large temperature gradients that may be important in facilitating local range shifts among many species. We use a moving window analysis in combination with a downscaled temperature model to highlight these places. The two approaches are complementary and reveal different aspects of the Northeast landscape.

Introduction

The term "range shift" refers to the colonization of new geography by a species through dispersing juveniles, propagules, seeds, eggs, or adults. A successful colonization requires that the species locate, establish, and reproduce in a new territory, and that their offspring reproduce. Thus, range shifts are a population process that occurs over generations, and species populations are constantly adjusting their distributions in response to local and regional conditions.

Climate change can cause range shifts through changes in mean climate, short-term climate extremes, or interactions with other species. However, understanding and predicting range shifts is complex, in part because species tolerances are not fixed. Davis and Shaw (2001) reviewed tree taxa shifts in latitude or elevation in response to changes in Quaternary climate, and stressed the complexity of climate changes. Summer and winter temperature, seasonality, and the distribution and amount of precipitation, all changed in different ways that produced new combinations of climate. They questioned the assumption that taxa disperse seed and establish in new regions more readily than they evolve a new range of climate tolerances, or even that the tolerance range for a species remains stable given wide intraspecific variation.

In spite of the complexities, it is clear that over the last two decades many species have shifted their geographic distributions toward higher elevations and latitudes in response to climate change. Evidence of this is strong and consistent across many taxa groups and across several continents (Chen et al. 2011). Upslope movement has been documented for over 1,000 species and appears to be greatest among plants and herptiles, followed by mammals, invertebrates, and fish (Table 2.1). Indeed, with the exception of birds, the evidence for significant upslope migrations now seems overwhelming regardless of the position along latitudinal or elevational gradients (Lenoir et al. 2010). Northward movements have also been well

Table2.1 Summary of elevational and latitudinal observed range shifts from 30 studies (Modified from Chen et al. 2011). ORS = observed range shift, SE = standard error. "Margin" refers to whether the studies focused on changes in the upper leading margin or average distribution. The list of sources for Chen et al 2011 may be found at http://www.sciencemag.org/content/333/6045/1024/suppl/DC1

Observed Elevational Range Shifts

Taxa group	# of Species	Margin (Upper / Average)	Duration (yrs.)	Mean ORS (m)	Min ORS (m)	Max ORS (m)	SE of ORS (m)	Temp change (C)	# Studies
Invertebrates	554	U/A	20-42 yrs.	37.7	7.4	108.6	12.3	0.62	5
Fish	15	U	25 yrs.	32.7	32.7	32.7	12.7	0.65	1
Herptiles	30	A	10 yrs.	65.3	65.3	65.3	24	0.24	1
Birds	326	A/U	11-25 yrs.	-4.75	-19.3	7.6	9.3	0.795	4
Mammals	37	U/A	25-88 yrs.	50	31	69	71.6	3.05	2
Plants	495	U/A	22-94 yrs.	62.4	21	89	16.2	0.97	7

Observed Latitudinal Range Shifts

Taxa group	# of Species	Margin	Duration (yrs.)	Mean ORS (m)	Min ORS (m)	Max ORS (m)	SE of ORS (m)	Temp change (C)	# Studies
Invertebrates	332	U	8-25 yrs.	59.1	7.9	104.2	15.9	0.6	3
Fish	15	U	25 yrs.	47.2	47.2	47.2	15.4	0.65	1
Birds	361	U/A	12-31 yrs.	24.2	3.6	46	19	0.49	4
Mammals	9	U	25 yrs.	22.4	22.4	22.4	38.4	0.45	1
Algae	37	A	50 yrs.	61.4	61.4	61.4	31.6	0.74	1

documented for 754 species across many taxa groups particularly algae, invertebrates, fish, mammals, and birds (Table 2.1). Recent meta-analysis of over 51 studies of elevational and latitudinal range shifts for various taxonomic groups suggest values ranging from 6.1 m to 11.0 m upslope, and from 6.1 km to 16.9 km northward (Chen et al. 2011, Parmesan and Yohe 2003, Lenoir et al. 2008). In most places, upslope range shifts are more likely than latitudinal shifts as elevational temperature gradients are steep and vastly greater than the latitudinal gradients. For example, in the tropics there is a 5.2°Cto 6.5°C decrease in temperature per 1000 m elevation, nearly 1000 times as much as the latitudinal rate of decrease (Colwell et al. 2008)

Current evidence makes a compelling case for upslope movement, but there is substantial variation in the data. Species showing downslope shifts, or no shifts, have been documented. An illustrative, non-comprehensive survey of such studies (Lenoir et al. 2010) suggests that about 65% of the species have shifted their mid-range positions upslope, 10% have not changed their mid-range positions, and 25% have shifted their mid-range positions downslope. According to a global review of the literature (Parmesan and Yohe 2003) about 20% of the species have adjusted their ranges towards lower elevations or southern latitudes. Recent papers have demonstrated a direct link between temperature change and range shifts (Chen et al. 2011), but other factors create variation in species response: competitive release, habitat modification, or changes in precipitation regime, snow cover duration, water balance, or seasonality.

Current climate change differs from historic climate change because humans have modified the landscape, fragmenting habitats and disrupting natural movements. These modifications create resistance that may prevent species from colonizing new habitat creating instead a range constriction. Our goal in modeling range shifts was to understand where species would likely move if there were no anthropogenic resistance, and then to add in the resistance and identify where the pinch points, blockages, or flow concentration areas occur. Accordingly, we modeled species range shifts in response to climate change in four compounding ways in order to fully understand the fourth integrated response:

1. **Anthropogenic**
2. **Upslope**
3. **Upslope and Northward**
4. **Upslope and Northward with Anthropogenic Resistance**

The anthropogenic model is based solely on human-modified barriers such as roads and development and the resistance they create. The upslope model uses land position and slope to simulate where species will move to get the greatest temperature change with the least amount of effort. Species in this model may move in any direction as long as they are going upslope. The upslope and northward model directs species movement northward while still modeling upslope movement. Species in this model may move upslope, northward, or both. The final integrated model, combines the resistance from human modifications with the upslope and northward model. In this model, the flow of species in an upslope or northward direction is channeled around areas of high resistances identifying pinch points or diffuse areas of high flow.

Circuitscape Model

All modeling of estimated species movement was done using Circuitscape (McRae and Shah 2009), an innovative software program that models species and population movements as if they were electric current flowing through a landscape of variable resistance (see McRae 2006; McRae and Beier 2007; McRae et al. 2008; Shah and McRae 2008). Circuit modeling recognizes that movement through a landscape is affected by a variety of impediments (resistances) and quantifies the degree to which these impediments will affect movement and the directional outcomes of the compounding effects.

The Circuitscape program calculates the amount of "current" moving directionally across a landscape based on an input grid of cells with values indicating their degree of "resistance." One output of the program, a current map, shows the behavior of directional flows, analogous to electric current flowing across a surface with varying levels of resistance. Like water moving across an uneven watershed, the flow of current over the resistance surface results in patterns of high and low concentrations very similar to the rills, gullies, braided channels, eddies, and main channels associated with flowing water. The program's ability to highlight flow concentration areas and pinch-points make it particularly useful for identifying key linkages for permeability. Concentration areas are easily recognized in the Circuitscape output by their high current density.

We used Circuitscape to generate comprehensive flow density surfaces using two approaches that both create a continuous surface: 1) wall-to-wall and 2) moving window. The wall-to-wall approach tends to highlight regional patterns and is discussed first. The moving window approach (as we applied it) highlights local patterns within a 10 km window.

Anthropogenic Resistance Grid

In a Circuitscape analysis, the current flows across the landscape through a resistance grid, with lower resistance being more permeable and higher resistance less permeable. The grid we used for anthropogenic resistance was land cover, but in theory resistance can be any factor that impedes movement (in later examples we use slope as well). When based on land cover, obstructions to species movement are assigned high resistance scores based on the degree to which they impede movement.

In the Circuitscape program, the landscape is converted into a graph, with every cell in the landscape represented by a node (or a vertex) in the graph and connections between cells represented as edges in the graph with edge weights based on the average resistance of the two cells being connected (Shah and McRae 2008). The program performs a series of combinatorial and numerical operations to compute resistance-based connectivity metrics, calculating net passage probabilities for random walkers passing through nodes or across edges. Unlike a least cost path approach, Circuitscape incorporates effects of multiple pathways, which can be helpful in identifying critical linkages where alternative pathways do not exist (McRae and Beier 2007). More detail about the model, its parameterization, and potential applications in ecology, evolution, and conservation planning can be found in McRae and Beier (2007) and McRae and Shah (2009).

In developing an anthropogenic resistance grid, we applied a weighting scheme to the 2011 National Land Cover Database (NLCD, Jin et al. 2013) such that natural lands had the least resistance, agriculture, or modified lands had more resistance and developed lands had the highest resistance (Table 2.2). The NLCD is the most recent national land cover database for the United States and it is mapped at a 30 meter scale. For Canada we used the Agriculture and Agri-food Canada Annual Crop inventory (AAFC 2013, Fisette et al. 2013). This is the most recent land use dataset for Canada, also at 30 meter resolution, and created through a methodology similar to the NLCD (satellite interpretation). It is primarily used for crop identification, but also includes information on water, barrens, shrublands, wetlands, and forests. We visually compared AAFC crop dataset with current aerial photos and older land use data to confirm its accuracy, and we matched the resistance weights in Canada with those in the US (Table 2.3)

Our assumption was that the resistance between cells increases with their contrast to natural land. Contrasting elements, like development or agriculture, were considered less permeable because of differences in structure, surface texture, chemistry, temperature, or exposure. Wildlife and plants do cross various landscape elements, but sharp contrasts such as forest adjacent to developed land disrupts movement because an animal may prefer to avoid the risk inherent in the crossing more exposed habitat or a plant may fail to establish in the new environment. The three basic landscape elements were as follows:

Natural lands: landscape elements where natural processes are unconstrained and unmodified by human intervention such as forest, wetlands, or natural grasslands. Human influences are common, but are mostly indirect, unintentional, and not the dominant process.

Agricultural or modified lands: landscape elements where natural processes are modified by direct, sustained, and intentional human intervention. This usually involves modifications to both the structure

(e.g. clearing and mowing), and ecological processes (e.g. flood and fire suppression, predator regulation, nutrient enrichment).

Developed lands: landscape elements dominated by the direct conversion of physical habitat to buildings, roads, parking lots, or other infrastructure associated with human habitation and commerce. Natural processes are highly disrupted, channeled or suppressed. Vegetation is highly tended and controlled.

Table 2.2. The National Land Cover Database (NLCD 2011) Attributes. This table shows the available attributes and the resistance score assigned to the land cover category. Resistance scores range from "1," no resistance to "20," very high resistance

Landcover Code in NLCD (if Applicable)	Landcover description	Resistance	Source
21	Developed, Open Space	8	NLCD 2011
22	Developed, Low intensity	8	NLCD 2011
23	Developed, Medium Intensity	9	NLCD 2011
24	Developed, High Intensity	20	NLCD 2011
31	Barren Land, non-natural	9	NLCD 2011
32	Barren Land, natural	1	NLCD 2011
41	Deciduous Forest	1	NLCD 2011
42	Evergreen Forest	1	NLCD 2011
43	Mixed Forest	1	NLCD 2011
52	Shrub/Scrub	1	NLCD 2011
71	Herbaceous	1	NLCD 2011
81	Hay/Pasture	3	NLCD 2011
82	Cultivated Crops	7	NLCD 2011
90	Woody Wetlands	1	NLCD 2011
95	Emergent Herbaceous Wetlands	1	NLCD 2011
11	Open Water, Shoreline Distance <200 m	1	NLCD 2011
11	Open Water, Shoreline Distance 200-400m	3	NLCD 2011
11	Open Water, Shoreline Distance >400 meters	5	NLCD 2011
	Major Roads	20	Tiger 2014
	Minor Roads	10	Tiger 2014
	Transmission Lines	9	Ventex 2014
	Pipelines	9	Ventex 2014
	Railroads	9	ESRI 2009
	Unpaved Roads /Tracks	1 point added to the above score	OpenStreet Map 2014

Table 2.3. The Agriculture and Agri-food Canada (AAFC 2013) Annual Crop Inventory. This table shows the available attributes and the resistance score assigned to the land cover category. Resistance scores range from "1," no resistance to "20," very high resistance

Landcover Code in AAFC	Landcover Description	Resistance Value
20	Water	1,3,5
30	Exposed Barren	9
34	Urban/Developed	9
36	Greenhouses	9
50	Shrubland	1
80	Wetland	1
110	Grassland	1
122	Pasture/Forages	3
120 – 199 (except 122)	Agriculture (This maps one of 52 crops (e.g. Barley, Potatoes) or undifferentiated cropland, fallow, or too wet for seeding.	7
200	Forest (undifferentiated)	1
210	Coniferous Forest	1
220	Broadleaf Forest	1
230	Mixedwood Forest	1

Although the 2011 NLCD and the 2013 AACF Crop Inventory were the most current datasets available, we made several improvements to them that substantially improved their performance as resistance grids. These included: 1) updating the roads and railroads, 2) adding transmission line data, 3) adding dirt roads, 4) reclassifying barrens, and 5) reclassifying water polygons.

All of the NLCD products (2011, 2006, and 2001) have an older, inaccurate roads layer burned into them from the Bureau of Transportation Statistics. These roads do not line up with the more commonly used and more accurate Tiger Road dataset (US Census 2014). To correct for this, we removed the older roads from the dataset using the following steps. First, cells in the developed open space class (which contains the roads) were shrunk by one pixel in order to remove linear road pixels, but not the larger actual developed open space areas. Values for these cells were replaced with the majority value of the surrounding pixels. Next the Tiger Roads dataset was "burned in" on top of the NLCD, greatly improving the spatial accuracy of the roads data set. We also burned in the latest railroad layer from ESRI (Tele Atlas North America, Inc., 2009)

We added in the location of transmission lines to the NLCD and AACF datasets. For this step we obtained access to power industry GIS data (Ventyx 2014), which was used with permission through a TNC agreement. We selected all transmission lines in service by voltage class, and all in-service natural gas pipelines. These were incorporated into the land cover dataset using power industry standard right of way widths: transmission lines less than 230 volt = 30 meter width, greater than 230 volts = 180 meter width, and all pipelines = 30 meter width (Duke Energy 2014). We compared the dataset to aerial photos, confirm that these widths were reasonable and to ensure that we added only features that left a distinguishable footprint on the ground.

Dirt roads or unpaved forest management roads are unevenly mapped in both the NLCD and AAFC datasets, even though they may create substantial road networks in some parts of the region. To map unpaved roads we used data from OpenStreetMap (2014) which is an open source global dataset built by a community of mappers that contribute and maintain data about roads and trails. We extracted roads tagged as "track" which includes roads for mostly agricultural use, forest tracks, etc., and are usually unpaved but may include paved roads suitable for two-track vehicles such as tractors or jeeps. This dataset excludes trails and paths that are not wide enough for a two-track vehicle. Although the quality and consistency of this dataset is not known, visual inspection suggested that it was more comprehensive than any other available dataset for mapping unpaved roads. Grid cells were assigned an extra resistance point for if they contained one or more unpaved roads (for example the resistance of hay/pasture with track roads increases from a "3" to a "4").

In the NLCD dataset, the land cover category "barrens" often included misclassified developed lands such as oil and gas well heads or airport runways. To distinguish natural barrens (e.g. beaches and summits) from highly developed barrens (e.g. airport runways). We used a spatial analysis of the land cover types in a 100 m buffer surrounding each cell of barrens to separate barrens associated with industry or commercial development from barrens associated with bare rock, exposed beach, lake shorelines, and other natural settings. Although we may have missed small anthropogenic barrens surrounded by forest, visual inspection of the enhanced dataset, with barrens classified into natural and non-natural, suggests that we fixed the more egregious errors.

Finally, we created a variable weighting for waterbodies following methods in Anderson et al. (2014). This weighting adjusts the resistance score of "open water" to reflect the size of the water body based on the assumption that large waterbodies are a greater impediment to the movement of terrestrial species than small ponds or headwater streams. To create the weighting, we selected all water pixels in the NLCD, converted the pixels to polygons, and buffered inward 200 and 400 meters. We assigned water within 200 m of shoreline a resistance value of "1" (natural), water between 200 and 400 meters of shoreline was given a resistance value of "3", and water greater the 400 meters from shoreline was given a value of "5" The final values assume there is no barrier effect from a small stream but a large lake creates a moderate barrier to species movement (Figure 2.1).

All improvements to the land cover grid were performed on the 30 meter grid cells and integrated with the NLCD and AAFC into one dataset (Figure 2.2). For the Circuitscape analysis, processing limitations required us to coarsen the data to 150 meter cell resolution which we did using the "aggregate" function by mean in Arctoolbox.

Figure 2.1. Waterbodies and the zones used in the resistance weighting. Waterbodies are shown in blue on the figure with darker blues indicating higher resistance at 0-200, 200-400, and 400+ meters.

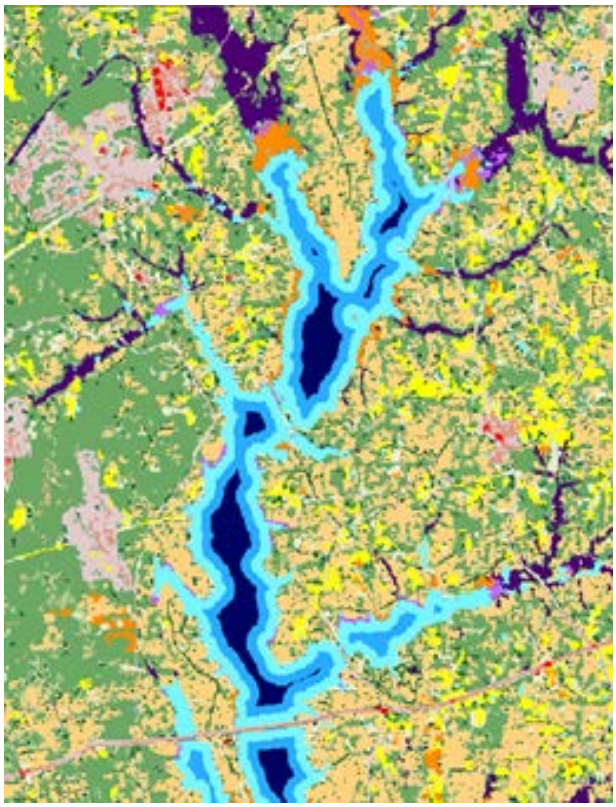

Figure 2.2. Anthropogenic resistance grid used in the Circuitscape analysis. The figure shows improved and integrated land cover map with each cell reclassified to its assigned resistance score.

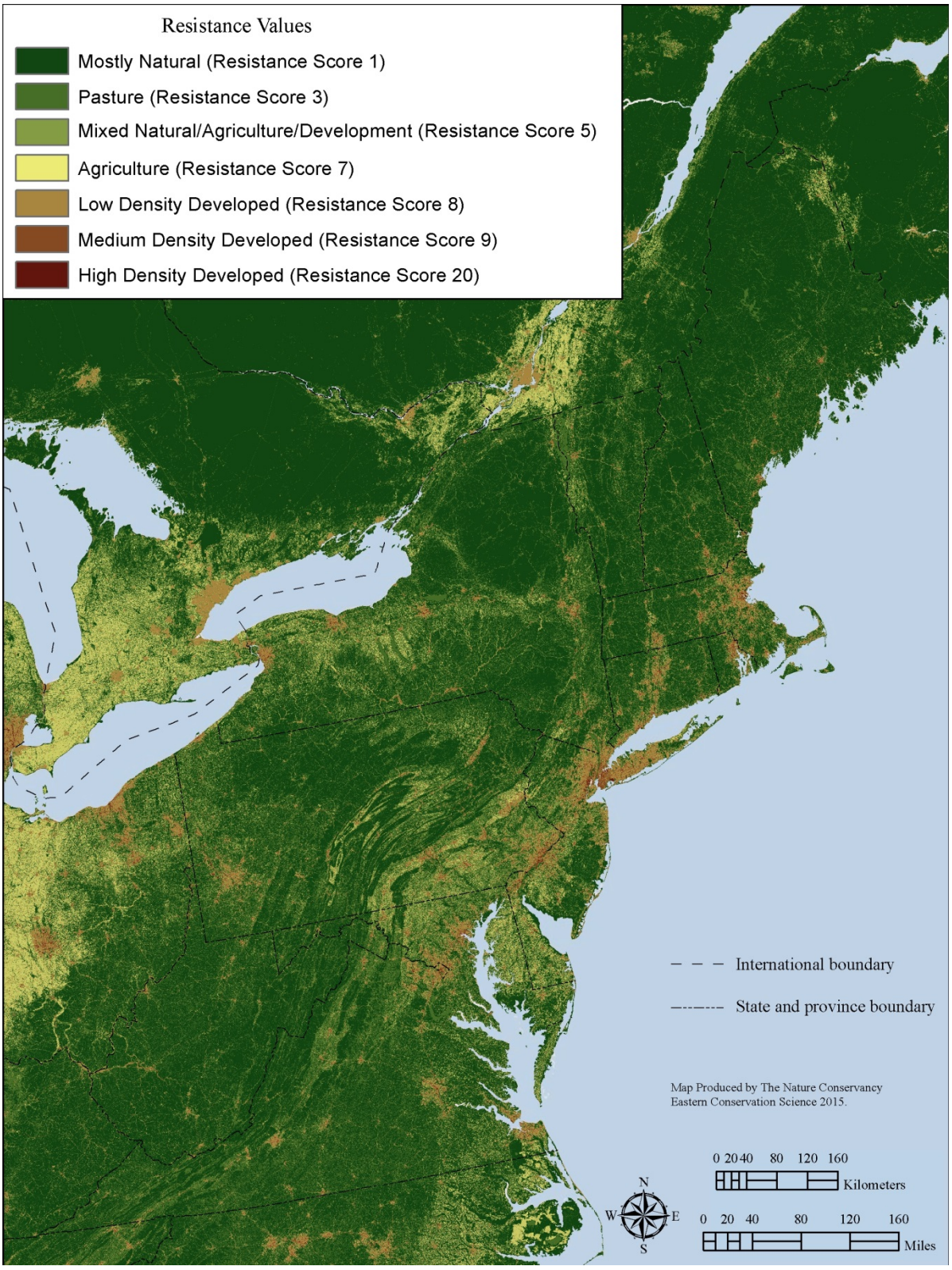

Wall-to-Wall Model: Anthropogenic Resistance Only

Circuitscape was originally designed to function in a point-to-point or patch-to-patch fashion, calculating resistance-based connectivity metrics from one focal area to another. As discussed previously, this approach can limit the utility of assessing connectivity over very large areas, in highly fragmented systems, or in evaluating climate change response where there may be so many habitat patches of interest that assessing connectivity among all possible combinations is prohibitive. To overcome these conceptual and practical limitations, we used a minor adaptation of the Circuitscape model that allows for the creation of omnidirectional connectivity maps illustrating flow paths and variations in the ease of travel across a large study area. Our methods are described in Anderson et al. 2013 and Pelletier et al. 2014, and we review them briefly below. Essentially, to obtain complete wall-to-wall coverage of the region we ran the model in gridded landscape tiles where one whole side was assigned to be source and the other side the ground, repeating the run for each of four directions: east-west, west-east, north-south, south-north, and then summing the results. This method gave stable and repeatable results for the central region of each tile, which we then clipped out and joined with other tile centers to create a continuous grid. All calculations were performed on the latest version of Circuitscape (4.0) with a cell size of 150 meters.

To run the analysis, the study area was divided into 54 tiles – or calculation areas –comprised of 3200 cells by 3200 cells (~ 480 kilometers), and each tile was intersected with the resistance map. The analysis was run for all tiles with complete land cover information, but tiles that were solely water were ignored.

Next, within each tile we identified a focus area that was one quarter the size of the total calculation area (Figure 2.3). We used only this central focus area because the results in this region stayed consistent even as the calculation area increased. This eliminated the margin of the calculation area, which appeared, based on many trials to have considerable noise created by the starting points.

Figure 2.3: Diagram of tiles used in Circuitscape. The image on the left shows the focus area in comparison to the calculation area. The image on the right shows how current is injected from every cell on the source (on the left) and can flow to any cell in the ground (right).

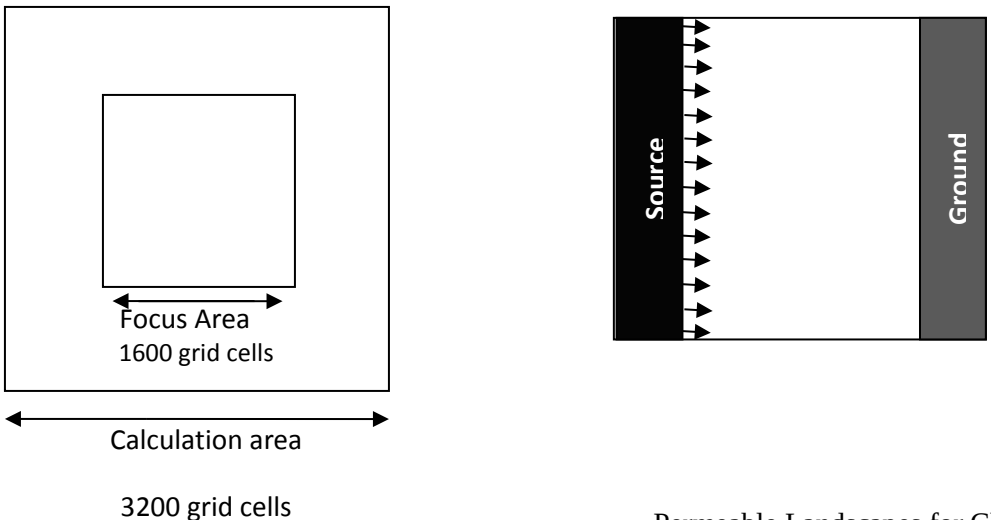

Third, we ran Circuitscape for each of the 54 calculation areas. To calculate the resistant surface, we set one side of the square to be the source and the other side area to be the ground (Figure 2.3). Current was injected into the system from each grid cell on the source side of the square. Because current seeks the path of least resistance from the source cells to any grid cell on the ground side, a run with the west edge as source and the east side as ground will not produce the same current map as a run with the east edge as source and west edge as ground. To account for these differences, we ran the program for all four of the direction possibilities - west to east, east to west, north to south, south to north, and summed the results.

To inject current in the coastal tiles, where a proportion of the tile is filled by Ocean or Great Lake we used a new method developed by Jeff Cardille of McGill University (personal communication, December 2015). We created a random raster with the same mean and standard deviation as the land resistance and replaced the large waterbodies (Ocean and Great Lake) with this random raster on the resistance grid. When current is injected along the "water" side of the tile it runs equally along the grid until it encounters a shoreline, allowing for equal current flow potential for coastal areas. In earlier runs (Anderson et al. 2012) we had assigned the two waterbodies a resistance weight slightly higher than the average land average. This encouraged current to follow from the oceans onto the land, but there was still a slight preference for the current to enter the land in the closest point possible. The new method corrected this problem.

Lastly, the focus area was clipped out of each calculation area and joined together to create a continuous coverage of results for the region. To normalize the scores across tiles, a cell of overlap was retained between all adjacent focus areas. Starting with the center focus area of the study area, the overlap between a center focus area and its neighboring focal area were compared (they should be in theory the same since they are the same area). The neighboring cell's score was then adjusted so the overlapping areas had the same mean score. This was repeated for all cells starting at the center and working outward in a starburst pattern. This created a more seamless surface than our previous method (Anderson et al.2013) of using a standard normal transformation (Z-scores) to convert focus areas to the same scale and then joining the focus areas together (Figure 2.4). That method had minimized differences between areas that had very different mean score such as a largely agricultural focal area adjacent to a largely natural focal area.

The model using only anthropogenic resistance revealed three basic patterns in the current flow reflecting how the human modified landscape is spatially configured (Figure 2.5): 1) Low flow (brown) indicates areas low permeability and many blockages to movement, 2) diffuse flow (yellow) are highly permeable areas where natural cover is intact and thus current can spread out, and 3) concentrated flow (dark green) are places where flow accumulates or is channeled through a pinch point. The results suggest important linkages where species movement is estimated to become concentrated, and form the anthropogenic resistance layer we later integrate with the upslope and moving window models.

Figure 2.4: Edge Mapping Overlap. The figure on the top shows the artifacts of tiling on the middle bottom tile. The bottom figure shows the same tile with the edge artifacts smoothed out.

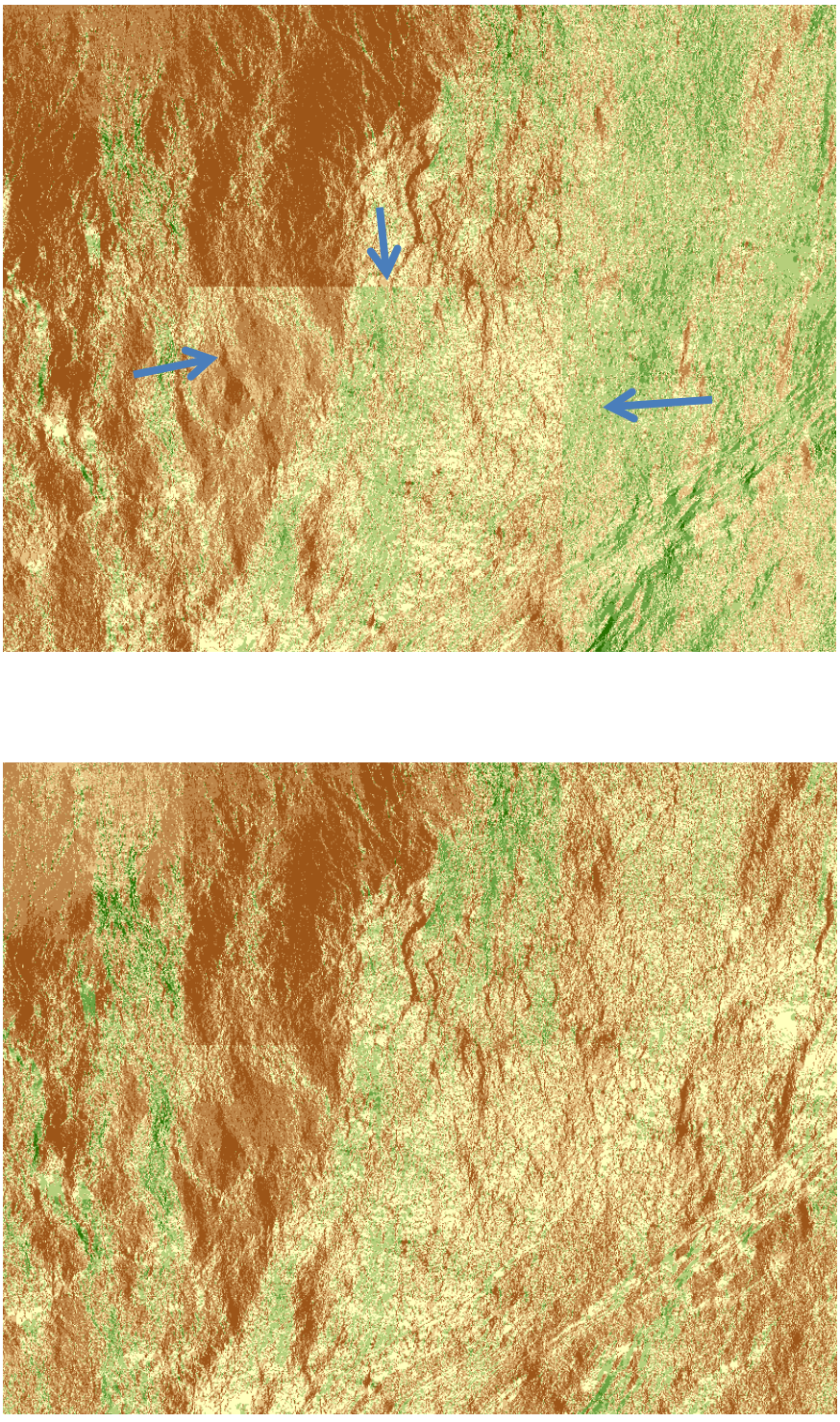

Figure 2.5. Results of the wall-to-wall Circuitscape model applied to the anthropogenic resistance grid. Brown indicates areas with low permeability where movement may be blocked. Yellow indicates areas of moderate flow; often highly natural settings were species movements are diffuse. Green indicates areas of concentrated flow where movements will accumulate or be channeled through a pinch point.

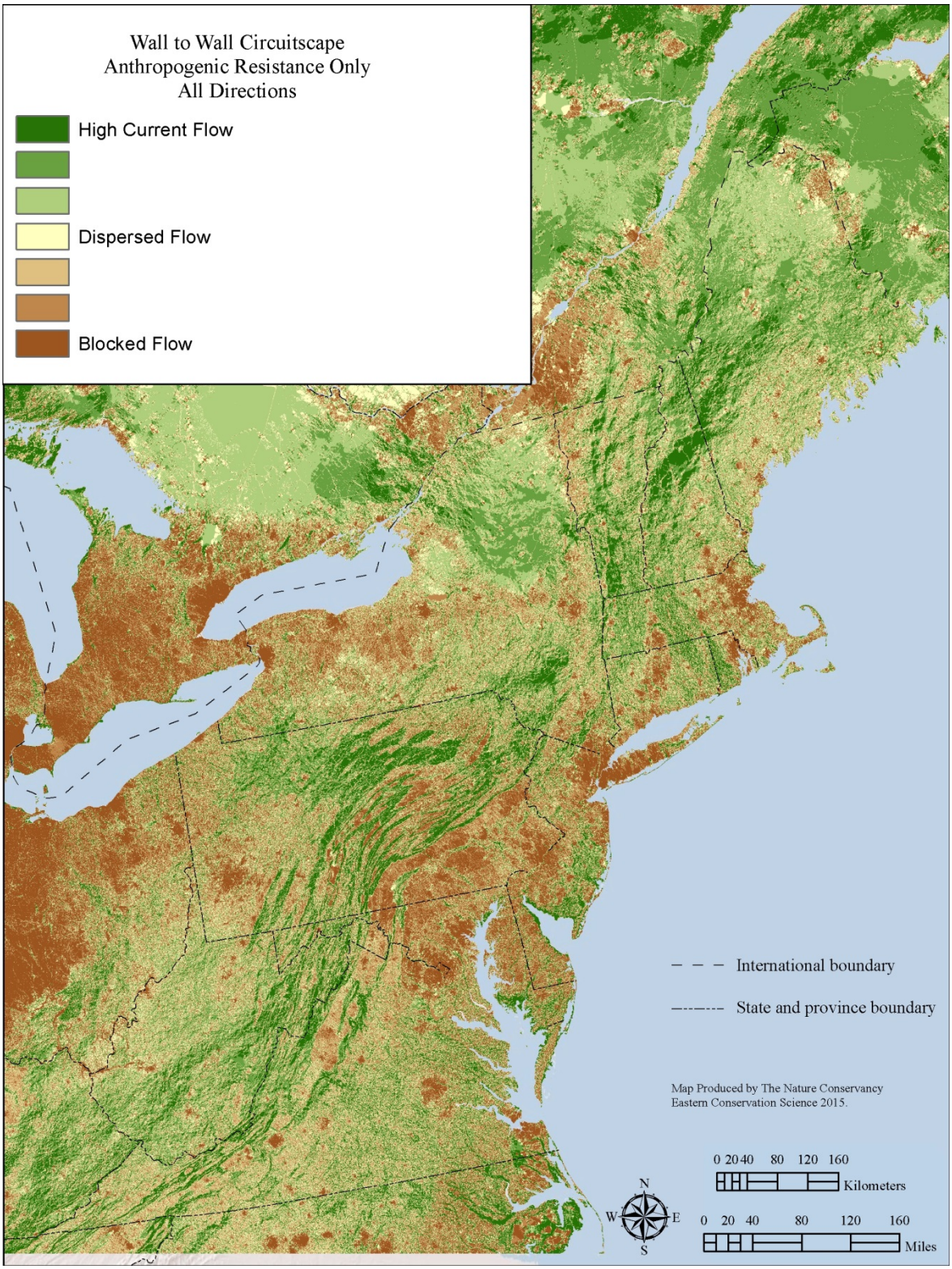

Wall to Wall Model: Upslope and Northward for Range Shifts

The evidence for species distributions shifting in response to climate change suggests that populations are already moving at impressive rates: 1.1 m (3.6 ft.) upslope per year and 1.7 km (1.1 miles) northward per year (Table 1). Theoretically, a plant or animal population with a leading edge ending on the banks of the Charles River in Boston might appear on top of Beacon Hill or northward halfway to the New Hampshire border in just 20 years. In one century the populations could occur north of Portland, Maine, or have already topped the summit of Mount Agamenticus. Of course, there are many factors besides temperature determining where a species occurs and a riverbank species might not be able to tolerate the thin rocky soils of a mountaintop. However, temperature is a well-documented and well understood factor limiting the northward expansion of many species, even if other factors such as moisture and soil type determine where a species is found within its range. Paleoecological studies show that movement was a near universal response to past changes in climate (Pardi and Smith, 2012).

In this section we explore the implications of human modification of the landscape in light of this directional movement driven by temperature change. Our objective was to model northward and upslope movements as if there were no human modification, than integrate the resistance layer and re-run the model to identify key pinch points, barriers, flow concentration areas, and facilitating landscapes. Our essential question was: if species populations are tracking temperature changes by moving upslope and northward, then how and where does the fragmented human-dominated landscape impede such movement? The wall-to-wall Circuitscape approach is well suited to exploring this question because it assumes that every cell in the region is a starting point for some species and the directional thrust upslope and northward can be thought of in terms of electrical sources and grounds, or as resistance. “Movement” in this case matches the conceptual foundation of the wall-to-wall approach because it refers to a population tracking a set of changing conditions, as opposed to moving between fixed patches of suitable habitat.

To get to our final results, we broke the model into three parts. First we developed a fine-scale model to simulate upslope movement. Second we added latitudinal direction to the upslope model by setting the “sources” and “grounds” to a North-South direction. Third we added in the anthropogenic resistance grid to identify how the directional pathways intersect with the human uses.

The upslope model was created using a 30 m continuous landform model (Anderson 1999, Anderson et al. 2012), which in turn is based on a cell’s relative land position and slope. We converted this to a resistance grid by first isolating the relative land position value and assigning increased resistance to moving downslope and decreased resistance to moving upslope. Current injected into this grid will flow upslope to the highest land position. Next, we modified the resistance score using the cell’s slope value, to reflect the relative degree of effort versus gain in temperature differences. For example, moving upward along a gentle slope is easy but provides little gain in temperature differences (moderate resistance), moving upward along a moderate slopes provides larger gains in temperature differences for moderate effort (low resistance), moving upward along a steep slopes is too difficult for most species in spite of the temperature gains (high resistance) (Figure 2.6). We combined the land position and slope into one resistance score that scales the model such that a theoretical species would move upslope preferentially along areas of moderate slope where they would experience the greatest temperature differences relative to effort (Table 2.4, Figure 2.6, and Figure 2.7).

Figure 2.6. Conceptual model of how a species population (black arrows) might move upslope and northward over five generations.

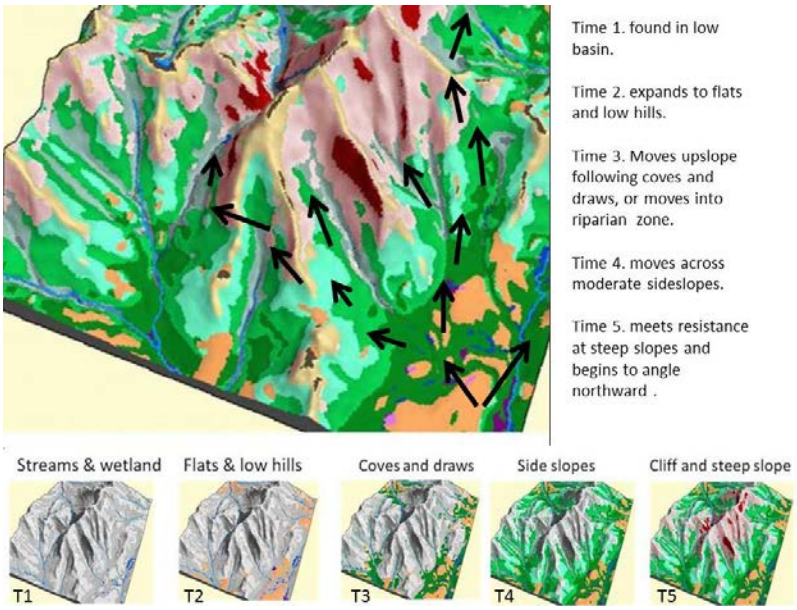

Table 2.4. Resistance Scores applied to the Landform Model. Land position ranks (LP_rank) were ordered so they decrease towards higher land positions. Slope ranks (S_rank) were ordered so that they increase at the extremes of no slope (no temperature gain) and steep slopes (too difficult to transverse) and are lowest at moderate values (most gain for least effort.).

Landform	code	Slope	Position	LP_rank	S_rank	Sum	Weight
Slope crest	13	3mod	highest	1	1	2	1
Ridgetop	12	2gentle	highest	1	4	5	2.5
N-sideslope	23	3mod	high	4	1	5	2.5
S-sideslope	24	3mod	high	4	1	5	2.5
Flat summit	11	1flat	highest	1	7	8	4
hill/gentle slope	22	2gentle	high	4	4	8	4
Lower side	33	3mod	low	7	1	8	4
Hilltop flat	21	1flat	high	4	7	11	5.5
Valley/toeslope	32	2gentle	low	7	4	11	5.5
N-cove	43	3 mod	lowest	10	1	11	5.5
S-cove	44	3 mod	lowest	10	1	11	5.5
Dry flat	30	1flat	low	7	7	14	7
Wet flat	31	1flat	low	7	7	14	7
Slopebottom	42	2gentle	lowest	10	4	14	7
Slopebottom flat	41	1flat	lowest	10	7	17	8.5
Steep slope	4	4 High	any	NA	9	18	9
Cliff	5	5 Highest	any	NA	10	20	10

Figure 2.7. The resistance scores applied to the landform model. This picture shows a three dimensional model of Mt Mansfield in Vermont. The left image shows the landform model with the low land position flats in purple and blue, mid land position and moderately sloped sideslopes in green, and high position and steep sloped steep slopes and cliffs in orange and red. The second image shows the resistances where low resistance corresponds to areas with the most temperature gain for the least effort (moderately steep sideslopes). Flat valley bottom flats and steep slopes have higher resistance

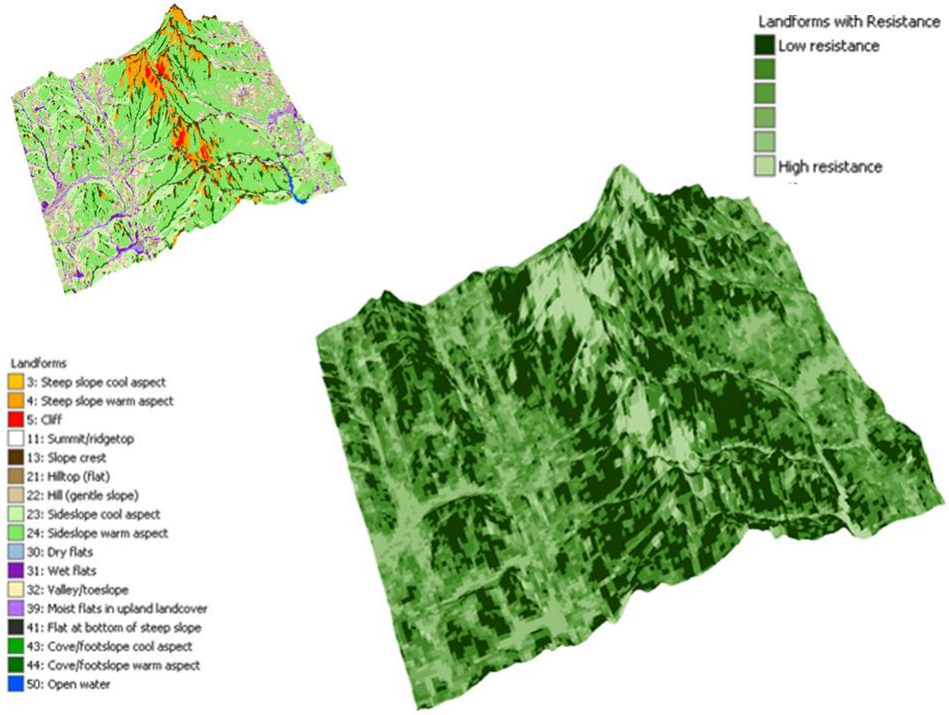

Results: Upslope and Northward

The Circuitscape analysis on the landform-based resistance grid shows how the areas with high potential for upslope range shifts are arranged within the region (Figure 2.8). The regional patterns broadly emphasize the Appalachian Mountains, but the detailed output also highlights local occurrences of moderate slopes (Figure 2.9). The high flow areas on the map are important because the rate of current climate change is faster than the historic rate and the moderate slopes offer the easiest access to meaningful temperature gradients (Corlett and Westcott 2015).

Adding anthropogenic resistance to the upslope analysis results in a 2-way integrated map (Figure 2.10) that shows a much more compressed picture than anthropogenic resistance alone, highlighting the dissected landscape of the Cumberland Mountains, the ridges of the Central Appalachians, and a broad linkage from the New Jersey highlands northward through the prongs of the White and Green mountain of Vermont and New Hampshire (Figure 2.10). The east side of the Adirondacks and the east side of the Connecticut River Valley are also highlighted.

In our next analysis, we added North-South directionality to the upslope model by limiting the "source" and "ground" inputs of current to the South-North axis. This analysis approximates a species population expanding both northward and upslope thus simulating the general response of most taxa to a warming climate (Figure 2.11 and 2.12). Not surprisingly this map is similar to the upslope map but emphasizes linear north-south running topographic features like the Appalachian Mountains and it also highlight north-south linkages across more resistant areas like the Mohawk valley between the Catskills and the Adirondacks.

For the final analysis of this section we created a 3-way integrated map that combines 1) anthropogenic resistance with the 2) upslope model using 3) North-South directionality (Figure 2.12). At the scale of the whole region significant flow concentrations are centered along the spine of the Green and White Mountains all the way to the Gaspe Peninsula in the Northern Appalachian ecoregion, and in the northern and southern portions of the Central Appalachian ecoregion (Figure 2.13). The map further emphasizes the importance of the Appalachian Mountain chain in facilitating range shifts.

In order to examine finer-scale patterns we stratified the 3-way results (Figure 2.12) by ecoregion (Figure 2.15 and see 2.26 for ecoregion map) in effect scaling the results within each individual region to identify ecoregionally significant flow concentration areas. For example, in the North Atlantic Coast ecoregion the Pine Barrens region of New Jersey, Eastern portion of Long Island, and coastal margin on central Connecticut are highlighted as areas of high flow (Figure 2.15).

It is possible that the 3-way integrated map gives to much weight to latitudinal North-South flows. In most places, local upslope range shifts are more likely than latitudinal shifts as elevational temperature gradients are steep and much greater than the latitudinal gradients (Colwell et al. 2008). If this is the case then the 2-way model of upslope with anthropogenic resistance (Figure 2.10) may give a more accurate picture of important linkages. When the maps are compared (Figure 2.13) the differences are not dramatic but smaller complexes of slopes in the High Allegheny and Cumberland Mountains have more flow in the 2-way model, and the very high scores of the Central and Northern Appalachians are muted. A zoom-in of the Mohawk Valley between the Catskills and the Adirondacks (Figure 2.14) is instructive. The upslope and resistance model (bottom left) emphasizes the importance of the sloped landforms crossing the valley that probably offer the most temperature change to species in the dryer flat areas. In the 3-way model (bottom right) there is so much northward pull because of the Catskill-Adirondacks linkage that the entire valley has average flow even the dry flat areas. Perhaps the movement of poor dispersers is similar to the 2-way model while populations of better dispersers are more similar to the 3-way model.

Figure 2.8. The Upslope Model. This figure shows the results of a wall-to-wall Circuitscape analysis applied to a resistance grid derived from landforms. There is no anthropogenic resistance shown.

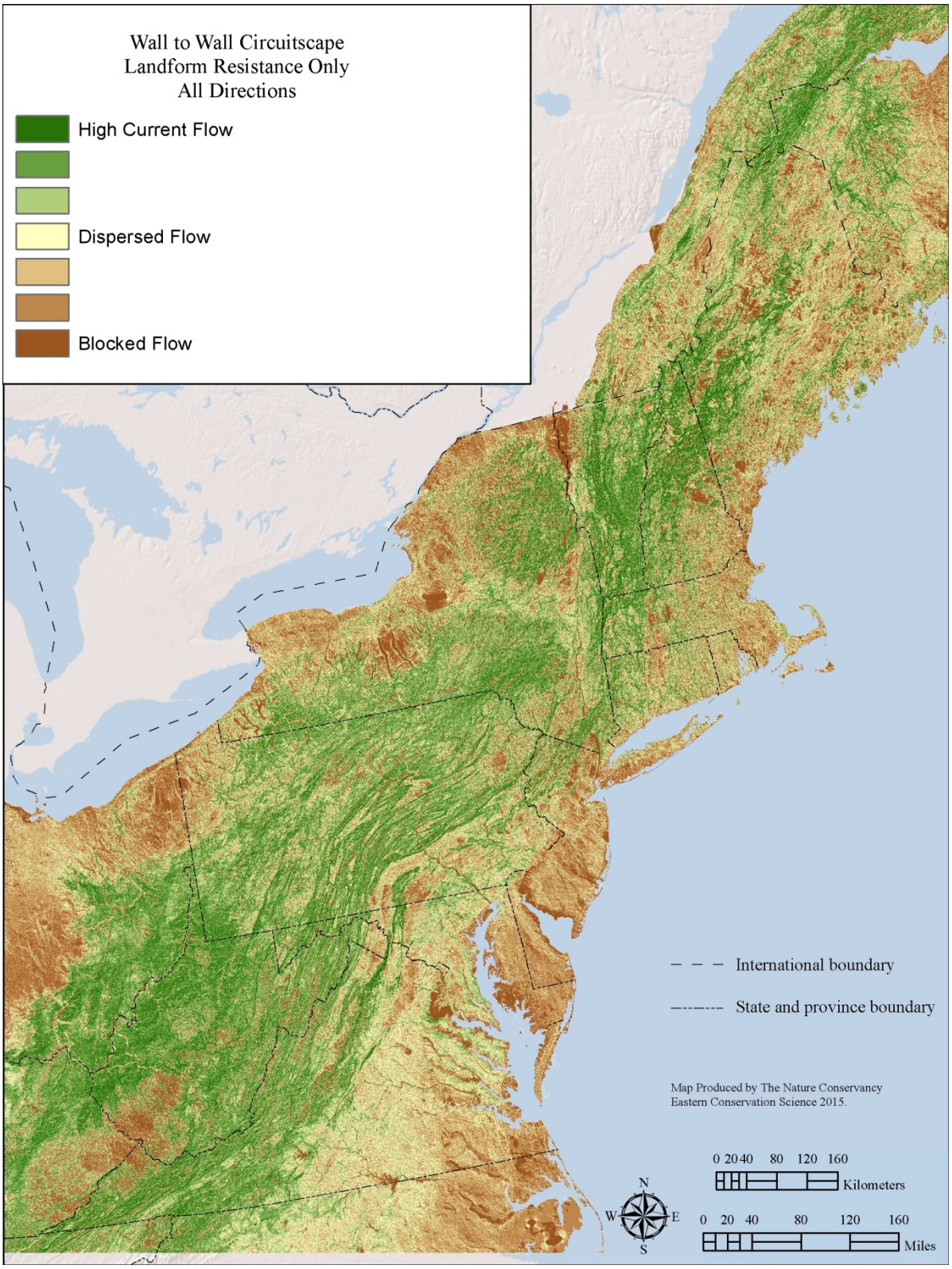

Figure 2.9. Zoom-in of the Upslope results (Figure 2.8) for the Mohawk Valley between the Adirondacks and Catskills, NY. Areas of high current flow are expected to be important channels of upslope movement

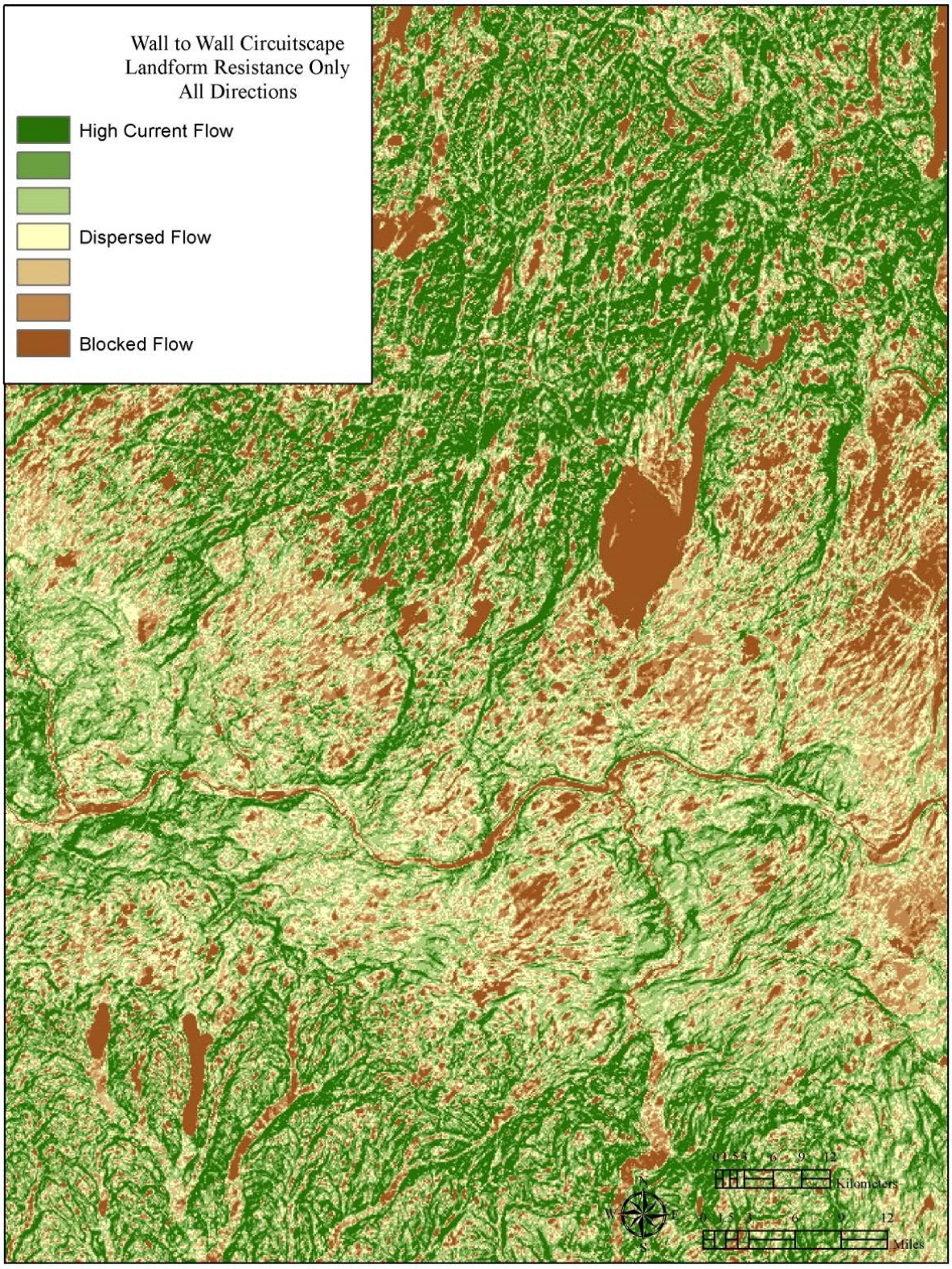

Figure 2.10. The Upslope Model with Anthropogenic Resistance. This figure shows the results of a wall-to-wall Circuitscape analysis applied to a resistance grid derived from landforms and anthropogenic resistance. Areas of high current flow are predicted to be important for upslope range shifts AND because human fragmentation patterns also channel flow through these areas

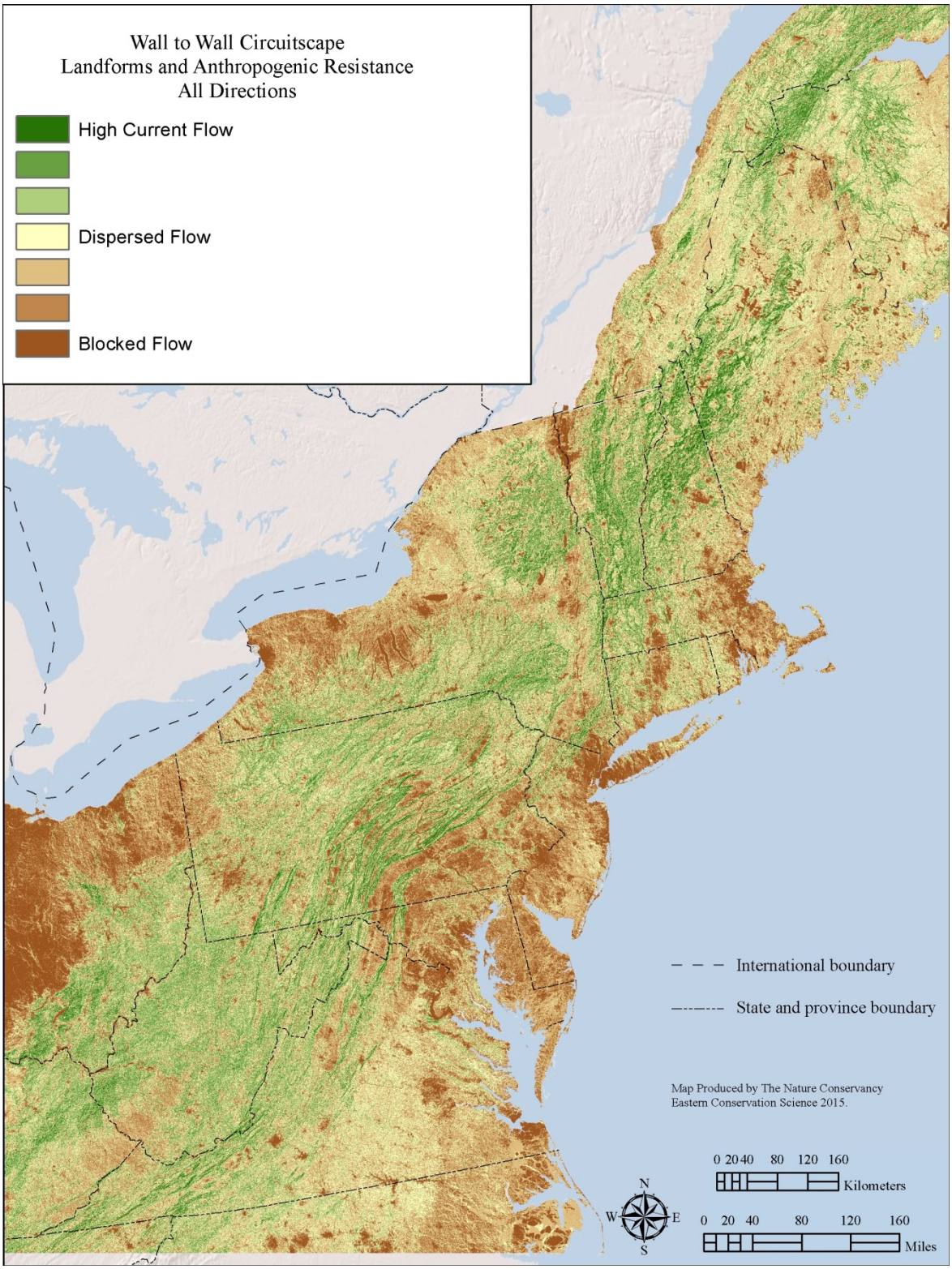

Figure 2.11. Upslope and Northward with No Anthropogenic Resistance. This map shows the results of a wall-to-wall Circuitscape analysis applied to a resistance grid derived from landforms, and run only for the North-South direction. Areas with high current flow are predicted to be important for facilitating upslope and northward range shifts.

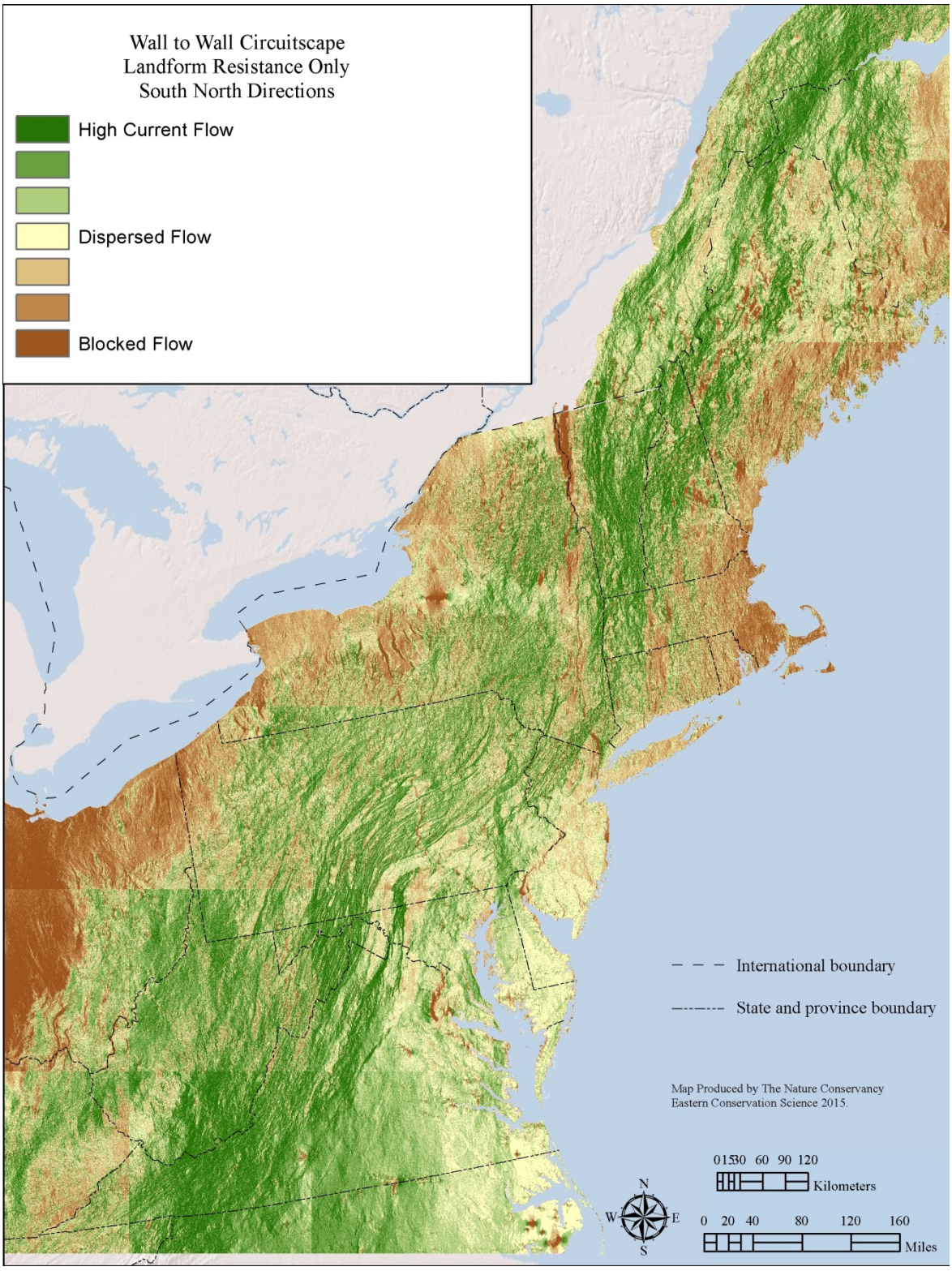

Figure 2.12. Upslope and Northward with Anthropogenic Resistance. This map shows the results of a wall-to-wall Circuitscape analysis applied to a resistance grid derived from landforms, and run only for the North-South direction. Areas with high current flow are predicted to be important for facilitating upslope and northward range shifts.

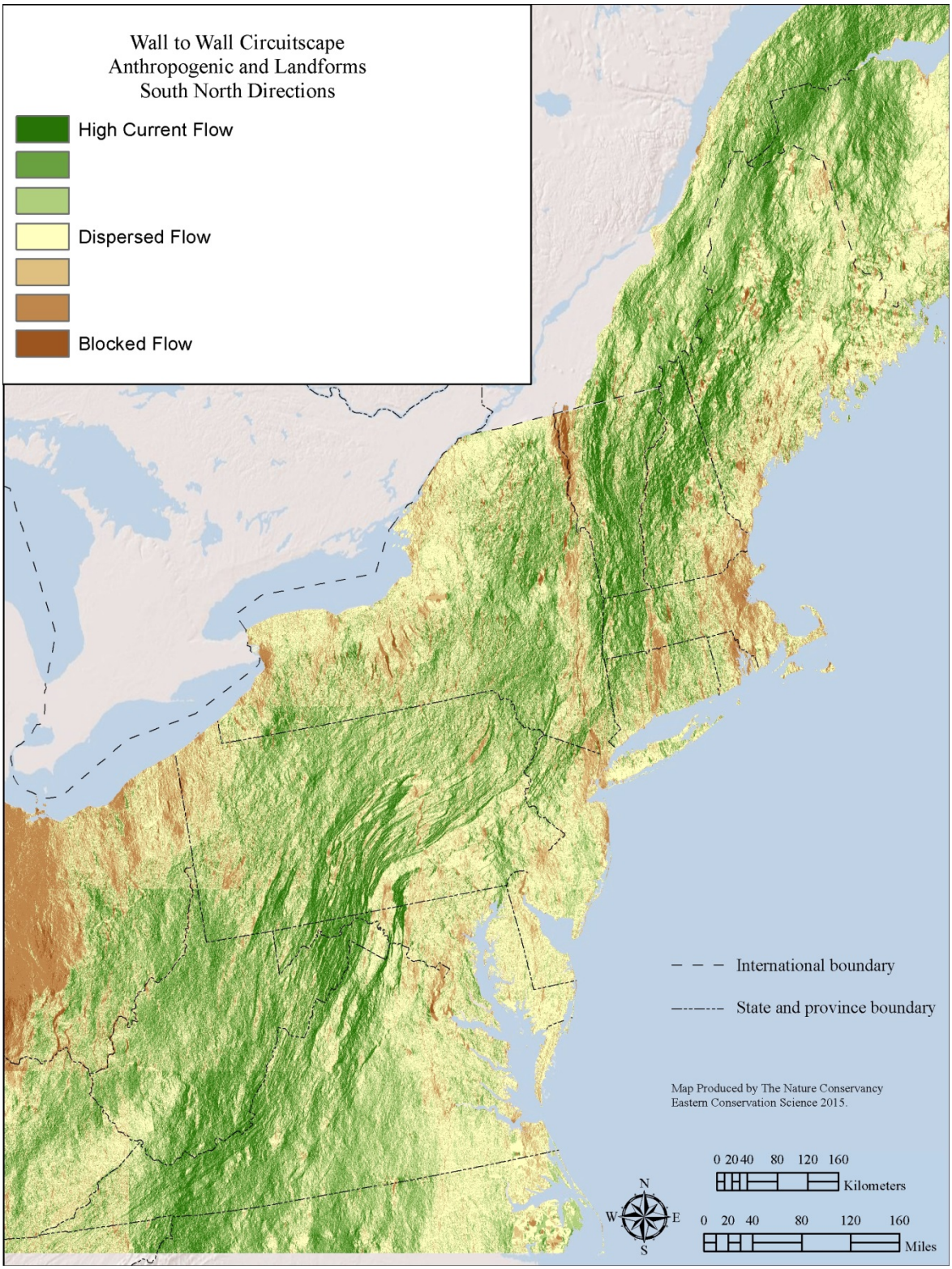

Figure 2.13. Comparison of Results: Upper maps are single variables. Lower maps show the 2-way (c) and 3-way (d) models. Arrows were added by hand to emphasize trends.

a. Anthropogenic Resistance Only

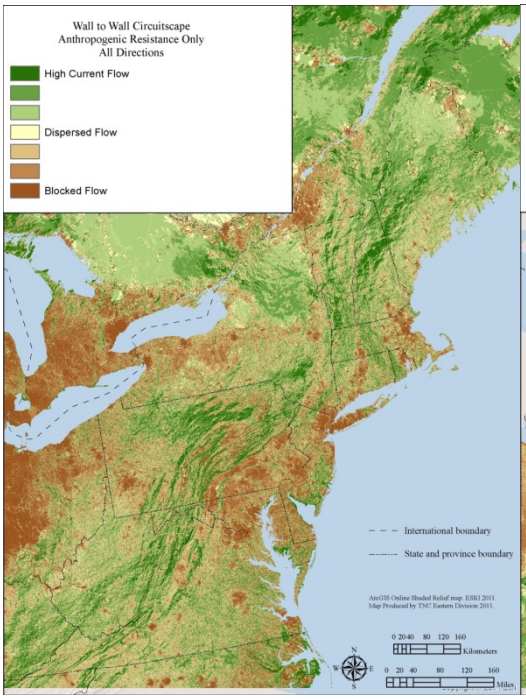

b. Upslope Only

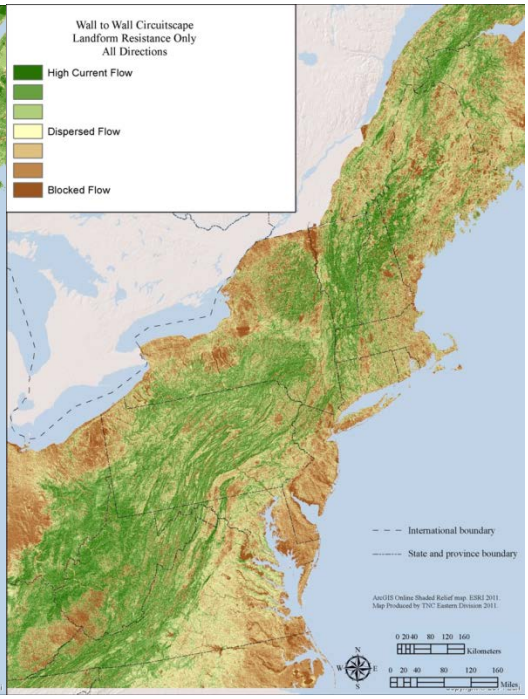

c. Upslope + Resistance

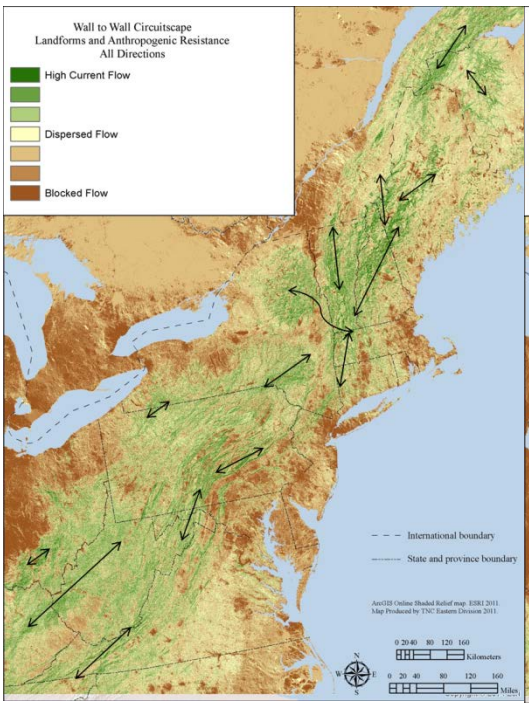

d. Upslope+ Northward+ Resistance

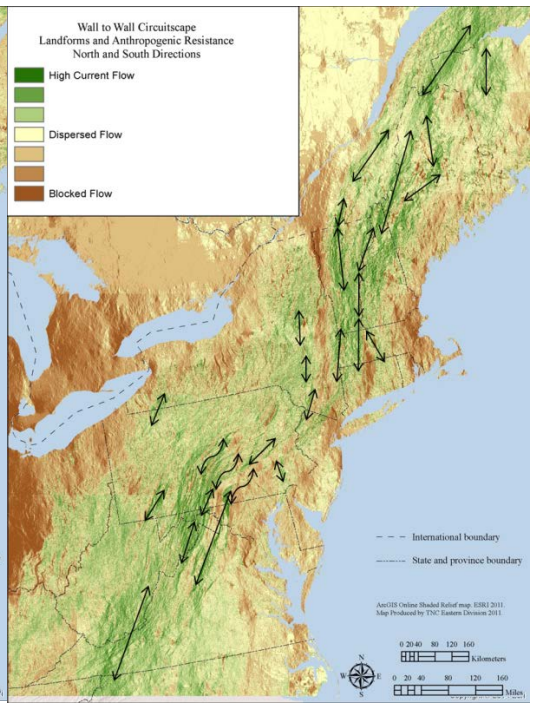

Figure 2.14. Comparison of Results –Zoom in. Maps focus on the Mohawk Valley in New York between the Catskills in the south and Adirondacks to the north. The upper maps are single variables. Lower maps show the 2-way (c) and 3-way (d) models.

a. Anthropogenic Resistance Only

b. Upslope Only

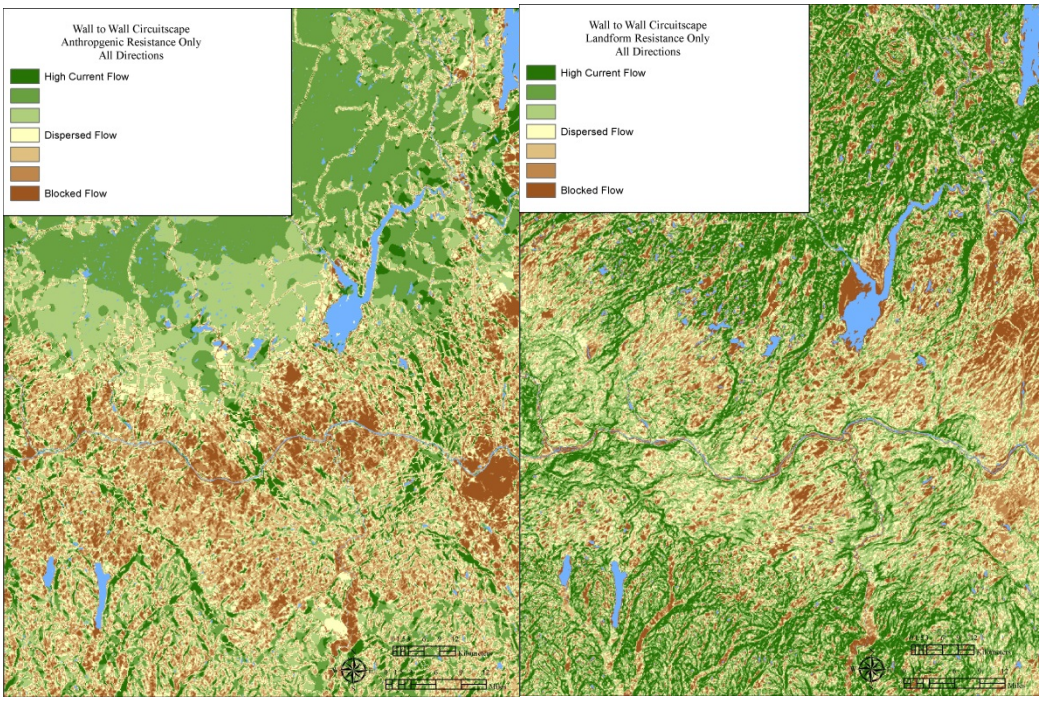

c. Upslope + Resistance

d. Upslope+ Northward+ Resistance

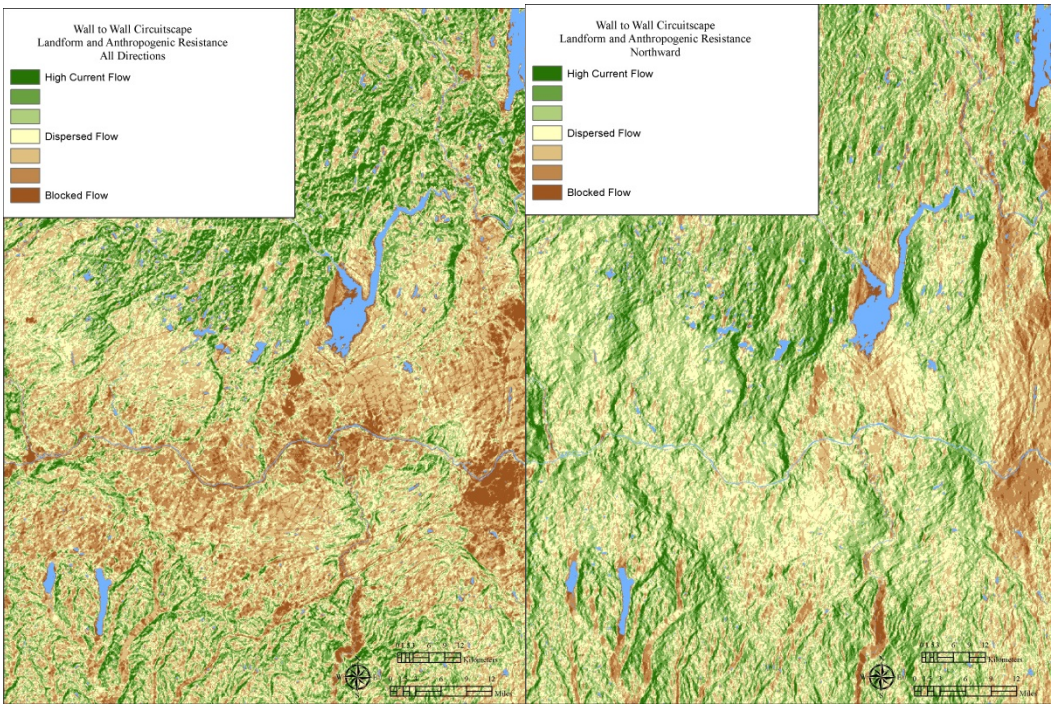

Figure 2.15. Upslope and Northward with Anthropogenic Resistance stratified by Ecoregion. This map shows the results of a 3-way wall-to-wall Circuitscape analysis using 1) the upslope model, 2) a North-South directional axis, and 3) the anthropogenic resistance grid. Areas with high current flow are predicted to be important for facilitating upslope and northward range shifts.

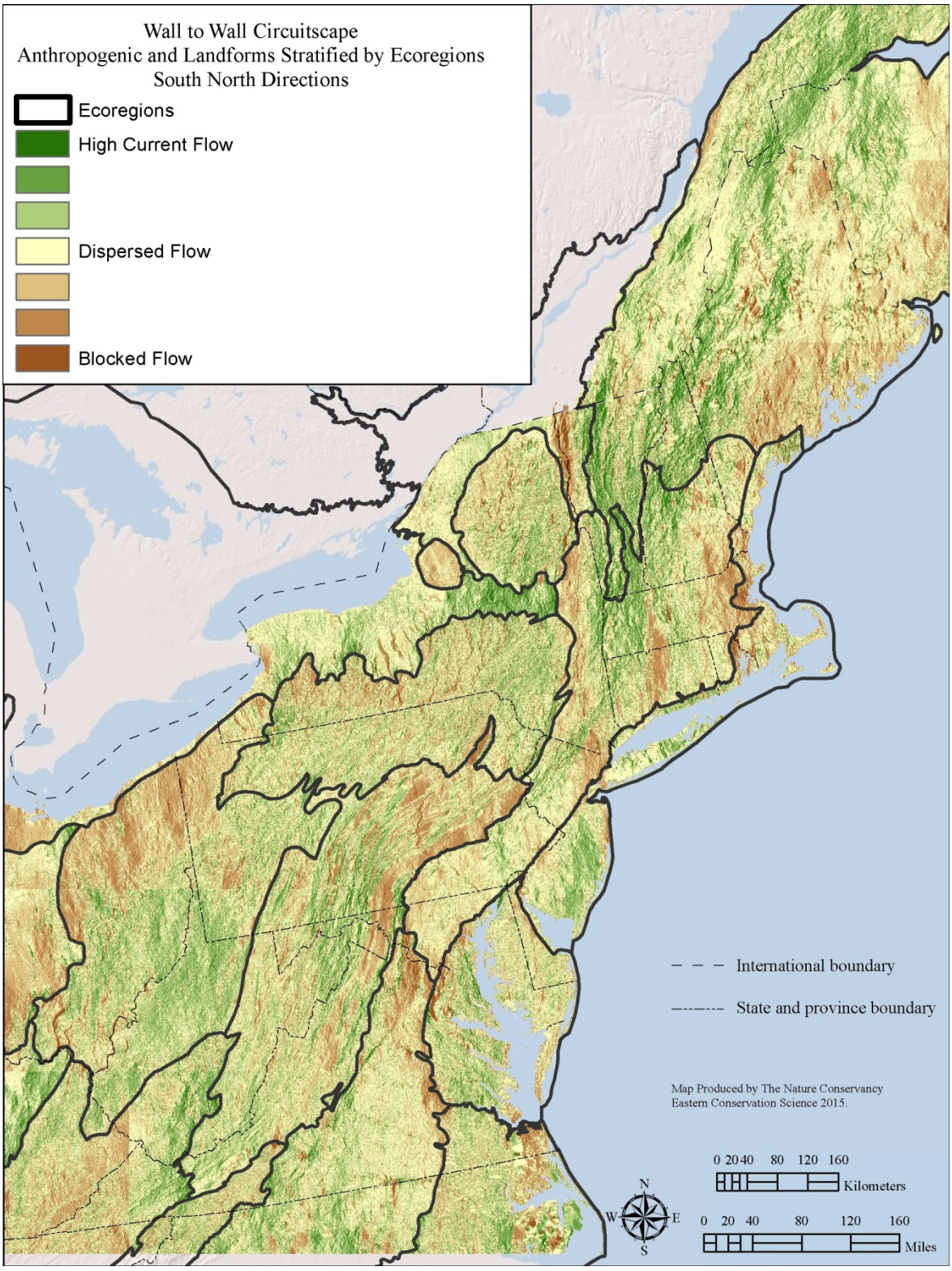

Moving Window Model for Local Range Shifts

The goal of this section was to model locally intact natural areas containing many climate gradients. These areas will likely be important for wildlife and plants responding to climate change because species can move within these areas to find cooler temperatures. The approach shares similarities with the climate-resilient sites identified by Anderson et al. (2014) which identified locally connected areas with high microclimate diversity using the latter as a proxy for climate options. Both approaches are concerned with connected areas with many climate options, but in this study we look specifically at a single variable – temperature – and we model temperature gradients at a much larger scale (10 km) appropriate to population range shifts. In contrast, the Anderson et al. microclimate diversity metric evaluates landform-based temperature and moisture combinations at a very local scale (0.4 km^2) appropriate to species persistence at sites.

The moving window approach connects natural areas to one another in a way that models movement from warm to cool areas. The method was inspired in part by the work of Nuñez et al. (2013), which modeled corridors connecting large blocks of natural land across temperature gradients. A key assumption is that although there is considerable uncertainty about the magnitude of climate change in different areas, temperature gradients are likely to be conserved. In other words, areas that are cooler than neighboring areas today will be cooler than neighboring areas in the future, even as all areas become warmer.

The approach also shares similarities with the riparian climate corridors discussed in the next chapter which identifies intact floodplains with long climate gradients. A major difference between the two is that the riparian corridors have simple linear climate gradients while the moving window approach measures climate gradients radiating out in all directions from a central point. To measure these temperature gradients we first had to create a downscaled temperature model using a 30 m digital elevation model (DEM), and then combine the temperature grid with the anthropogenic resistance grid described in the previous section.

This work differs from Nuñez et al. (2013) in two major respects. First, Nuñez et al. required identifying discrete patches to connect. We wished to avoid delineating such patches because dividing the landscape into a binary representation of patch and matrix adds arbitrary decisions and parameters to the modeling process, and strongly influences connectivity modeling results (Carroll et al. 2010). Instead, we used a continuous, moving window that begins by creating a 10 km circle around each 30 m cell of land cover, connecting all natural pixels within the circle that differ in temperature, and scoring the central cell with a value that reflects the density of connect temperature gradients.

The second difference is that Nuñez et al. used least-cost corridor modeling to identify discrete corridors between patches. We used Circuitscape (McRae et al. 2013), which takes into account multiple pathways and also facilitates the creation of continuous connectivity maps (e.g., Anderson et al. 2012, Koen et al. 2014, Pelletier et al. 2014). Circuitscape treats landscapes as conductive surfaces and models current flow across them to identify important movement pathways, particularly pinch points where the loss of a small amount of habitat can disproportionately reduce connectivity.

Methods: Downscaled Temperature Model

Downscaling is a method to increase the resolution of a dataset by establishing statistical relationships between a large-scale variable of interest and a local-scale variable, then using the relationships to approximate a finer-scale model based in-part on the local-scale variable. In our model we begin with 800 m PRISM temperature data (PRISM Climate Group 2013) and downscaled it using a 30 m elevation model, based on the statistical relationship between temperature and elevation (Figure 2.16 and 2.17). We selected mean annual temperature because it is often used for temperature analysis and future predictions of climate (NRC 2010, Meehl et al. 2007, Hansen et al. 2010, Krosby et al. 2015), and correlates well with the distribution of many species.

PRISM data (PRISM Climate Group 2013) is one of the most widely used climate datasets for the US. It is based of weather station data and is itself downscaled to an 800 m cell size and peer-reviewed for accuracy and consistence. We compiled mean temperature for all months of the year normalized over the last 30 years. Methods to further downscale the 800 meter scale to a resolution more appropriate for local analysis have been developed and applied in the western US and are available in the Climate Western North America mapper. We used the same methodology (Wang et al. 2006, 2012) that allows for the downscaling of climate data using elevation, latitude, and longitude. The method uses combination of bilinear interpolation and elevation adjustment to downscale the baseline climate data to specific points of interest or a regional grid. We followed the method exactly as described in Wang et al. 2012, using the parameters and steps shown in Table 2.4. These steps are shown graphically in Figure 2.18 with a detailed area shown in Figure 2.19.

Table 2.4. Parameters and steps used to downscale the PRISM data following Wang et al. (2012).

Inputs:
800 m PRISM dataset, 30 meter DEM, 30 meter latitude, 30 meter longitude grid
STEPS

1. Convert the PRISM datasets to points
2. Use extract value to points to assign the Elevation, Latitude, latitude and Longitude to PRISM Points
1. Use the attribute table to calculate a spatial regression for Mean Annual Temperature (MAT) using all variable combinations.
2. Interpolate from the point values (using Spline) 30 meter values for Temperature and Elevation.
3. Take the 1st derivative of the regression equation to get change in MAT, which is the change in MAT between the splined value and the Interpolated value. Equation A is the regression equation. Equation B is the first derivative of Equation A.

Equations

A. MAT = 146.6 + 1.244 * xcord – 3.318 * ycord – 0.2274 * elev – 0.03058 * xcord * ycord – 0.002863 * xcord*elev + 0.005228*ycord*Elev +0.00006745*xcord*ycord*elev

B. Delta MAT = Delta Elev * (0.2274 + 0.002863*xcord + 0.005228*ycord + 0.00006745*

Caveats: Our downscaled data is highly correlated with elevation, and it does not take into account topography, aspect, moisture, slope, canopy cover or other aspects of microclimate diversity, and thus it smooth's out the local temperature variations important to resilience. The data is useful for estimating regional patterns, but will not correspond to actual measured temperature data at a given location.

Figure 2.16. Original 800 m PRISM data showing mean annual temperature for the Northeast US.

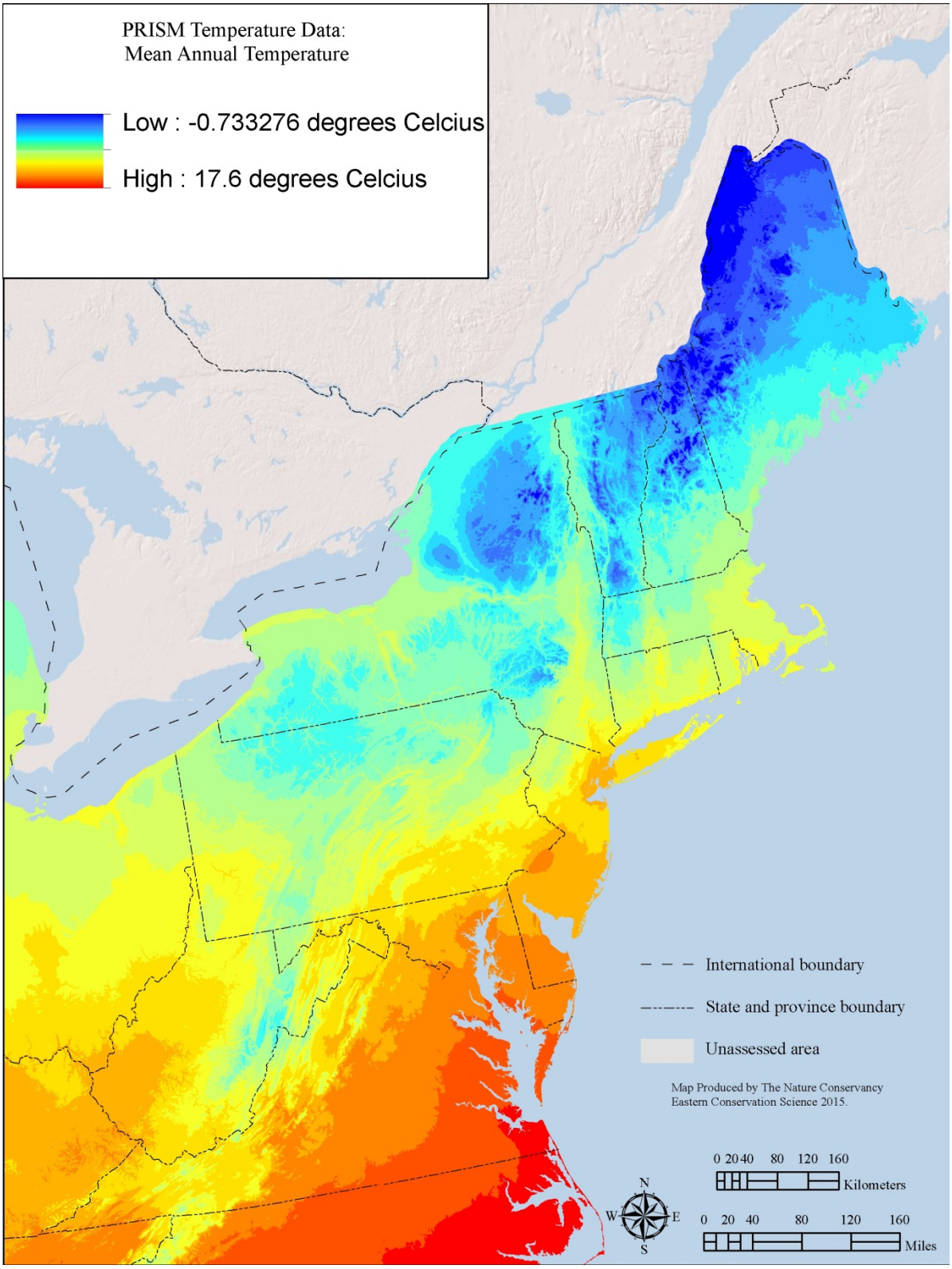

Figure 2.17: Downscaled PRISM data showing mean annual temperature for the Northeast US.

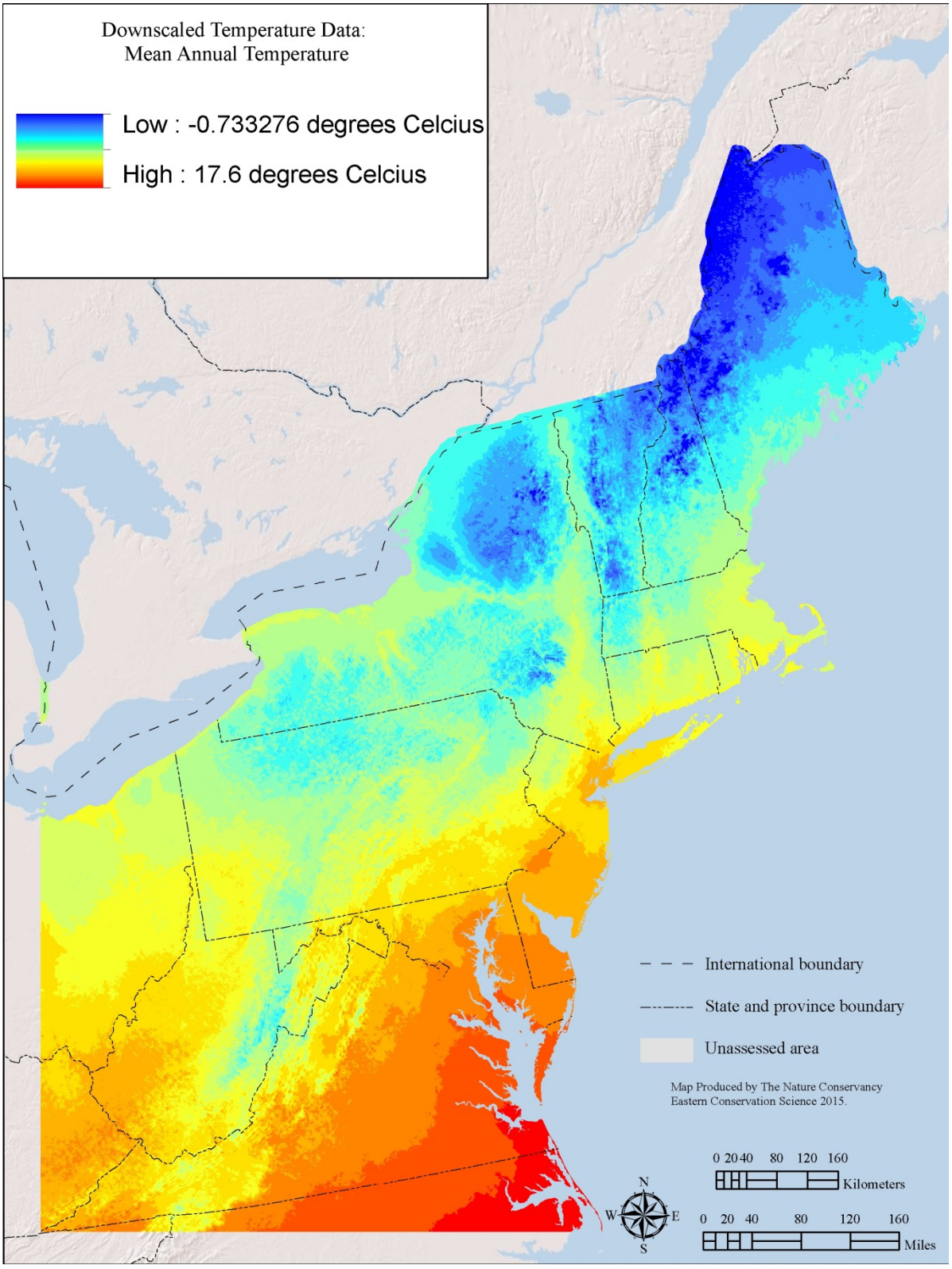

Figure 2.18 Effects of the downscaling process in the Hudson River Valley in NY. (A) DEM at 30m; (B) MAT generated by PRISM at 800 m; (C) interpolated MAT using spline interpolation; (D) elevation adjusted MAT using nearest data values from PRISM data and elevation adjustment function developed in Wang et al. 2012; (E) downscaled MAT using a combination of spline interpolation and elevation adjustment; (F) the downscaled MAT (E) overlaid on the DEM to show the trend of MAT along topography

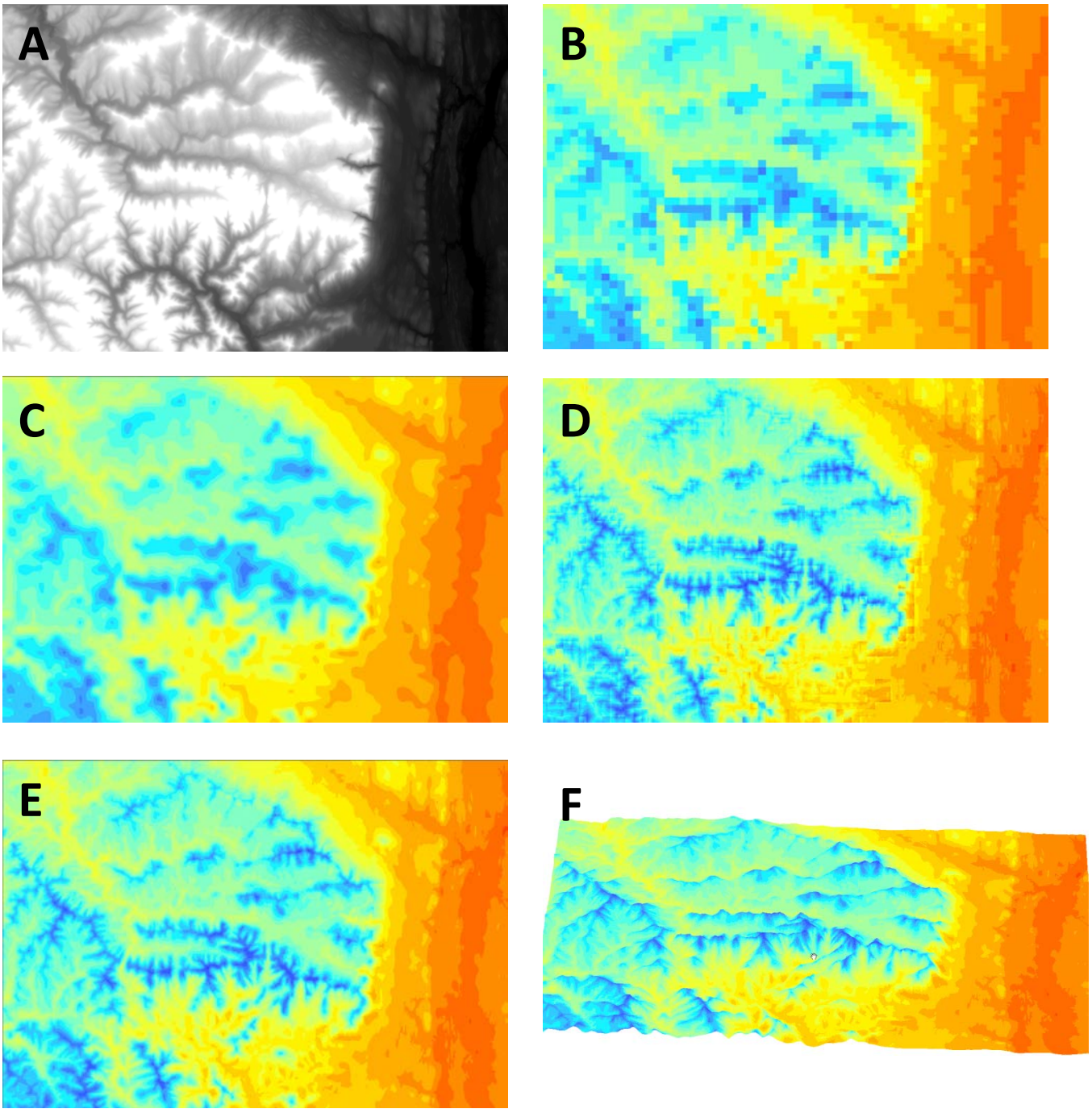

Figure 2.19: Zoom in comparing the PRISM 935 meter data with the downscaled 30 meter data. Figure A is the downscaled 30 m data. Figure B is the original 800 m data.

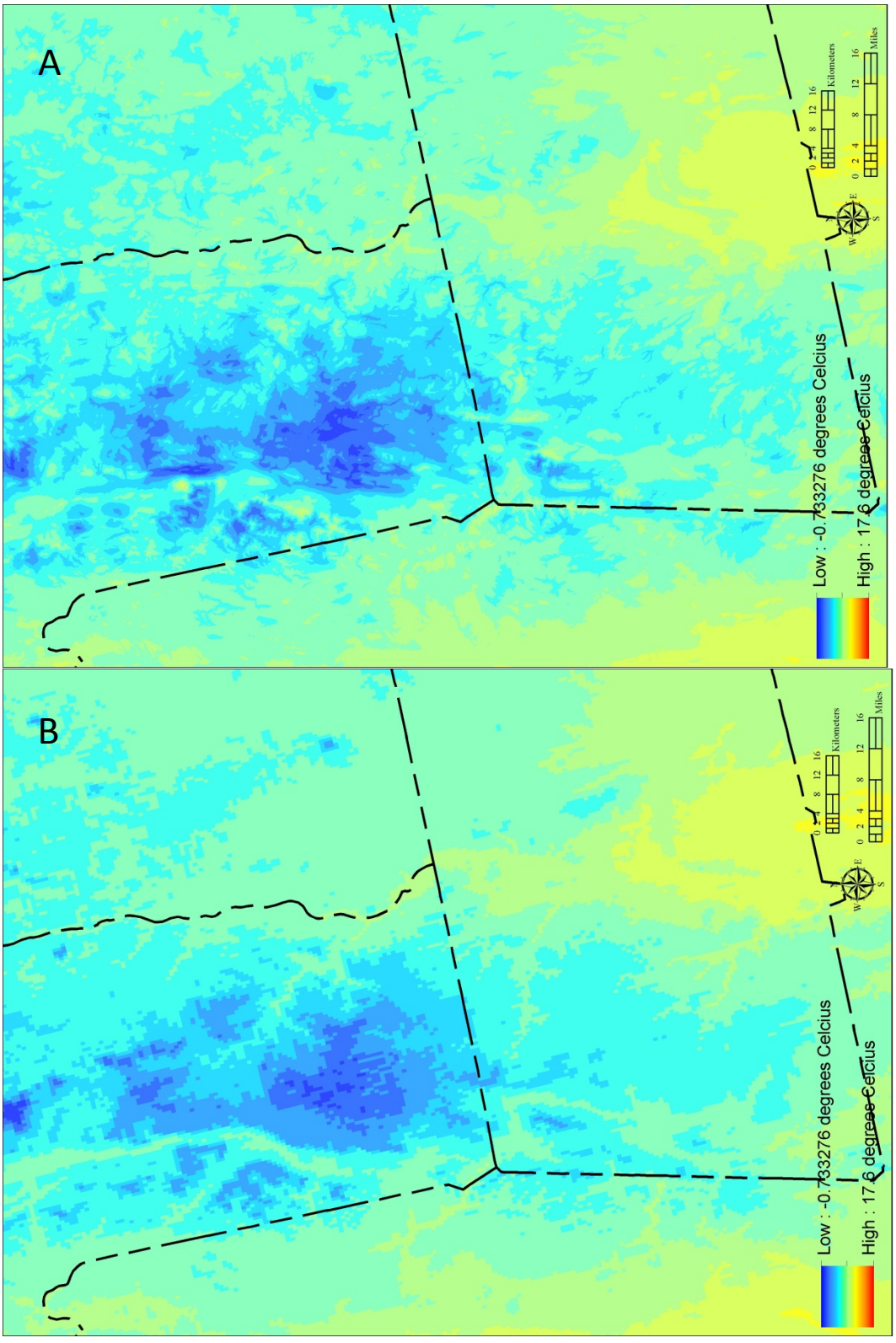

Methods: Moving Window Model

We modeled connectivity between natural pixels based on the same landcover-based resistance grid described in the previous section, although for this model, the resistance values were squared to create more differentiation between them. "Natural" pixels were those with a resistance of "1", reflecting sites that fell in natural land cover classes and had no roads, railroads, transmission lines, or pipelines running through them. The essence of the model was that within each 10 km window, all natural pixels were connected if their temperatures differed by a given threshold (Figure 2.20). We tested four temperature thresholds (T_{cutoff}) and these were 0.25^0, 0.5^0, 1^0 and 2^0 C (equal to 0.45^0, 0.90^0, 1.8^0, 3.6^0 F), and we ran an additional analysis with T_{cutoff} = to 0, i.e., connecting all natural pixels regardless of their temperatures.

In preliminary development of the method, we passed a circular moving window with a radius of 10 km across the study area. If the window centered on a natural pixel, we then connected all warmer natural pixels within 10 km to that pixel, provided they were warmer by at least T_{cutoff}. We did this by treating each warmer pixel within the radius as a source, with 1 Amp of current injected into each, and with current flowing to the (cooler) center pixel (Figure 2.21, left panel). Calculations were performed only for the moving window area; we created subsets of the resistance layer with any areas outside the window masked out.

Figure 2.20. A simple example landscape with a variety of land uses. Natural and semi-natural lands have low resistance, and human modified lands have high resistance. Hard barriers such as buildings and highways are shown in black. Locations of natural pixels to be connected are shown by dots, with colors indicating temperature. This over-simplified example is just for illustrative purposes; in our models temperature would not differ strongly at scales this fine, and there would often be many more natural pixels to connect.

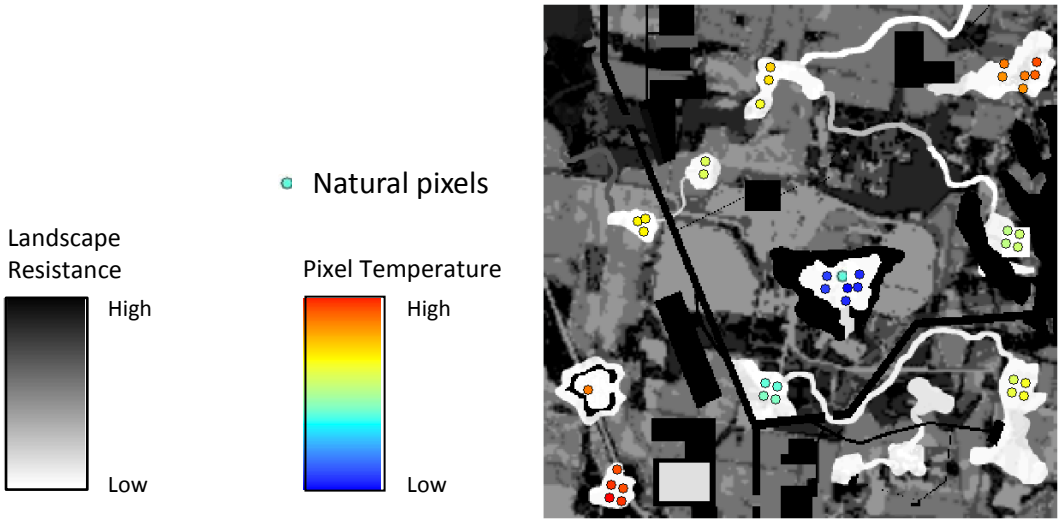

Figure 2.21. Illustrations of the moving window approach. The left-hand panel shows a circular moving window (red circle) centered on one of the natural pixels (green circle). This pixel becomes the target, and all pixels that are warmer than this pixel by at least T_{cutoff} are treated as sources. In this case, warmer pixels would each have 1 Amp injected at their locations (represented by green arrows), and the center pixel would be connected to ground. The right-hand panel illustrates our computational shortcut, where the moving window centers on a block of pixels. All candidate source pixels are given current sources equal to the number of cooler pixels inside the block. Here, green arrows represent 4 Amps of current flowing to the block, and red arrows represent 3 Amps (in each case the current equals the number of target pixels in the block that are cooler than the respective source).

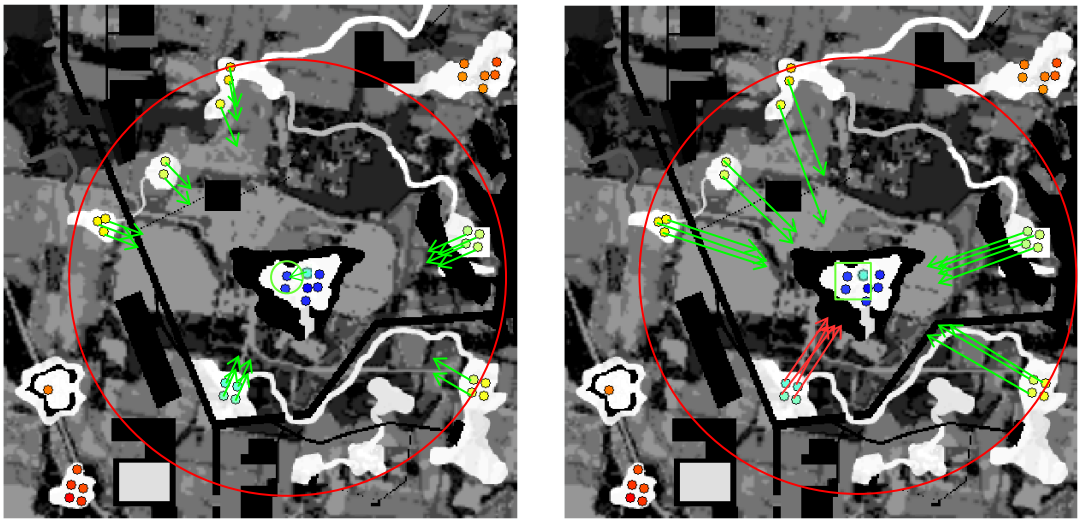

In experiments with test landscapes, this approach closely approximated current flow patterns that would be mapped when all pixels within the threshold distance were connected in a pairwise fashion (i.e., creating a separate current flow map for every pair of source and target pixels, and summing the results). This meant that for a study area with n natural pixels, n many-to-one calculations would closely approximate results from $(n^2\text{-}1)/2$ pairwise calculations.

We connected all natural pixels within 10 km of each other that differed in temperature by at least T_{cutoff}. We then ran Circuitscape in advanced mode with the source, ground, and resistance layers as inputs for each target pixel. We summed and mosaicked all current maps from individual moving window iterations into a cumulative current flow map for the study region

In practice, this method proved computationally prohibitive (requiring weeks of processing time) when calculations had to be repeated with the moving window centered on each and every natural pixel in the study region. As a computational shortcut, we ran the analysis with the moving window centered not on individual pixels, but on blocks of 15 x 15 pixels. Natural pixels in the 15 x 15 block were considered potential targets for flow, and natural pixels in the remainder of the 10 km radius area were considered potential sources. For each block, we iterated through all natural target pixels. For each target pixel, we identified all valid sources (i.e., those natural pixels within 10 km that met temperature criteria, if any). For each potential source that met the criteria, we added 1 Amp to the source location. After iterating through all targets, the result was a single source layer, with each source pixel having as many Amps of current injected into it as there were targets in the 15 x 15 block that met the temperature criteria for that

source (Figure 2, right panel). We then set the pixel at the center of the block to ground, and ran Circuitscape in advanced mode with the source, ground, and resistance layers.

After each computation, the window would move over 15 pixels and the process would begin again. In several test landscapes, the results closely approximated results achieved with having the moving window center on a single pixel, but with computation time cut dramatically, replacing up to 225 (15 x 15) calls to Circuitscape with a single call.

We performed our analyses with five T_{cutoff} values of 0^0, 0.25^0, 0.5^0, 1^0 and 2^0 C.

After running the results for the whole region, we stratified the results by ecoregion to identify the most intact places with the most temperature options within each ecoregion. However, because the mean annual temperature range varies considerably between ecoregions we varied the T_{cutoff} value depending on the ecoregion. In the coastal plain, which is largely flat and has little elevation-based temperature variation, the 10 km local range in mean annual temperature is only 0.34^0 C, whereas in the mountainous area of the Appalachians local mean annual temperature ranges vary from 2.1^0C in the Northern Appalachians to 3.4^0C in the Central Appalachians. To account for this variation, we selected T_{cutoff} values for each ecoregion based on the local mean annual temperature range (Table 2.5). We combined the results into one integrated map, and smoothed the ecoregional boundary to create a more gradual transition in our maps.

Table 2.5. Neighborhood Mean and Standard Deviation of Mean Annual Temperature for each ecoregion. Using a 10 km neighborhood the range of T_{mean} was calculated. This was summarized for each ecoregion to determine which grid to temperature grid to use.

MEAN	STD	Ecoregion Name	Grid of degrees temperature difference
0.3886	0.1445	Mid-Atlantic Coastal Plain	0.25
0.5282	0.2575	Chesapeake Bay Lowlands	0.50
0.6593	0.3485	North Atlantic Coast	0.50
1.0498	0.7359	Piedmont	1.00
1.2305	0.9360	Great Lakes	1.00
1.2557	1.0959	St. Lawrence - Champlain Valley	1.00
1.3377	0.5054	Western Allegheny Plateau	1.00
2.1315	1.4479	Northern Appalachian / Acadian	2.00
2.1360	0.9776	Lower New England / Northern Piedmont	2.00
2.4699	0.8698	Cumberland and Southern Ridge and Valley	2.00
2.7002	1.0138	High Allegheny Plateau	2.00
3.3238	0.9805	Southern Blue Ridge	2.00
3.4357	1.1405	Central Appalachian Forest	2.00

Results: Intact Areas with Large Temperature Gradients

The results of the resistance-only analysis highlight the areas of the region with the most intact forest cover and the least amount of roads: Northern Maine, The Adirondacks, the Catskills, the Allegheny Plateau, and the southern portion of the Central Appalachians (Figure 2.21). This results because areas with high numbers of natural pixels had high current flows. The current flowing into any target block will be a function of how many pairs of sources and targets there are in the window. For the non-climate model, the current flowing into a block would be $N_{targets} * N_{sources}$.

For any of the models incorporating temperature criteria, the current would reflect the number of source-target pairs meeting the criteria, with a maximum possible value being $N_{targets} * N_{sources}$ when all targets are cooler than all sources by at least T_{cutoff}. Thus, subsequent maps with increasing temperature differences are easy to interpret as they show increasingly smaller subsets of the "resistance only" map (Figure 2.21-2.25). Temperature gradients are correlated with elevation gradients, and as we increased the temperature difference criteria the results increasingly highlighted mountainous areas with steep elevation gradients. The 2^0 C map shows the summits of Mount Katahdin, the upper peaks of the White and Green Mountains, and the high peaks of the Adirondacks and Catskills (Figure 2.25).

The mountainous regions are indeed the most intact areas with the steepest temperature gradients but these areas are unlikely to benefit species in much of the region, especially low-relief ecoregions like the North Atlantic Coast. The stratified map by ecoregion (Figures 2.26 and 2.27) shows the location of relatively intact areas with the best temperature options within each ecoregion. The map highlights several linkages, such as the NJ High Peaks to the Green Mountains, the Catskills to the Adirondacks, and the Central Connecticut coast, that may provide the best local movement options for wildlife and plants.

The moving window method is experimental, but is promising in several respects. First, it readily identifies areas where large concentrations of natural lands exist along steep temperature gradients, i.e. those areas where species occupying natural lands could move short distances to reach cooler natural areas. Second, it produces continuous maps and does not require identifying discrete patches of natural lands to connect. Third, the method can also be used to identify important barriers (in a way similar to that described in McRae et al. 2012), some of which may represent restoration opportunities. The latter approach is in development, but preliminary results are in line with expectations. We now have the data and computer code needed to flesh out the barrier detection methods.

Comparing the moving window results (0.25^0 C) with the wall-to-wall 3-way results indicates considerable agreement between the two models (Figure 2.28). Both highlight the White and Green Mountains, the east side of the Adirondacks and the Central Appalachian ridges (the moving window was not run for Canada). They differ in that the wall-to-wall approach also emphasizes south central Virginia, while the moving window approach emphasizes the western Adirondacks, perhaps reflecting the latter's lack of directional flow and sensitivity to abundance of natural pixels within the window area.

Figure 2.21. Moving Window using Resistance only. This map shows the results of the 10 km moving window analysis connecting all natural cells. Areas with the highest flow have many interconnected natural cells and low resistance, indicating very intact regions.

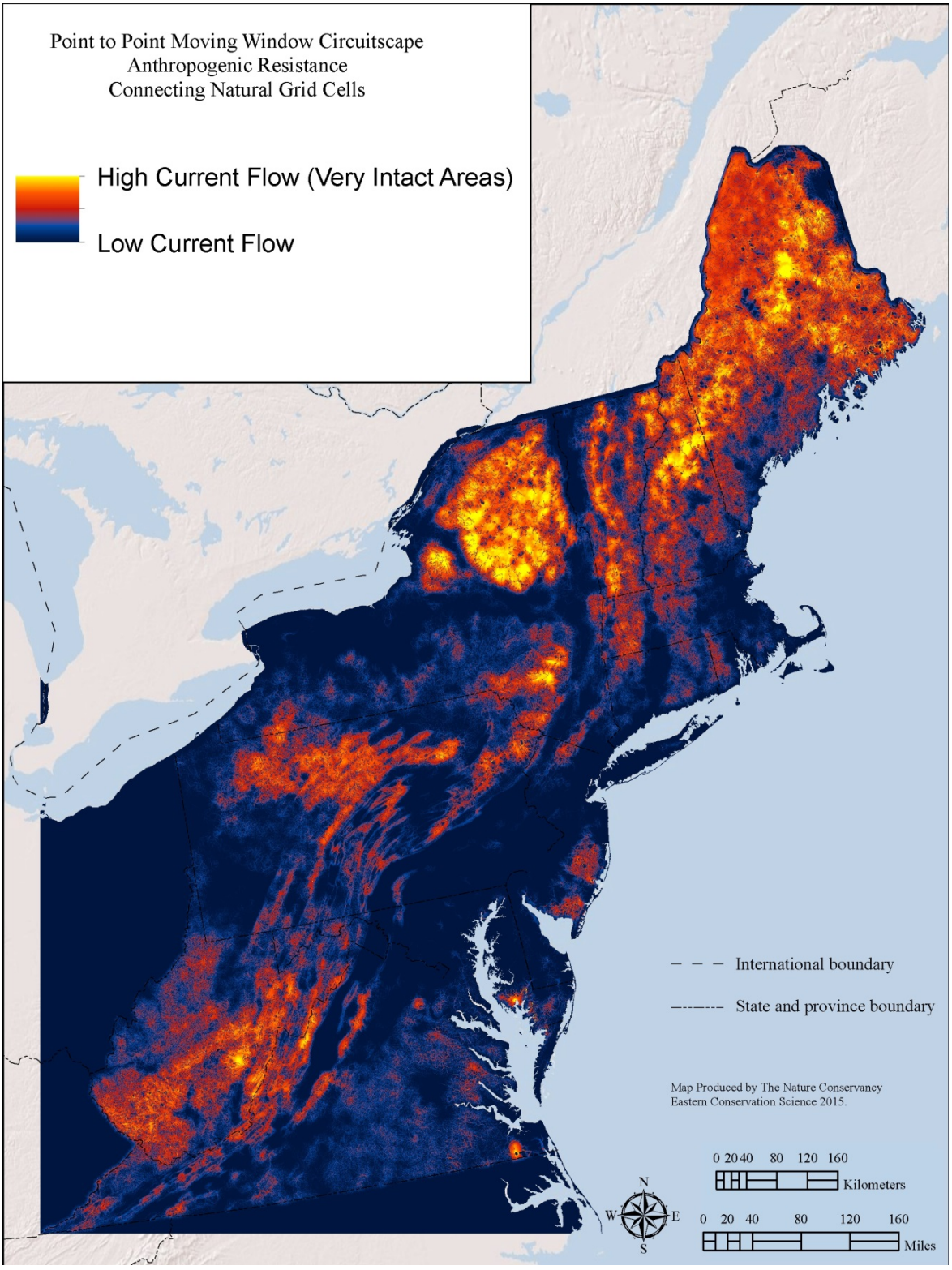

Figure 2.22. Moving Window using Resistance plus 0.25 C Mean Annual Temperature. This map shows the results of the 10 km moving window analysis connecting all natural cells that differ by at least 0.25 C in mean annual temperature. Areas with the highest flow have many interconnected natural cells, low resistance, and small to large temperature gradients.

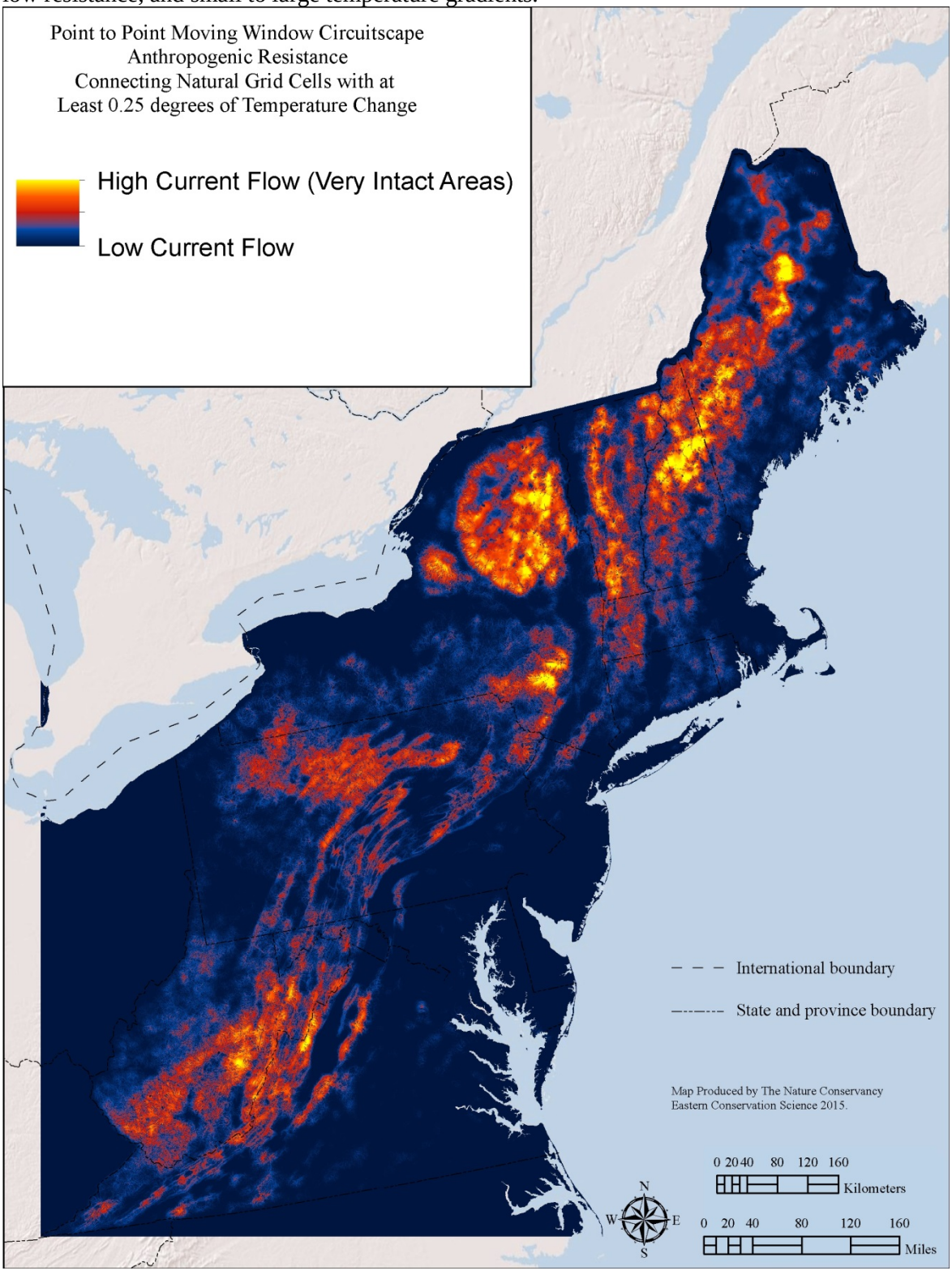

Figure 2.23. Moving Window using Resistance plus 0.50 C Mean Annual Temperature. This map shows the results of the 10 km moving window analysis connecting all natural cells that differ by at least 0.5 C in mean annual temperature. Areas with the highest flow have many interconnected natural cells, low resistance, and moderate to large temperature gradients.

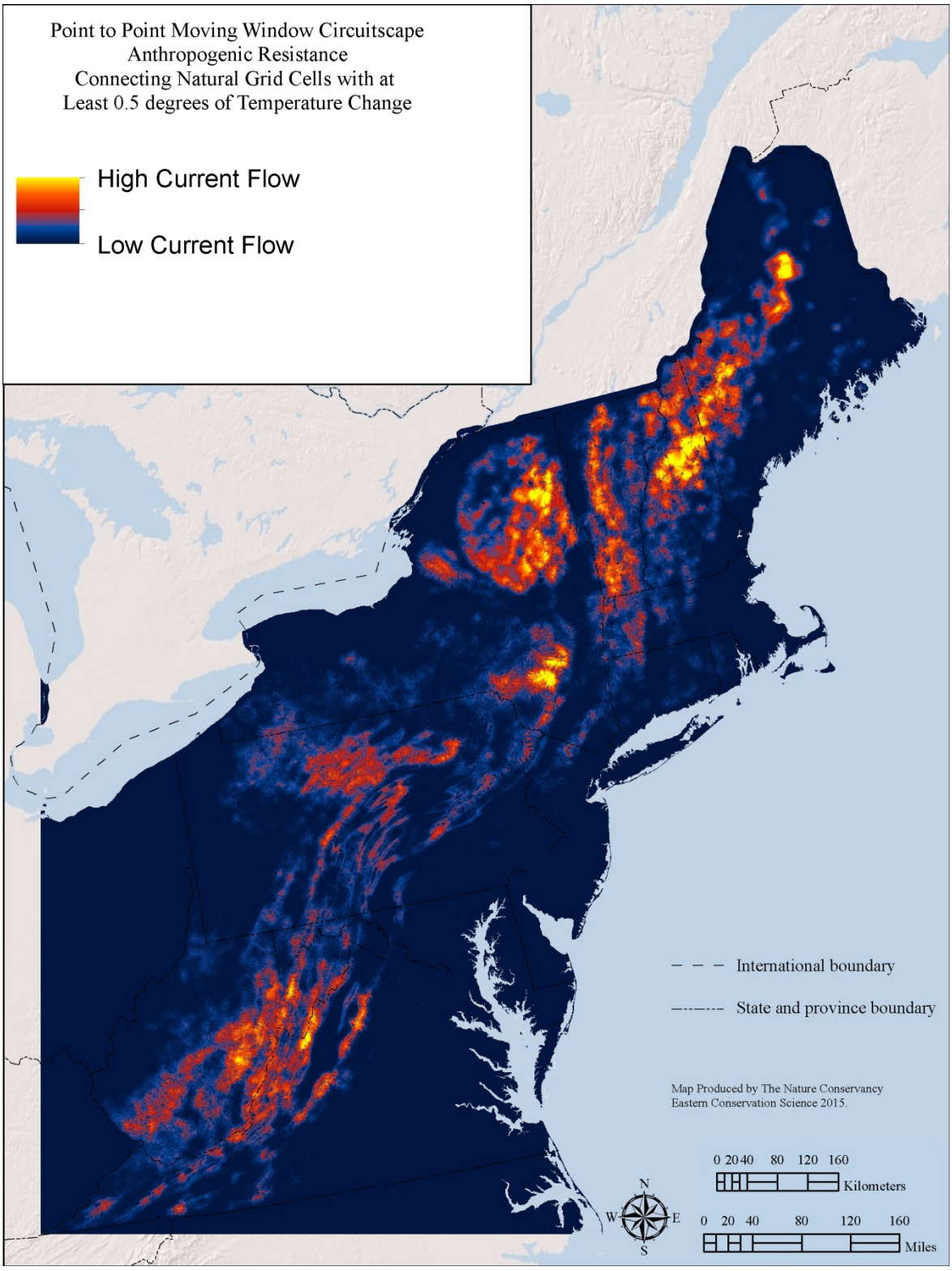

Figure 2.24. Moving Window using Resistance plus 1 C Mean Annual Temperature. This map shows the results of the 10 km moving window analysis connecting all natural cells that differ by at least 1 C in mean annual temperature. Areas with the highest flow have many interconnected natural cells, low resistance, and large temperature gradients.

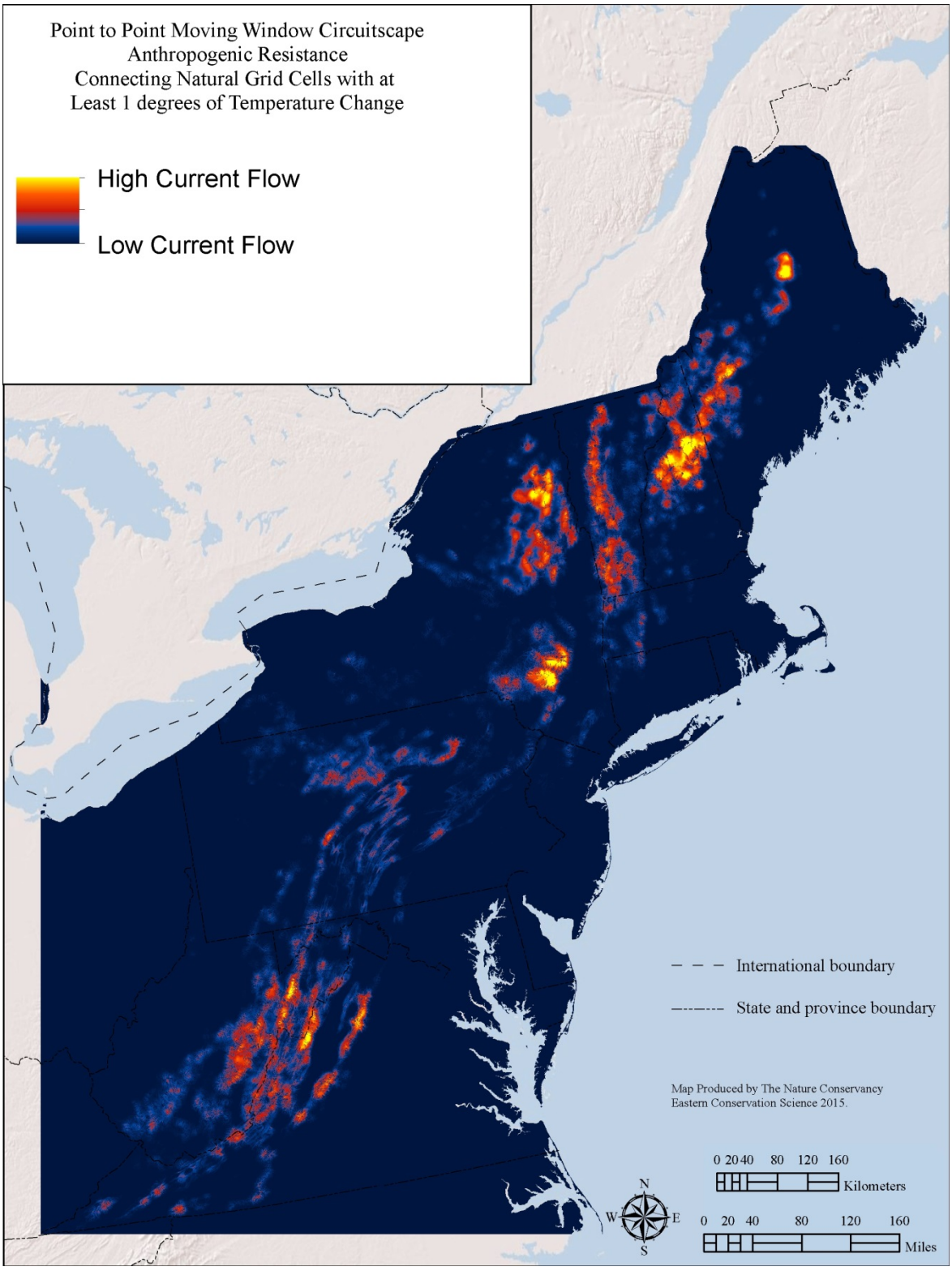

Figure 2.25. Moving Window using Resistance plus 2 C Mean Annual Temperature. This map shows the results of the 10 km moving window analysis connecting all natural cells that differ by at least 1 C in mean annual temperature. Areas with the highest flow have many interconnected natural cells, low resistance, and very large temperature gradients.

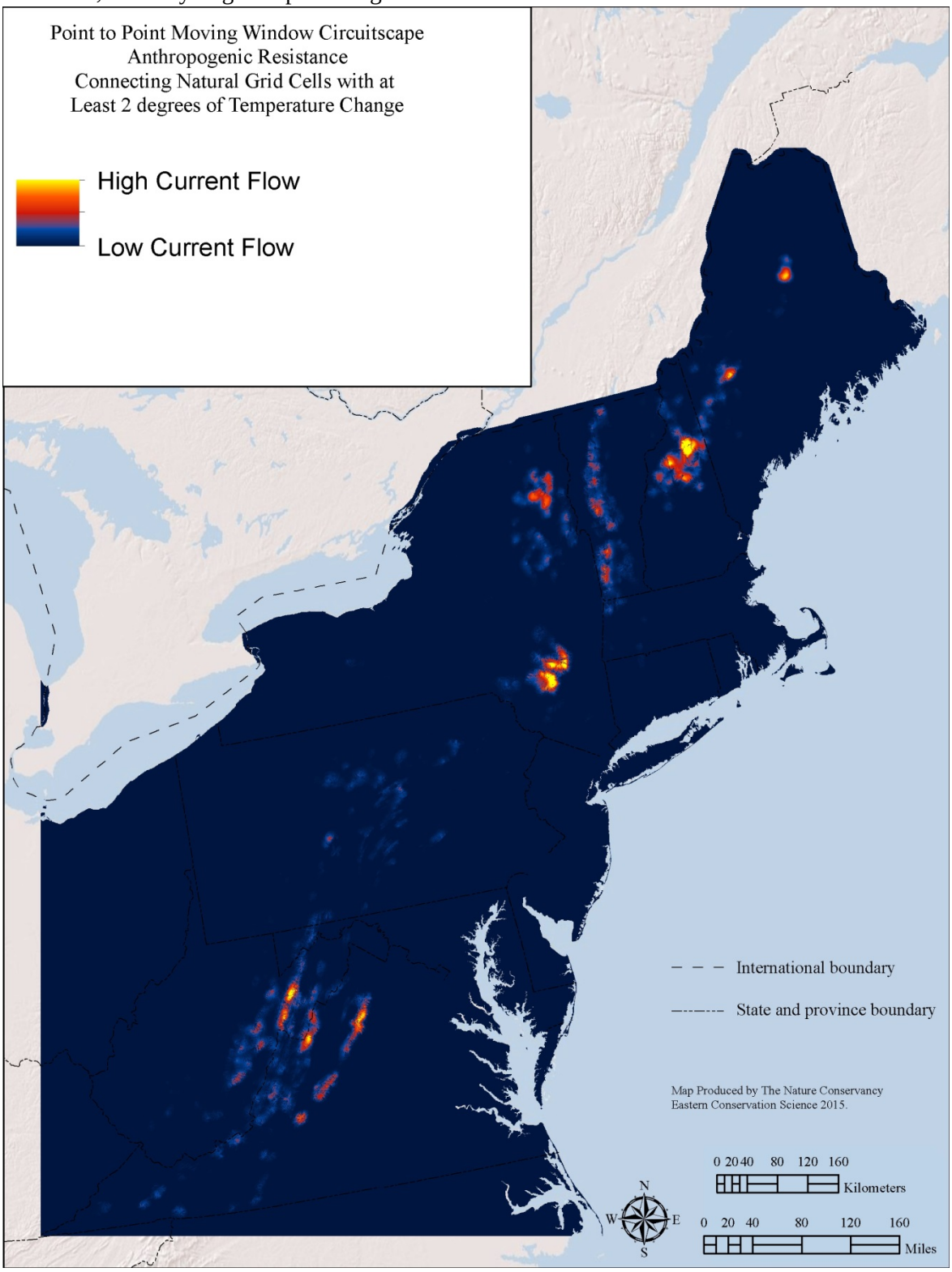

Figure 2.26. Ecoregions and their T_{cutoff} thresholds. The map shows the how the T_{cutoff} thresholds were distributed across ecoregions to produce the stratified results map (Figure2.27).

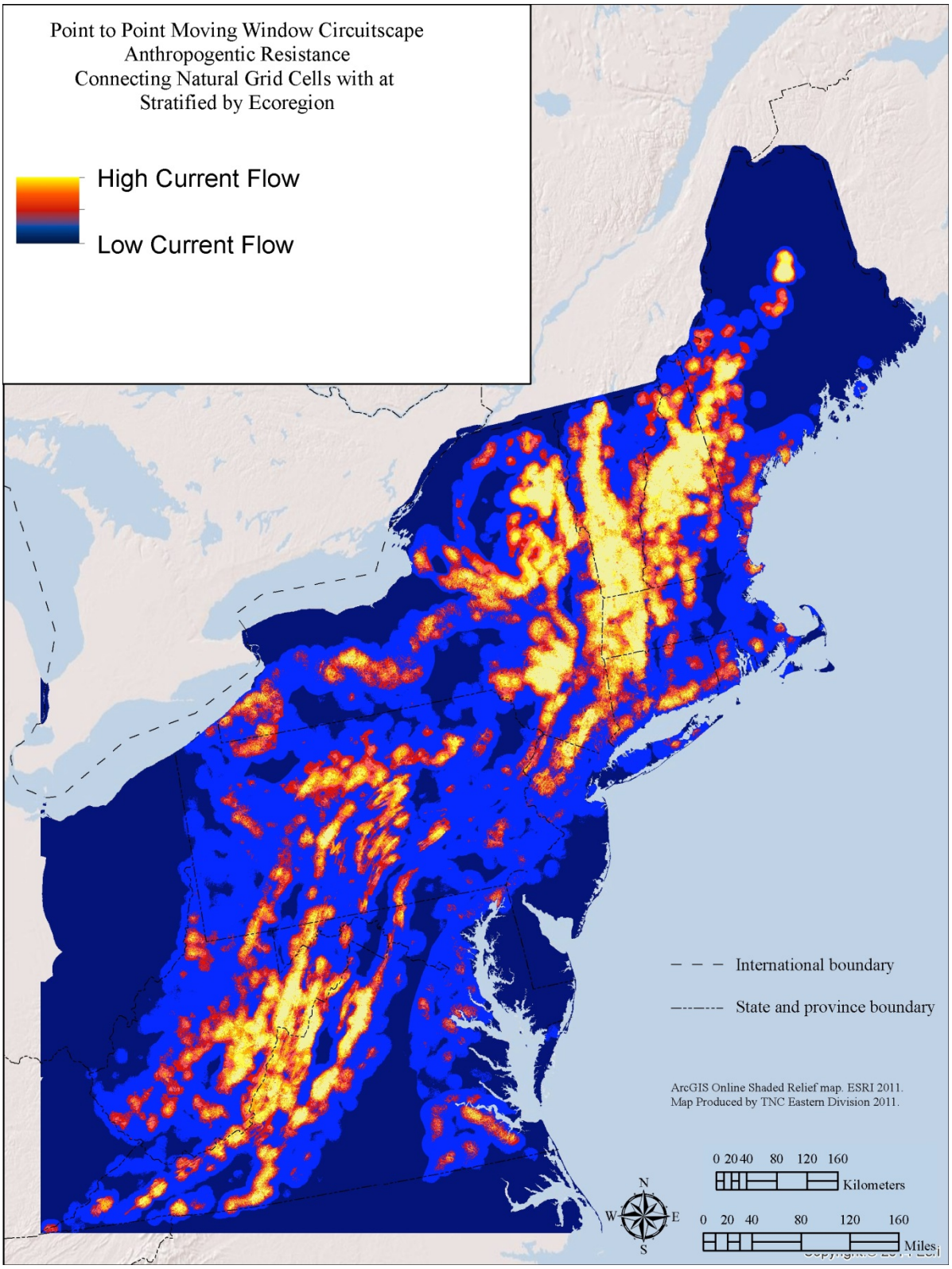

Figure 2.27. Moving Window results stratified by Ecoregion. The map shows the results of the 10 km moving window analysis connecting all natural cells that differ in mean annual temperature, using a variable temperature difference threshold depending on the ecoregion (see map 2.26). Areas with the highest flow have many interconnected natural cells, low resistance, and larger than average temperature gradients for their ecoregion.

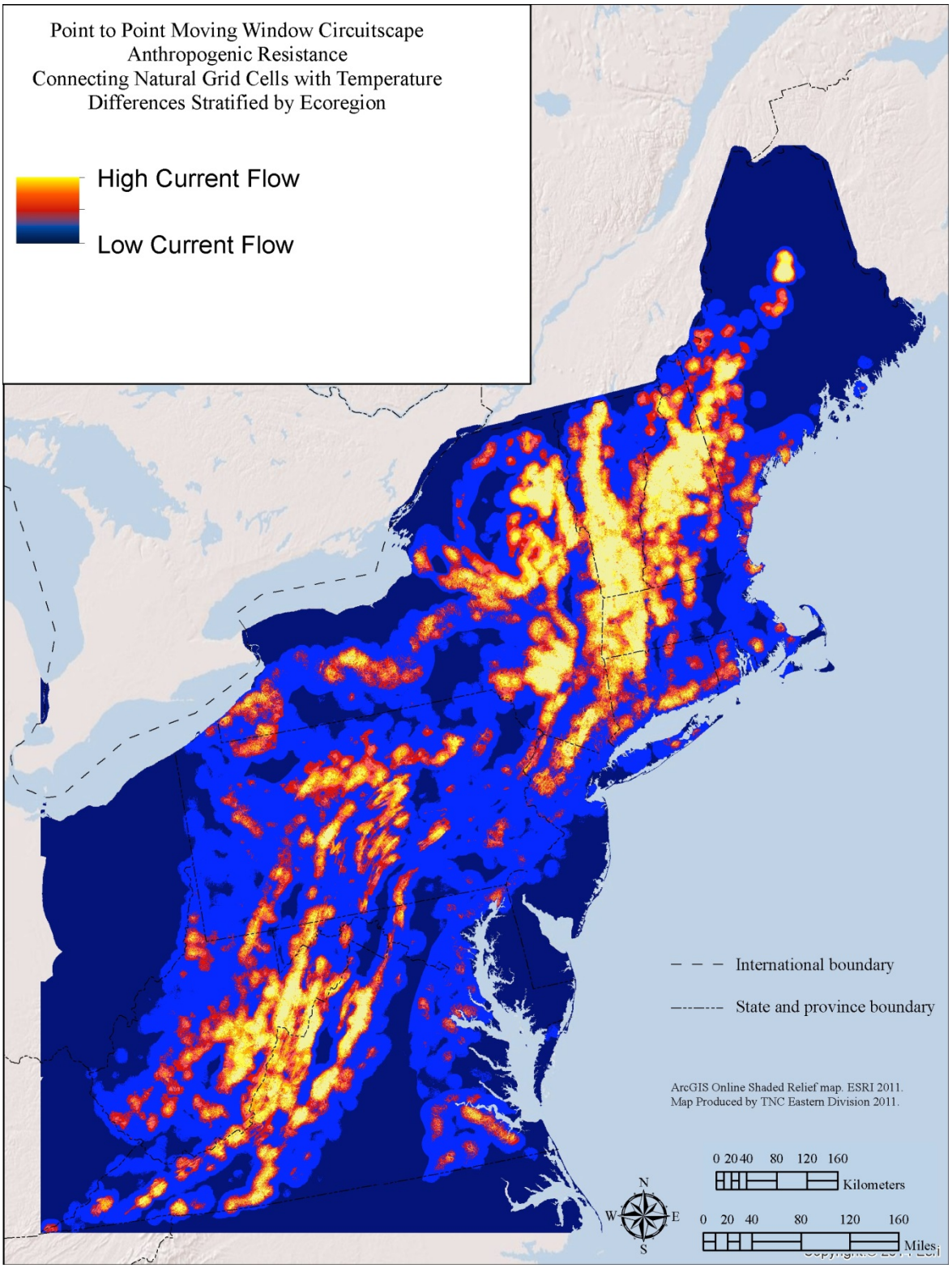

Figure 2.28. Combined Results with overlay of High-Scoring Areas. The map shows the high-scoring cells (top 40%) resulting from the wall-to-wall and moving window approaches overlaid to show combined and separate areas. Note that the moving window approach did not include Canada

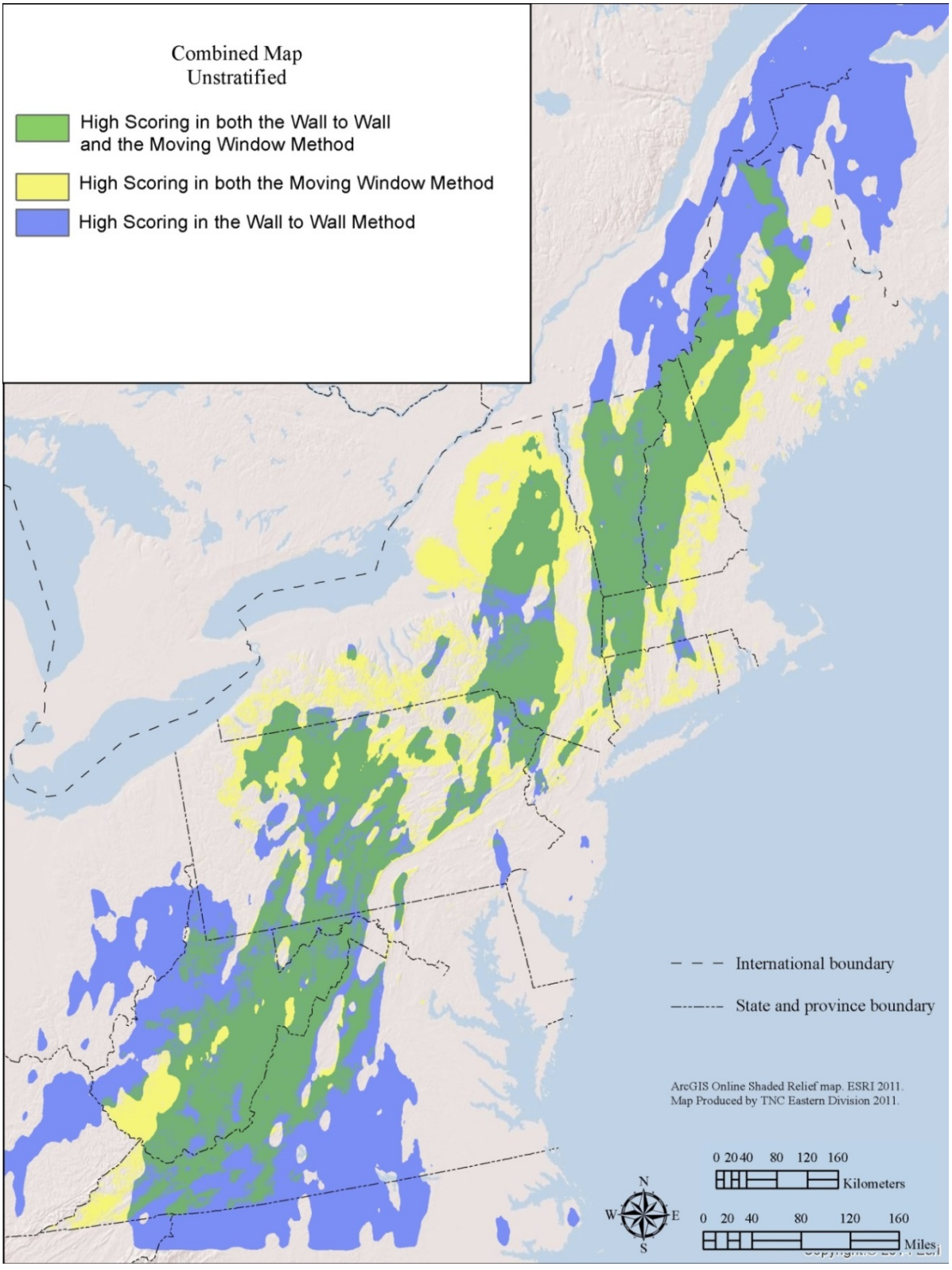

Riparian Climate Corridors

Introduction and Background

Riparian areas are the zones along water bodies that serve as interfaces between terrestrial and aquatic ecosystems. Although they compose a minor proportion of the landscape, they are typically more structurally diverse and more productive in plant and animal biomass than adjacent upland areas. Riparian areas supply food, cover, and water for a large diversity of animals, and serve as migration routes and connectors between habitats for a variety of wildlife (Manci 1989), particularly within highly modified landscapes (Hilty and Merenlender 2004). With respect to climate change, riparian areas feature micro-climates that are significantly cooler and more humid than immediately surrounding areas (Olsen et al. 2007), and are expected to provide micro-climatic refugia from warming (Seavy et al. 2009). Indeed, a climate resilience analysis based on microclimates and connectedness identified many riparian corridors as key landscape features in providing climate options (Anderson et al. 2014). Riparian areas that span climatic gradients and provide natural corridors that species may use to track shifting areas of climatic suitability have been called Riparian Climate Corridors or RCCs (Krosby et al. 2014).

In addition to their connectivity functions, riparian areas offer many other conservation values. They are important in mitigating nonpoint source pollution, and removing excess nutrients and sediment from surface runoff and ground water. Riparian vegetation modifies the temperature conditions for aquatic plants and animals, stabilizes streambanks, mitigates flooding, and contributes to the health of adjacent freshwater habitats (Pusey & Arthington 2003). Riparian areas typically contain high levels of species richness (Naiman et al. 1993).

Krosby et al. (2014) proposed a method for identifying priority riparian areas for climate adaptation. Their analysis, performed in the Pacific Northwest at a 90 m scale, identified potential riparian areas that span large temperature gradients, have high levels of canopy cover, are relatively wide, have low solar insolation, and low levels of human modification – characteristics expected to enhance their ability to facilitate climate-driven range shifts and provide micro-climatic refugia from warming. We were inspired by this work and aimed to develop a counterpart for the Northeast.

Our methods and results differ in several ways from Krosby et al. First, we aimed for a finer-scale result: the identification of *stretches of intact and connected floodplain* that crossed large temperature gradients. To this end, we partitioned the Northeast riparian areas into over 158,000 individual units and then we assessed each unit using data developed at a 30 m scale. Second, because the Northeast is largely forested we found that available canopy cover and solar radiation datasets provided little differentiation among riparian units. Thus we focused primarily on human modification, temperature gradients, and the size and area of each unit.

Mapping Riparian Climate Corridors

Our objective was to identify contiguous units of riparian floodplain that would facilitate movement of plants and wildlife across temperature gradients. In contrast to the upslope model of the previous section where populations were presumed to traverse the landscape starting at any point, here we assumed that the species of interest would stay within the floodplain, traveling linearly along it and taking advantage of the cooler moister environment.

Riparian Units

Our riparian model was based on the Active River Area (ARA) model previously developed to map the floodplain and other zones of rivers in the Eastern U.S. (Eastern Conservation Science 2009). The model uses a 30 m DEM and 1:100,000 hydrography NHD datasets to model the channels and riparian lands necessary to accommodate the physical processes that maintain habitat types and conditions in and along rivers and streams (Smith et al. 2008). This area interacts with the stream or river and includes the meander belt, riparian wetlands, and the 100 year floodplain. The mapped area accommodates the natural ranges of variability of flooding, sediment transport, processing of organic materials, and other key biotic interactions.

Our model included all of the ARA floodplain plus a 90m buffer around it and any mapped stream too small to have a floodplain (Figure 3.1). The buffer area, representing the material contribution zone, is higher in slope than the base zone and has less direct hydrologic connection to the stream. However, materials in this zone contribute to the input of woody debris, sediments, and nutrients. This area also provides critical habitat for terrestrial species associated with riparian ecosystems.

Figure 3.1. Zoom-in of the Active River Area showing base zone and the material contribution zone.

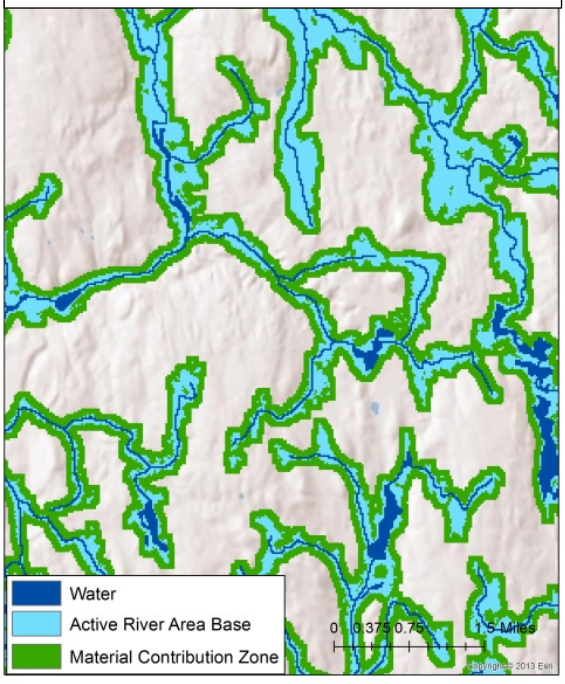

The ARA maps as a continuous network. In order to partition it into individual units we used a dataset of "local connectedness" (Anderson et al. 2014) to identify areas that were mostly natural and would allow movement through the floodplain. The local connectedness metric measures how impaired the structural connections are between natural ecosystems within a local landscape using a resistant kernel model. Roads, development, agriculture, and other barriers create resistance to species movement by increasing the risk or perceived risk of harm (for details on the local connectedness model see Anderson et al. 2014 or Anderson et al. 2012).

Local connectedness is a measure of human modification. The grid attributes every 30 m cell in the region with a score from 0 to 100 reflecting the degree to which the natural cell is connected with the cells in a 3 km radius surrounding it. A score of "0" indicates that the cell is completely surrounded by development and a score of "100" indicates a cell completely surrounded by natural land cover (Figure 3.2). We attributed the entire ARA will the connectedness scores and then separated the continuous ARA into individual units wherever the connectedness score was less than 15. This removed areas that have concentrations of roads, development, or intensive agriculture but allowed the units to include areas that cross an occasional low density development or agriculture

Figure 3.2: A gallery of satellite images and their corresponding local connectedness (lc) scores. The mean scores are based on a roughly circular site positioned at the center of each image (not shown).

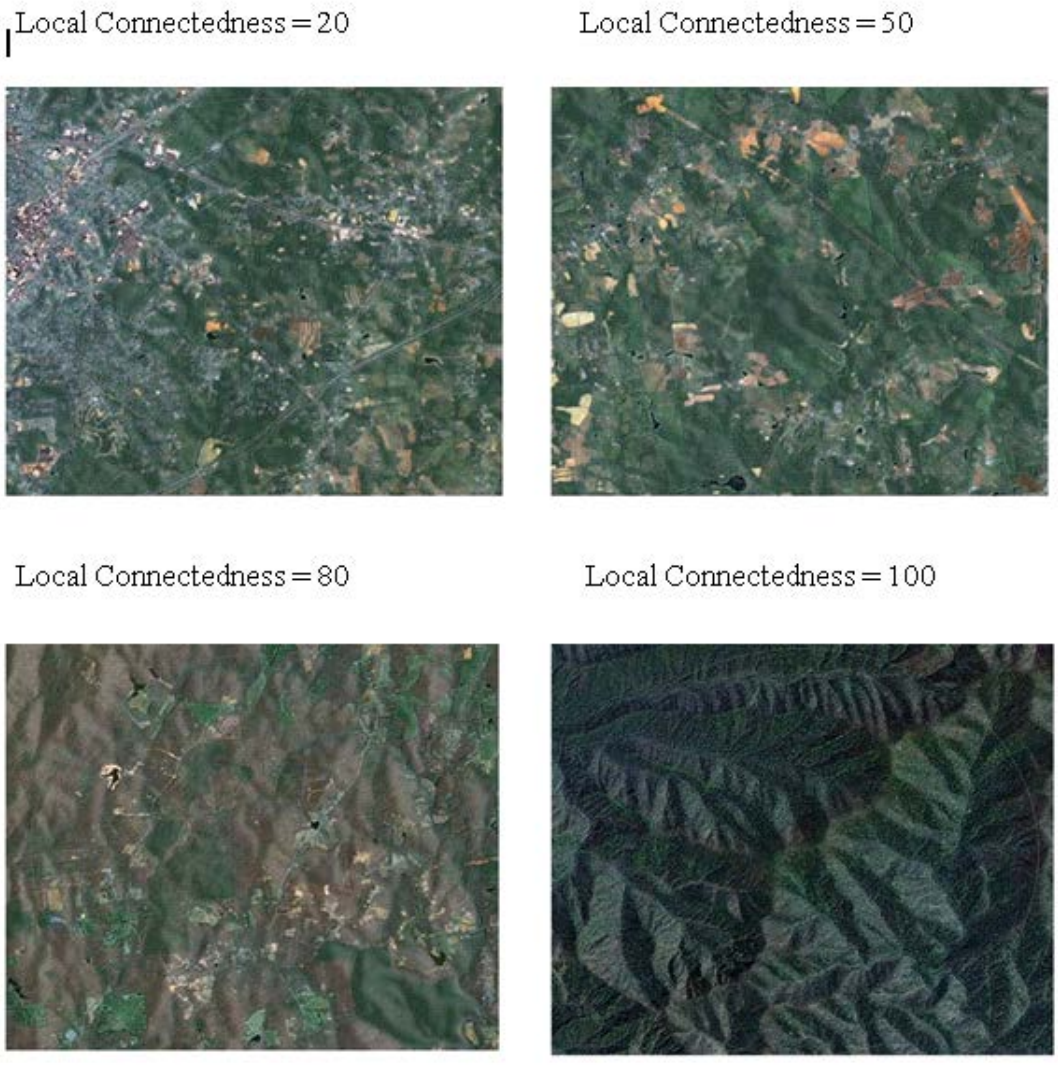

Dividing the ARA by the local connectedness score created over 300,000 units. We set a minimum size of 10 acres for a unit to be considered a potential riparian climate corridor because corridors smaller than 10 acres cannot offer the movement or temperature potential we were interested in. Additionally we eliminated large lakes (with centers more than 200 m from shoreline) to ensure that the units did not contain large open water stretches that would be difficult for terrestrial species to cross. Applying these criteria resulted in 158,402 riparian units for the region ranging in size form 10 acres to over 1,000,000 acres (Figure 3.3).

Figure 3.3: An example of unit creation using local connectivity scores . The figure on the left shows a stream and its buffered ARA in bright blue. The figure on the left in the same location, and shows the Riparian Unit outlined in black. The unit in bounded on the top and the bottom by a minor road.

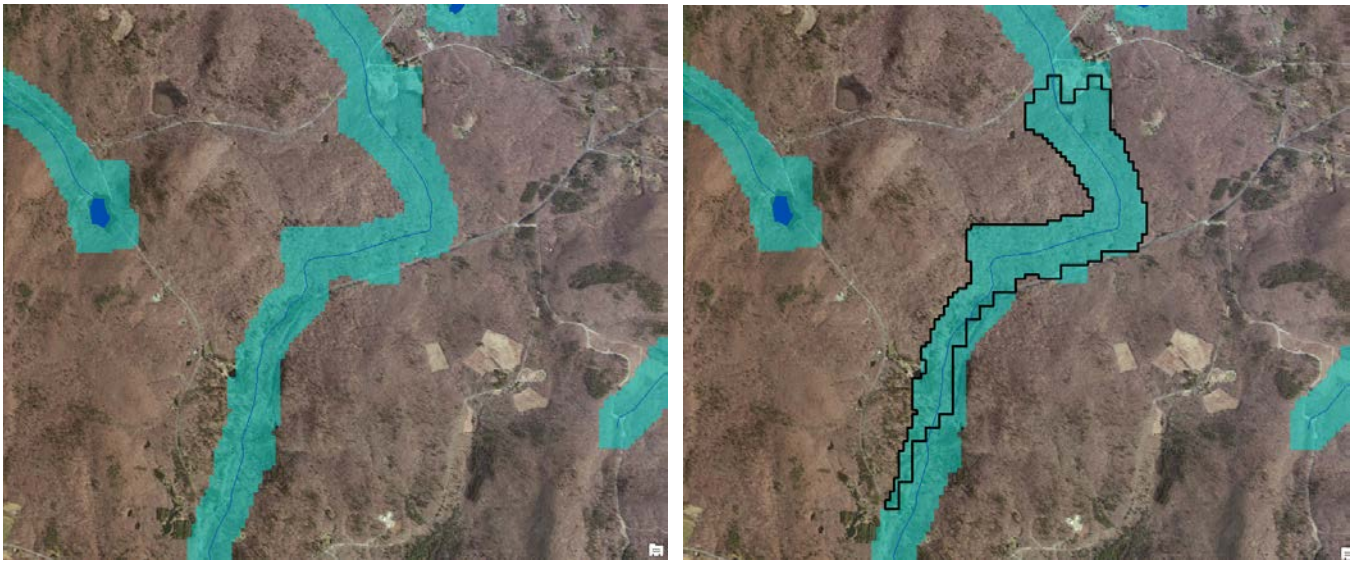

Riparian Unit Attributes

We attributed the 158,402 riparian units with six attributes associated with its ability to function as a climate corridor: size, mean temperature range, local connectedness, canopy cover, wetland density, and steepness.

Size

For each unit, we calculated its total area in meters and acres. Our assumption was that the larger the size of the unit the longer species could persist within it and the more likely it is to facilitate movement through large geographic areas. We used a cutoff of 100 acres as part of the riparian climate corridor definition to focus our analysis on the larger units. As with Krosby et al 2014, size also provided the closest approximation of length and width, as these characteristics proved difficult to summarize into a single value due to the complexity of some of the longer networks.

Mean Annual Temperature Range
For each unit, we overlaid the downscaled 30-year mean annual temperature model described in the previous section, and calculated the temperature mean and range for each unit as an indication of the length of the temperature gradient available in the unit.

Local Connectedness / Human Modification
We overlaid the local connectedness dataset (Anderson et al. 2014) and calculated the mean connectedness score for each unit as an indication of the degree to which the corridor has been impacted by human activity.

Steepness
Some stream corridors cross elevation gradients that appeared too steep to be used by most species for movement. To assess this, we overlaid a Digital Elevation Model (Gesch et al. 2002) on the riparian units and calculated its elevation range divided it by its total acres, as a metric of its steepness. Our assumption was that short steep units greater than 50 meters elevation per 10 acres were likely not conducive to movement by most species (this affected 2779 units and 3 RCCs).

Wetlands
We overlaid a dataset of wetland density for the region (Anderson et al. 2014) that was based on the number of National Wetland Inventory wetlands summarized within a weighted 100 acre and 1000 acre neighborhood around each 30-m cell. We calculated the average wetland density for each unit as a gauge of small-scale topographic diversity and patterns of freshwater accumulation. This attribute was not used for identifying the RCC classes but is included in the final dataset

Canopy Cover
We overlaid the 2011 NLCD percent tree canopy cover dataset (Jin et al. 2013) on the riparian units and calculated the mean percent cover for each unit, as an indication of forest cover in the riparian areas. This attribute is included in the final dataset, but was not used in identifying RCC classes due to perceived inaccuracies in the data and the lack of differentiation between units provided by this data.

Definition of Riparian Climate Corridor

We defined an RCC as an intact stretch of floodplain of at least 100 acres with a temperature gradient longer than the mean for its ecoregion. To identify RCCs, we first calculated the mean annual temperature gradient for all riparian units over 100 acres within each ecoregion (Table 3.1). Mean temperature range varied by ecoregion from a low of 0.14^0 C in the Mid Atlantic Coastal Plain to 1.3^0 C in the Central Appalachians. For each unit, we transformed the values to a standard normal distribution (Z-scores) based on the mean and SD of mean annual temperature of the ecoregion it occurred in. Units over 100 acres that had temperature ranges > 0.5 SD above their ecoregional mean were identified as potential RCCs.

Table 3.1. Temperature Gradients within Riparian Units. This table shows the number of riparian units over 100 acres within each ecoregion and the mean and standard deviation of the mean annual temperature score.

Ecoregion	Mean Mean Annual Temperature Range	SD Mean Annual Temperature Range
Mid-Atlantic Coastal Plain	0.141877	0.044748
Chesapeake Bay Lowlands	0.220081	0.074156
North Atlantic Coast	0.245211	0.093256
Piedmont	0.421882	0.169777
St. Lawrence – Champlain Valley	0.455968	0.213315
Western Allegheny Plateau	0.594606	0.178008
Great Lakes	0.726212	0.345052
Lower New England / Northern Piedmont	0.774548	0.330938
High Allegheny Plateau	1.032997	0.417104
Cumberlands Southern Ridge and Valley	1.112109	0.335743
Southern Blue Ridge	1.11737	0.423664
Northern Appalachian / Acadian	1.231299	0.598963
Central Appalachian Forest	1.326468	0.468164

Results: Categories of Riparian Climate Corridors

There were 48,458 riparian units over 100 acres in the Northeast region. In order to understand their distribution and significance we identified four categories of potentially important RCCs based on their size, temperature gradient, local connectedness and steepness. Our criteria for group membership increased in difficulty as the area of the corridor got smaller. Small corridors 100-1000 acres in size had to be 2 SD above the mean in temperature gradient, above "35" in local connectedness and less than "50" in steepness, whereas huge riparian units over 50,000 acres only had to have temperature gradients above the mean (Table 2.2, Figure 3.4)

Table 3.2. Criteria for Riparian Climate Corridor Categories. The table gives the number of original units, the criteria, and the number of units meeting the criteria. We started with 158,402 units, 109,944 were less than 100 acres. Of the remaining 48,548 units, 5782 met criteria for group inclusion.

Size Class	Total Units	Criteria			Total meeting criteria
		Temp. Gradient	Connected-ness	Steep-ness	
A: Over 50,000 Acres	19	*> 0.5 SD*	-	-	19
B: 10,000 to 50,000 Acres	122	*> 0.5 SD*	-	-	19
C: 1,000 to 10,000 Acres	3,150	*> 1 SD*	*>25*	-	1,708
D: 100 to 1,000 Acres	45,167	*> 2 SD*	*>35*	*<50*	4,036
TOTAL	48,458				5,782

Figure 3.4. Distribution of the Four Types of Riparian Climate Corridors (definitions in Table 3.2).

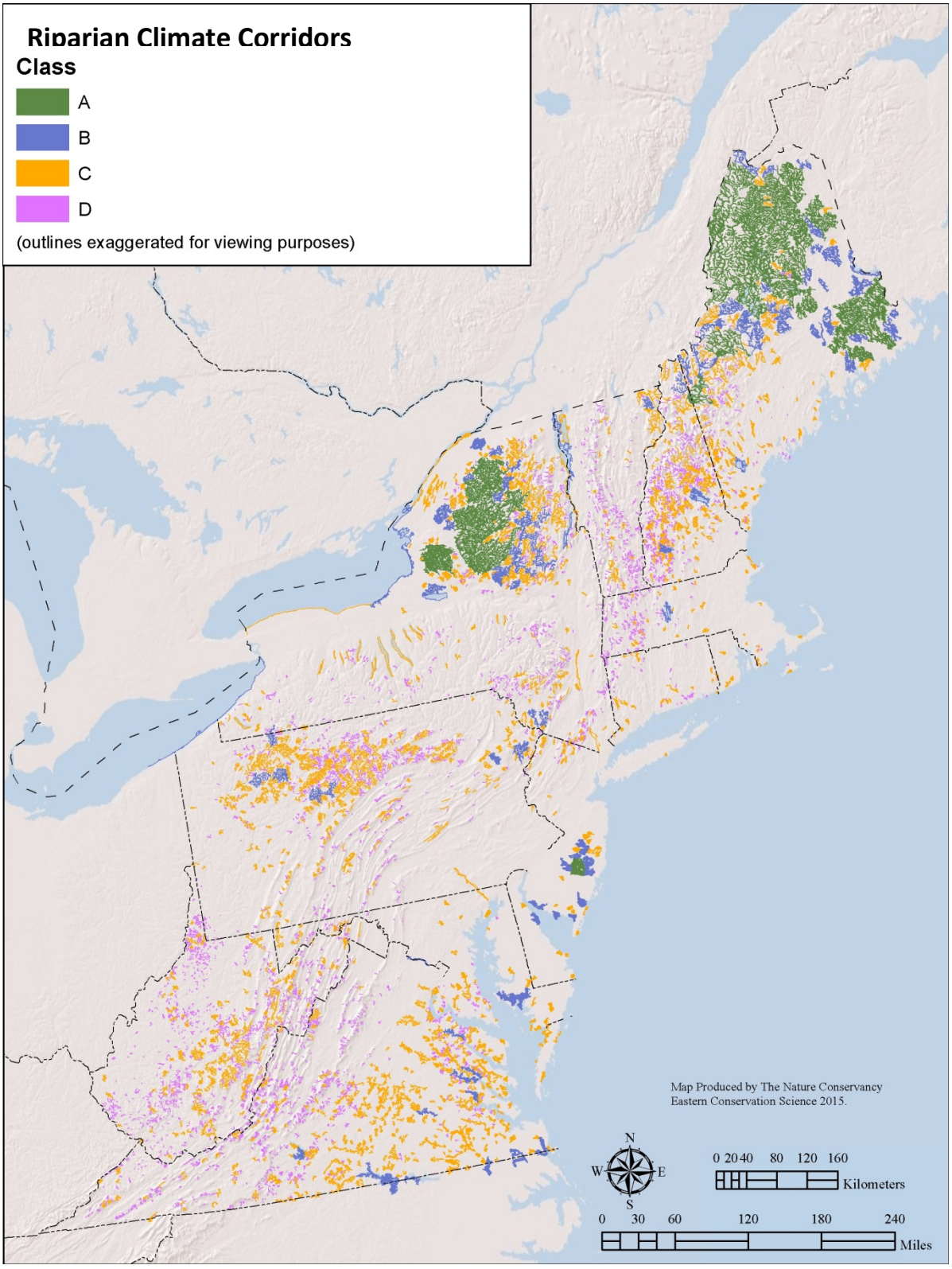

Temperature gradients were relatively short within the riparian corridors particularly within the low relief ecoregions. For example, in the Mid-Atlantic Coastal Plain with its average of only 0.14^0 C even a corridor with temperature gradients 2 SD above the mean offers only 0.22^0 C (less than one half degree F) temperature change. This may make a difference to some wildlife and plants, but it is unlikely to maintain a full complement of biodiversity over time. Nevertheless, the 31,000 riparian units with above average temperature gradients (Table 3.3) may be the best available option for many species and in aggregate may provide significant climate relief. The small amount of temperature change found in these results highlight the importance of topographically based micro-climates not captured by the temperature model, but offering more extensive climate options to local species.

Table 3.3. Distribution of the Temperature Gradients. These are for all sizes greater than 10 acres.

Temperature distribution		
>3SD	**3,087**	**2%**
<3 SD and >2SD	**4,130**	**3%**
<2SD and >1SD	11,129	7%
<1SD and >0.5 SD	12,706	8%
<0.5 to >-0.5 SD (the mean)	73,055	46%
<0.5 SD	54,295	34%

Characterization of the Riparian Climate Corridor Categories

Class A: 19 examples

These important RCCs are over 50,000 acres in size and have temperature gradients over 0.5 SD in their ecoregion (Figure 3.5). Most of the 19 Class A RCCs are in Maine and New York where there are extensive intact floodplains, however one corridor occurs partially in New Hampshire and one occurs in the Pine Barrens of New Jersey. Their local connectedness scores are very high, ranging from 50 to 90, with a mean of 76, and their mean temperature range is 2.36^0 C. All of these RCCs contain a wide range of stream types including size 1, 2, and 3 rivers (Olivero and Anderson 2008). By virtue of their large size and temperature gradients they connect many different habitats and are a regionally important priority for conservation for the refuge and options they offer. Examples include: West Branch of the Penobscot River (ME), Saint Croix River (ME), Machias River (ME), West Branch Wading River/Batsto River (NJ), and Raquette River (NY).

Class B: 108 examples

Class B RCCs are large corridors are between 10,000 and 50,000 acres with temperature gradients of over 0.5 SD for their ecoregion (Figure 3.6). Class B RCCs occur in every state except West Virginia, Connecticut, and Rhode Island. They are most common in Maine (35), New York (38), New Jersey (12)

and Virginia (11). Their mean temperature range is 1.18^{0}C indicating substantial temperature gradients. Their local connectedness scores have a mean of 65 and range from 29 to 91, suggesting a wider range of intactness than the Class A group. This widespread group is likely to be very important in facilitating movement and provide refuge under climate change. Examples include: Leipisic River/Duck Creek (DE), East Brach Swift River/Hop Brook (MA), Blackwater River (MD), Moose River/South Branch Brassua Stream (ME), Dead Diamond River (NH), Oswego River (NJ), Cedar River (NY), Lehigh River (PA), and Winooski River/Otter Creek (VT).

Class C: 1703 examples

Class C RCCs are moderately sized corridors between 1,000 and 10,000 acres with high temperature gradients (>1 SD above the mean), and good local connectedness scores (> 25). Class C corridors occur in all states and are among the most intact floodplains in the states with a mean local connectedness score of 53 and a range from 25 to 91 (Figure 3.7). They have a substantial temperature range averaging 1^0 C and may be particularly important to local populations because they offer a relatively large amount of temperature change in a smaller area. Examples include: Appoquinimink River/Blackbird Creek (DE), Westfield River (MA), North Branch Patapsco Creek (MD), Corson Brook (ME), Saco River/Dry River (NH), Cedar Creek (NJ), East Branch Trout Creek (NY), Coon Creek (PA), Green Fall River (RI), Appomattox River (VA), Moose River (VT), and Cheat River/Big Sandy River (WV).

Class D: 4036 examples

Class D RCCs are widespread short riparian areas with a high amount of temperature change (Figure 3.8). These 100 to 1000 acre floodplains are found in regions with considerable slopes and are absent from the relatively flat and developed states of Rhode Island and Delaware. By definition they have high temperature gradients (> 2 SD, mean of 1.2^{0}C), and are very intact (mean local connectedness score or 54, range 35-96). The three examples with extremely steep slopes (>50 steepness) were excluded from this group because they were likely to be too steep for many species to move across. Examples include: Farm Creek (MA), Hill Top Fork (MD), Mountain Brook (ME), Hanson Brook (NH), Coopertown Brook (NY), Deering Run (PA), Cold Brook (RI), Dirt Bridge Run (VA), Turkey Mountain Brook (VT), and Buffalo Creek/Grog Run (WV).

Comparison with the Terrestrial Range Shift Results

An overlay of the Class A, B and C riparian climate corridors on the high scoring areas for terrestrial range shifts indicates substantial geographic correspondence between the two (Figure 3.9). The majority of the RCCs nest within regions identified by the wall-to-wall or moving window approach or both. The Chesapeake Bay region is an exception where many RCCs are identified but few range shift areas. The Green Mountain region of Vermont identified by both the wall-to-wall and moving window methods is comprised almost entirely of Class D RCCs not shown on the overlay map (but see Figure 3.8) indicating that this region contains mostly short riparian areas with steep temperature gradients.

Figure 3.5. Class A Riparian Climate Corridors. This class contains RCCs over 50,000 acres in size with temperature gradients over 0.5 SD in their ecoregion.

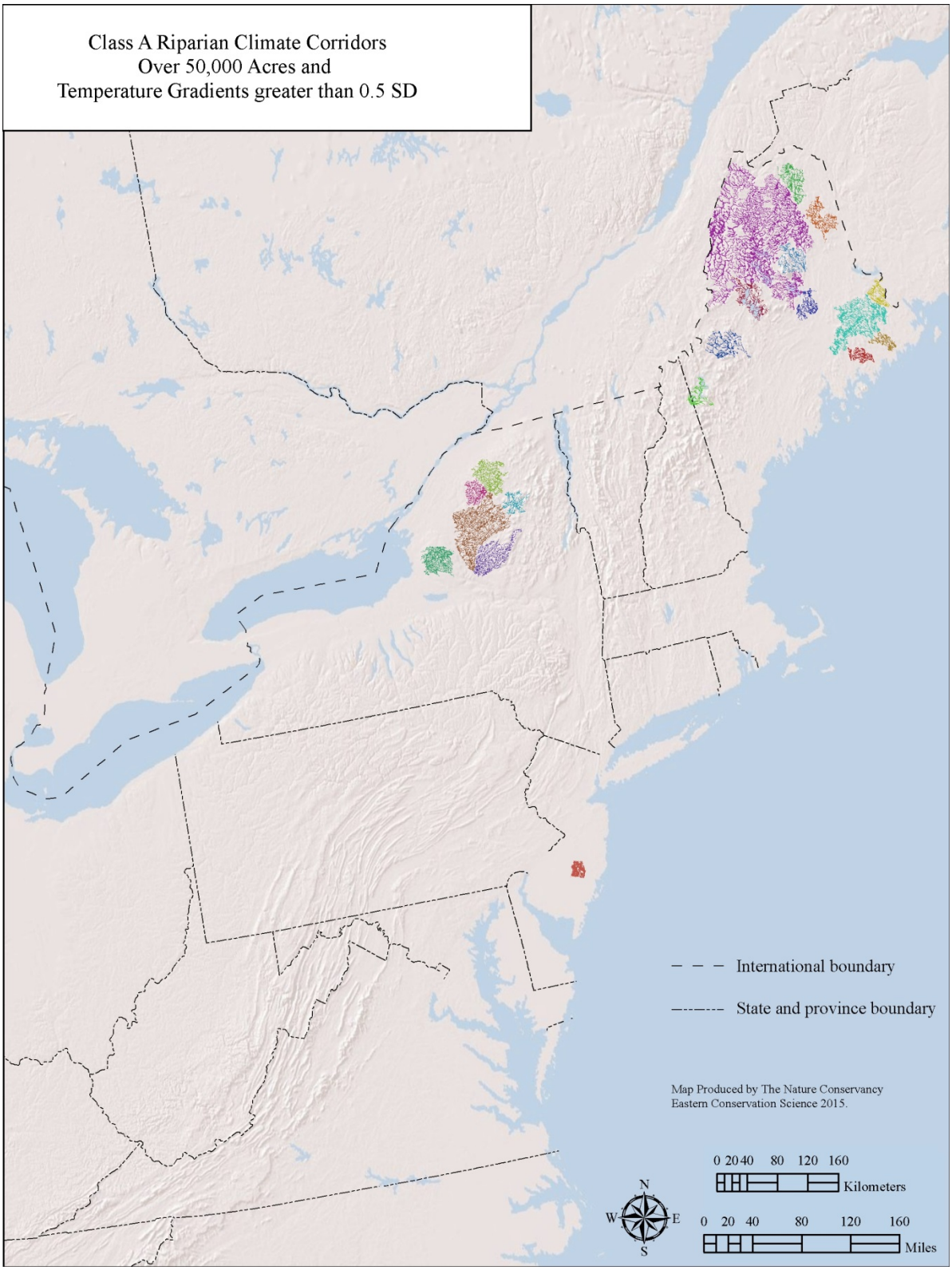

Figure 3.6. Class B Riparian Climate Corridors. This class contains large corridors between 10,000 and 50,000 acres with temperature gradients of over 0.5 SD for their ecoregion

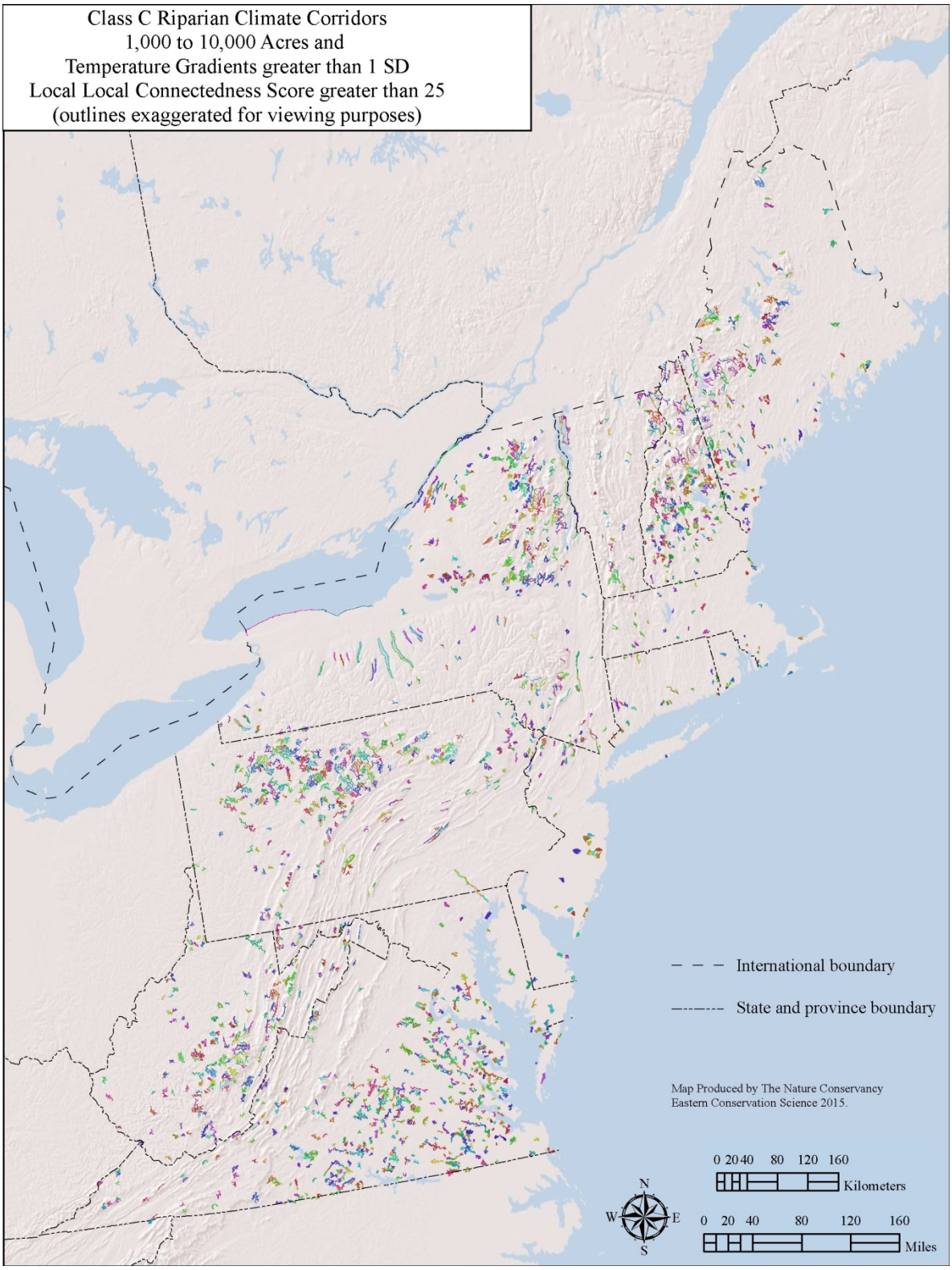

Figure 3.7. Class C Riparian Climate Corridors. This class contains large corridors between 1,000 and 10,000 acres, with temperature gradients of over 1 SD for their ecoregion, and have a Local connectedness score >25

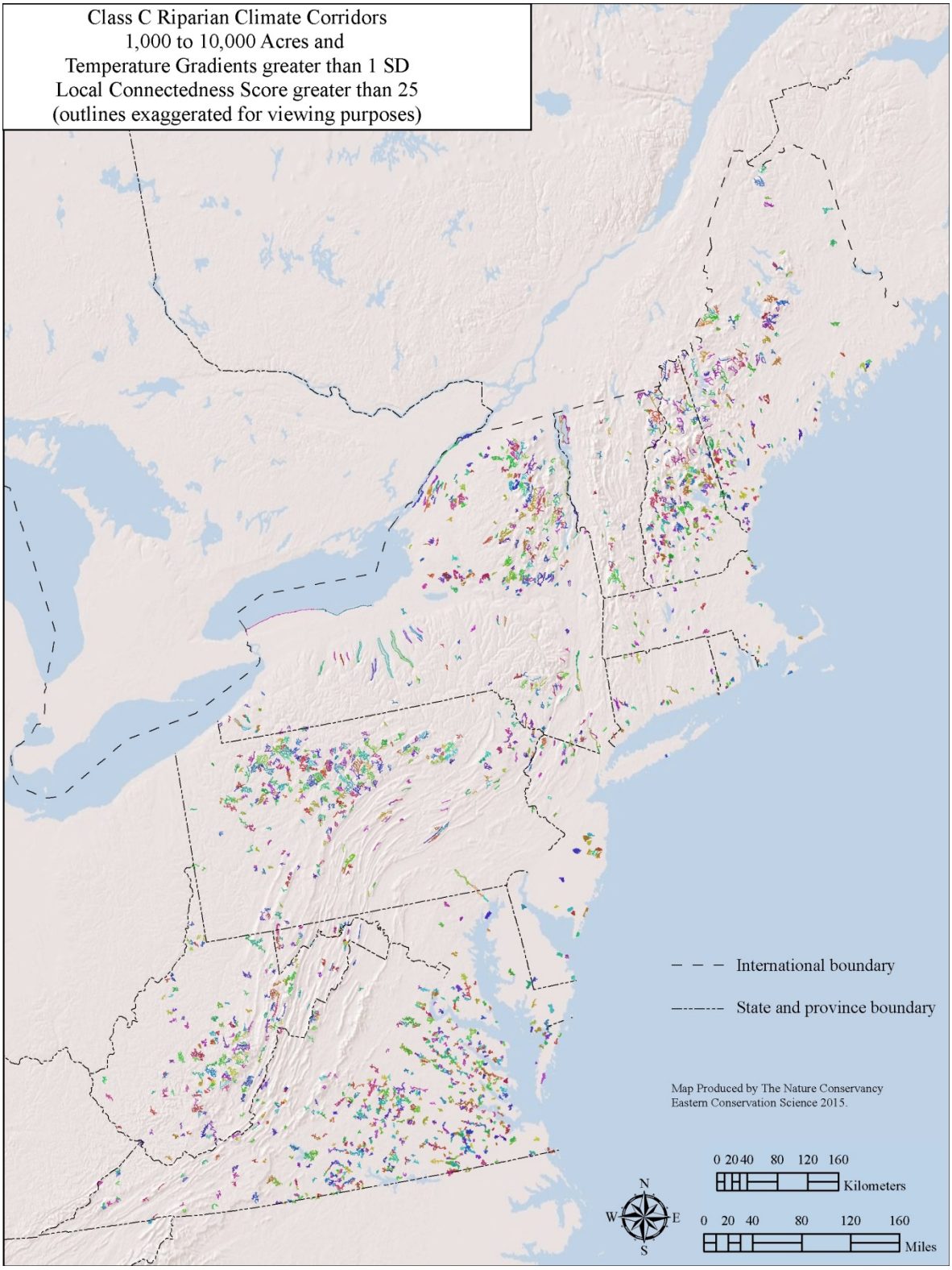

Figure 3.8. Class D Riparian Climate Corridors. This class contains large corridors between 100 and 1,000 acres, with temperature gradients of over 2 SD for their ecoregion, and have a Local connectedness score >35

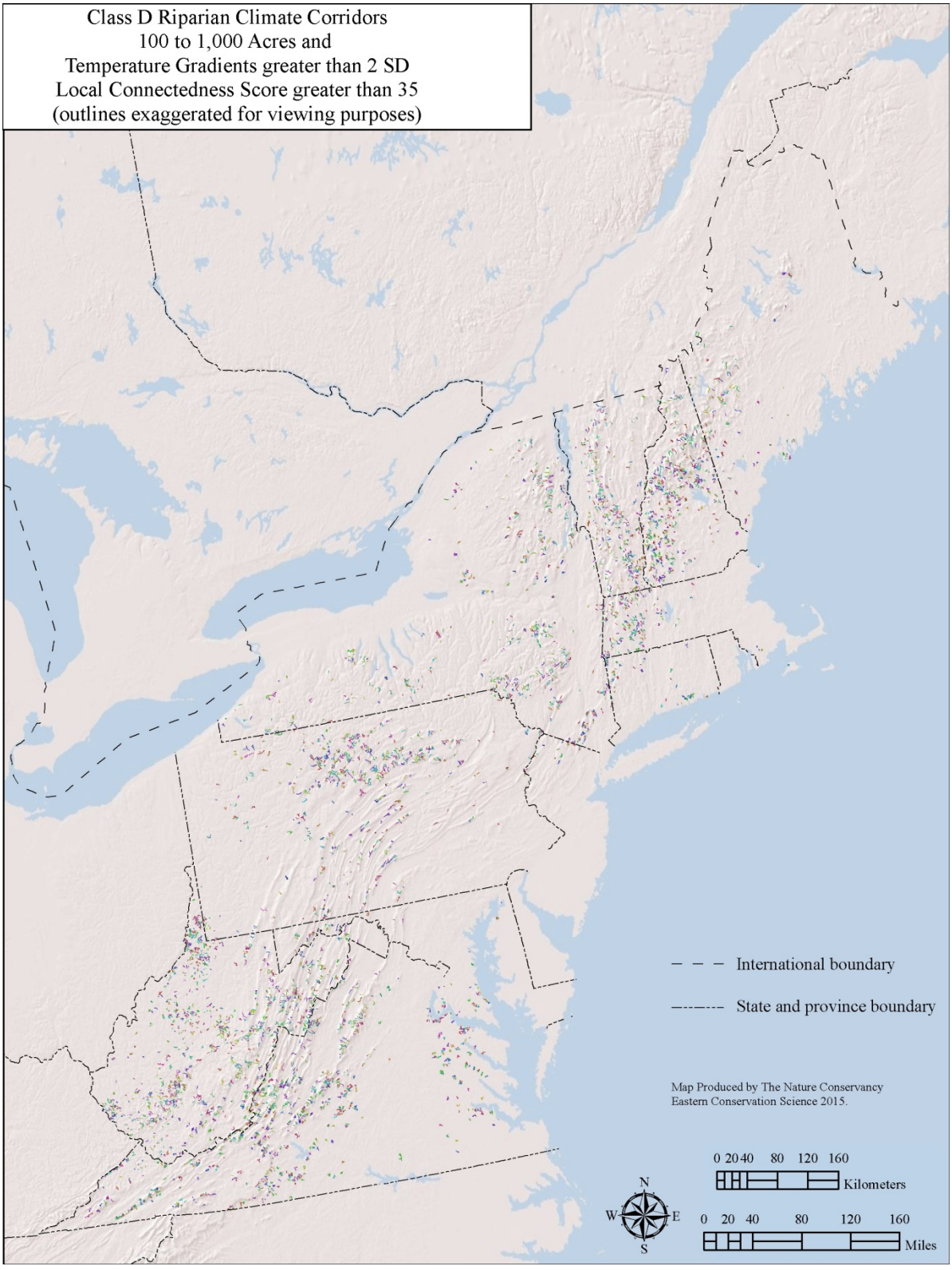

Figure 3.9. Correspondence between the RCCs and the Terrestrial Range Shift Results. The map shows areas with Class A, B or C riparian climate corridors overlaid on high-scoring cells (top 40%) identified by the wall-to-wall and moving window approaches described in the terrestrial range shift sections. Neither the RCCs nor the moving window approach covered Atlantic Canada.

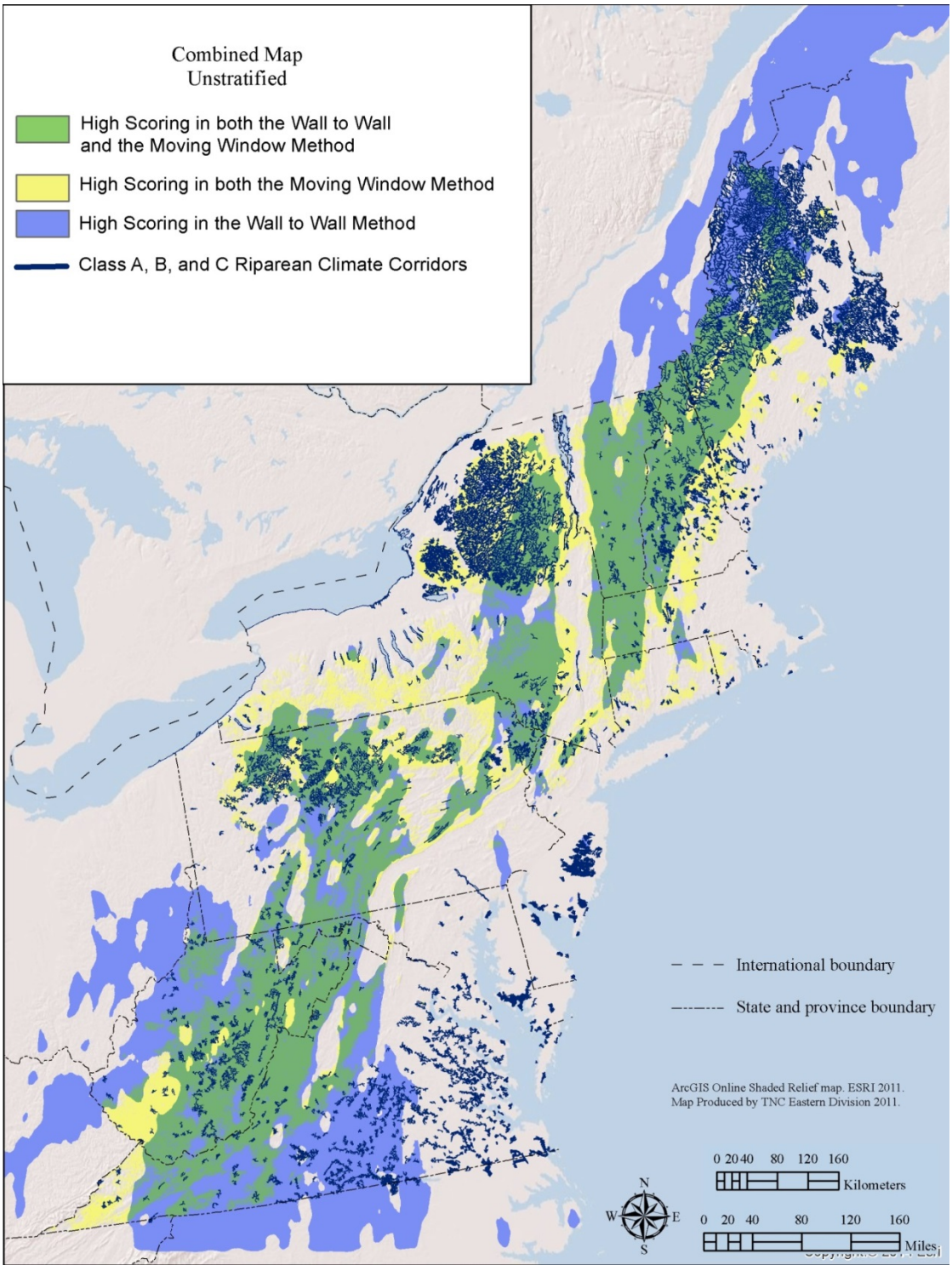

Next Steps

The concepts, analysis, and data presented here offer new tools to understand the permeability patterns of the Northeast region and the implications of those patterns on species populations responding to climate change. Although the results clearly emphasize the importance of the Appalachian Mountain chain in providing temperature options for species, there are many nuances and fine-scale patterns in the data that we are just beginning to understand.

Our overarching goal in developing this permeability data was to understand the geographic distribution of key linkage areas so that we could integrate the results with the "core areas" identified by the resilient site analysis (Anderson et al 2014) and design a network of cores and linkages that might sustain biodiversity under climate change. As this is a goal shared by The Nature Conservancy and the North Atlantic Landscape Conservation Cooperative we anticipate working closely with the LCC on this goal.

The methods and analysis presented here are very new and somewhat experimental. Prior to incorporating them into a core and linkage design, we plan to explore them further in several ways in order to fully understand their implication and use. First, we have compiled 20-30 spatially explicit datasets created by others to identify linkages at a local scale. Comparing and contrasting these datasets with the regional ones develop in this study will help us understand how connectivity changes across geographic scales. Second, we plan to experiment further with the moving window approach by adjusting the size of the search-area window to get an idea of the sensitivity of the results to the scale of analysis. Third, we hope to experiment with the relative weighting of the upslope and northward aspects of the wall-to-wall analysis to balance out the strong effect of the North-South axis

The challenge ahead is to integrate information on species ranges and range shifts with an understanding of potential and occupied habitat. Species occupy only a small portion of their range and exactly where they are found is determined by finer scale factors such as soils, geology, moisture, condition, historical changes and interactions with other species (Figure 4.1). We hope the range shift models developed here will contribute to the accumulating knowledge on species occupancy and prove useful in focusing conservation on the right places.

Figure 4.1. Spatial Relationship between a Species Range and Occupied Habitat.

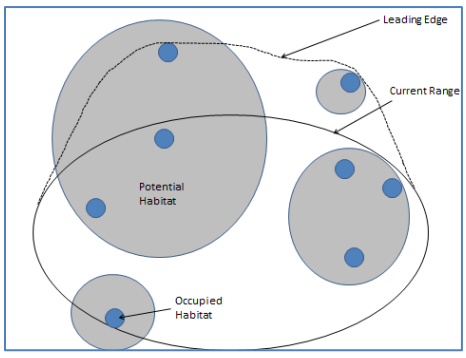

References

Anderson, M.G. (1999). Viability and Spatial Assessment of Ecological Communities in the Northern Appalachian Ecoregion. PhD dissertation. Univ. of New Hampshire. 224 pp.

Anderson, M.G., M. Clark, and A. Olivero Sheldon. (2012). Resilient Sites for Terrestrial Conservation in the Northeast and Mid-Atlantic Region. The Nature Conservancy, Eastern Conservation Science. 168pp

Anderson, M. G., Clark, M., & Sheldon, A. O. (2014). Estimating climate resilience for conservation across geophysical settings. *Conservation Biology*, *28*(4), 959-970.

Anderson, M.G., A. Barnett, M. Clark, C. Ferree, A. Olivero Sheldon, and J.Prince. (2014). Resilient Sites for Terrestrial Conservation in the Southeast Region. The Nature Conservancy, Eastern Conservation Science. 127 pp

Beier, P., Spencer, W., Baldwin, R. F., & McRae, B.H. (2011). Toward best practices for developing regional connectivity maps. *Conservation Biology*, *25*(5), 879-892.

Botkin, D. B., Saxe, H., Araujo, M. B., Betts, R., Bradshaw, R. H., Cedhagen, T., & Stockwell, D. R. (2007). Forecasting the effects of global warming on biodiversity. *Bioscience*, *57*(3), 227-236.

Carroll, C., Dunk, J. R., & Moilanen, A. (2010). Optimizing resiliency of reserve networks to climate change: multispecies conservation planning in the Pacific Northwest, USA. *Global Change Biology*, *16*(3), 891-904.

Chen, I. C., Hill, J. K., Ohlemüller, R., Roy, D. B., & Thomas, C. D. (2011). Rapid range shifts of species associated with high levels of climate warming. *Science*, *333*(6045), 1024-1026.

Colwell, R.R., Brehm, G., Cardelús, C.L., Gilman, A.C., Longino, J.T. (2008). Global Warming, Elevational Range Shifts, and Lowland Biotic Attrition in the Wet Tropics. *Science* 322, 258-261.

Corlett, R.T. and Westcott, D.A. (2015). Will plant movements keep up with climate change? Trends in Ecology & Evolution (in press)

Davis, M. B., & Shaw, R. G. (2001). Range shifts and adaptive responses to Quaternary climate change. *Science*, *292*(5517), 673-679.

Duke Energy (2014). Transmission Rights of Way. http://www.duke-energy.com/safety/right-of-way-management/transmission.asp

Eastern Conservation Science. (2009) Active River Area Riparian Component Model Using 30m DEM. http://easterndivision.s3.amazonaws.com/Freshwater/Full%20Region%20Final%20Data,ARA_RIP_ALL_090810.zip

Fischer, J., & Lindenmayer, D. B. (2007). Landscape modification and habitat fragmentation: a synthesis. *Global Ecology and Biogeography*, *16*(3), 265-280.

Fisette, T.; Davidson, A.; Daneshfar, B.; Rollin, P.; Aly, Z.; Campbell, L. (2014). Annual space-based crop inventory for Canada: 2009–2014. Geoscience and Remote Sensing Symposium (IGARSS), 2014

IEEE International, Issue Date: 13-18 July 2014. http://open.canada.ca/data/en/dataset/ba2645d5-4458-414d-b196-6303ac06c1c9

Hansen, J., Ruedy, R., Sato, M., & Lo, K. (2010). Global surface temperature change. Reviews of Geophysics, 48(4).

Hannah, L. (2011). Climate change, connectivity, and conservation success. Conservation Biology 25:1139–1142.

Heller, N. E., & Zavaleta, E. S. (2009). Biodiversity management in the face of climate change: a review of 22 years of recommendations. *Biological conservation*, *142*(1), 14-32.

Hilty, J. A., & Merenlender, A. M. (2004). Use of riparian corridors and vineyards by mammalian predators in northern California. *Conservation Biology*, *18*(1), 126-135.

Hodgson, J.A., Thomas, C.D., Wintle, B.A. & Moilanen, A. (2009). Climate change, connectivity and conservation decision making: back to basics. Journal of Applied Ecology 2009, 46, 964–969 doi: 10.1111/j.1365-2664.2009.01695.x

Jin, S., Yang, L., Danielson, P., Homer, C., Fry, J., & Xian, G. (2013). A comprehensive change detection method for updating the National Land Cover Database to circa 2011. *Remote Sensing of Environment*, *132*, 159-175.

Koen, E. L., Garroway, C. J., Wilson, P. J., & Bowman, J. (2010). The effect of map boundary on estimates of landscape resistance to animal movement. *PLoS One*, *5*(7), e11785.

Koen, E. L., Bowman, J., Sadowski, C., & Walpole, A. A. (2014). Landscape connectivity for wildlife: development and validation of multispecies linkage maps. *Methods in Ecology and Evolution*, *5*(7), 626-633.

Krosby, M., Tewksbury, J., Haddad, N. M., & Hoekstra, J. (2010). Ecological connectivity for a changing climate. *Conservation Biology*, *24*(6), 1686-1689.

Krosby, M., Norheim, R., Theobald, D. M., and B. H. McRae. (2014). Riparian climate-corridors: Identifying priority areas for conservation in a changing climate. Technical Report. Available at http://nplcc.databasin.org/datasets/46caec8762194138a8a6421322ea170d.

Lenoir, J., Gégout, J. C., Marquet, P. A., De Ruffray, P., & Brisse, H. (2008). A significant upward shift in plant species optimum elevation during the 20th century. *Science*, *320*(5884), 1768-1771.

Lenoir, J., Gégout, J. C., Guisan, A., Vittoz, P., Wohlgemuth, T., Zimmermann, N. E.,& Svenning, J. C. (2010). Going against the flow: potential mechanisms for unexpected downslope range shifts in a warming climate. *Ecography*, *33*(2), 295-303.

Manci, Karen M. (1989). Riparian ecosystem creation and restoration: A literature summary. U.S. Fish and Wildlife Service Biological Report 89(20):1-59. Jamestown, ND: Northern Prairie Wildlife Research Center Online. http://www.npwrc.usgs.gov/resource/habitat/ripareco/index.htm (Version 16JUL97).

McRae, B.H., V.B. Shah, and T.K. Mohapatra. (2013). Circuitscape 4 User Guide. The Nature Conservancy. http://www.circuitscape.org.

McRae, B. H., & Beier, P. (2007). Circuit theory predicts gene flow in plant and animal populations. *Proceedings of the National Academy of Sciences*, *104*(50), 19885-19890.

McRae, B. H., Dickson, B. G., Keitt, T. H., & Shah, V. B. (2008). Using circuit theory to model connectivity in ecology, evolution, and conservation. *Ecology*, *89*(10), 2712-2724.

McRae, B. H., & Shah, V. B. (2009). Circuitscape user guide. *ONLINE. The University of California, Santa Barbara. Available at: http://www. circuitscape.org*.

Meehl, G.A., T.F. Stocker, W.D. Collins, P. Friedlingstein, A.T. Gaye, J.M. Gregory, A. Kitoh, R. Knutti, J.M. Murphy, A. Noda, S.C.B. Raper, I.G. Watterson, A.J. Weaver and Z.-C. Zhao (2007). Global Climate Projections. In: Climate Change 2007: The Physical Science Basis . Contribution of Working Group I to the Fourth Assessment Report of the Intergovernmental Panel on Climate Change [Solomon, S., D. Qin, M. Manning, Z. Chen, M. Marquis, K.B. Averyt, M. Tignor and H.L. Miller (eds.)]. Cambridge University Press, Cambridge, United Kingdom and New York, NY, USA.

Meiklejohn, K., Ament, R. and Tabor, G. (2010). Habitat Corridors & Landscape Connectivity: Clarifying the Terminology. Center For Large Landscape Conservation. www.climateconservation.org.

Naiman, R. J., Decamps, H., & Pollock, M. (1993). The role of riparian corridors in maintaining regional biodiversity. *Ecological applications*, *3*(2), 209-212.

NRC (2010). Advancing the Science of Climate Change. National Research Council. The National Academies Press, Washington, DC, USA.

Nuñez, T. A., Lawler, J. J., McRae, B. H., Pierce, D., Krosby, M. B., Kavanagh, D. M., ... & Tewksbury, J. J. (2013). Connectivity planning to address climate change. *Conservation Biology*, *27*(2), 407-416.

Olivero, A, and M.G. Anderson. (2008). The Northeast Aquatic Habitat Classification. The Nature Conservancy, Eastern Conservation Science. 90 pp. http://www.rcngrants.org/spatialData

Olson, D. H., Anderson, P. D., Frissell, C. A., Welsh, H. H., & Bradford, D. F. (2007). Biodiversity management approaches for stream–riparian areas: perspectives for Pacific Northwest headwater forests, microclimates, and amphibians. *Forest Ecology and management*, *246*(1), 81-107.

Open Street Map (2014). Open Street map. http://www.openstreetmap.org

Pardi, M.I. and Smith, F.A. (2012) Paleoecology in an era of climate change: how the past can provide insights into the future. In Paleontology in Ecology and Conservation (Louys, J., ed.), pp. 93–115, Springer-Verlag

Parmesan, C., & Yohe, G. (2003). A globally coherent fingerprint of climate change impacts across natural systems. *Nature*, *421*(6918), 37-42.

Pelletier, D., Clark, M., Anderson, M. G., Rayfield, B., Wulder, M. A., & Cardille, J. A. (2014). Applying circuit theory for corridor expansion and management at regional scales: tiling, pinch points, and omnidirectional connectivity. *PloS one*, *9*(1), e84135.

PRISM Climate Group (2013). Oregon State University, http://prism.oregonstate.edu.

Pusey, B. J., & Arthington, A. H. (2003). Importance of the riparian zone to the conservation and management of freshwater fish: a review. *Marine and Freshwater Research*, *54*(1), 1-16.

Seavy, N. E., Gardali, T., Golet, G. H., Griggs, F. T., Howell, C. A., Kelsey, R., ... & Weigand, J. F. (2009). Why climate change makes riparian restoration more important than ever: recommendations for practice and research. *Ecological Restoration*, *27*(3), 330-338.

Shah, B.V. and McRae, B. (2008). Circuitscape: a tool for landscape ecology. In proceeding of the 7th Python in Science Conference.

Smith, M. P., Schiff, R., Olivero, A., & MacBroom, J. G. (2008). The active river area: A conservation framework for protecting rivers and streams. The Nature Conservancy, Boston, MA. 59p.

Tele Atlas North America, Inc. (2009). U.S. and Canada Railroads. 1:100,000. ESRI® Data & Maps: StreetMap. 2009 Data Update: North America. Redlands, California, USA. U.S. and Canada Railroads represent the railroads of the United States and Canada.

U.S. Census Bureau (2014). 2014 TIGER/Line Shapefiles (machine-readable data files). http://www.census.gov/geo/maps-data/data/tiger.html

Ventyx Corporation (2014) Velocity Suite: Transmission lines constrained or congested, transmission lines (In service by voltage class), and Natural Gas Pipelines (In service). http://www.ventyx.com/en/enterprise/business-operations/business-products/velocitysuite.
Accessed October 2014.

Wang, T., Hamann, A., Spittlehouse, D. L., & Aitken, S. N. (2006). Development of scale-free climate data for Western Canada for use in resource management. *International Journal of Climatology*, *26*(3), 383-397.

Wang, T., Hamann, A., Spittlehouse, D. L., & Murdock, T. Q. (2012). ClimateWNA-high-resolution spatial climate data for western North America. *Journal of Applied Meteorology and Climatology*, *51*(1), 16-29.